

Microplastics removal from water with organosilanes

zur Erlangung des akademischen Grades eines
DOKTORS DER NATURWISSENSCHAFTEN

von der KIT-Fakultät für Chemieingenieurwesen und Verfahrenstechnik des
Karlsruher Instituts für Technologie (KIT)
genehmigte

DISSERTATION

von

M. Sc. Michael Sturm
aus Bad Bergzabern, Deutschland

Erstgutachter: Prof. Dr. rer. nat. Harald Horn

Zweitgutachter: Prof. Dr.-Ing. Hermann Nirschl

Tag der mündlichen Prüfung: 15.07.2022

Meiner Familie

“You are the universe, expressing itself as a human for a little while.”

- Eckhart Tolle

Acknowledgment

Very special thanks belong to **Prof. Dr. Harald Horn** for his supervision, the generous provision of the laboratories and equipment, the constant control of the progress and quality of the doctorate, as well as the help with the planning of experiments and the evaluation of the results. Especially in the field of biofilms, I would not have come this far without his help.

Further special thanks also belong to **Dr. Katrin Schuhen**, for the constant support and close cooperation, the planning and discussion of experiments and results, the joint preparation of proposals, manuscripts, and presentations as well as the reassuring words in case the experiments did not go as they should. Without her, the doctorate would not have come about.

For the financial support, the provision and production of numerous special chemicals, the support with business trips, and visits to numerous conferences I thank the **abcr GmbH** - an essential partner for the doctorate. I particularly thank **Dr. Jan Schuricht** for the trust placed in me, which enabled me to work freely, and **Dr. Christoph Hussal-Raic**, who was always committed to helping me with organizational problems.

Another thank you goes to the **Wasser 3.0 gGmbH**, especially **Dennis Schober**, who made it possible to implement my laboratory tests on a pilot plant scale.

Furthermore, I would like to thank all employees of the **Engler-Bunte Institut - Water Chemistry and Water Technology** for their support. **Dr. Gudrun Abbt-Braun**, who always had good advice and helped me with numerous organizational tasks. **Dr. Michael Wagner** for discussing and optimizing measurements and results. **Prof. Dr. Gisela Guthausen** for the support with the NMR measurements. All the technicians, **Stephanie West, Axel Heidt, Matthias Weber, Reinhart Sembritzki, Ulrich Richert**, and **Rafael Peschke**, who helped me with test setups, measurements, and finding various laboratory equipment. My fellow doctoral students, especially - **Luisa Gierl** for the OCT measurements **Florian Ranzinger** for the 3-D images of biofilms, and the secretaries **Sylvia Heck** and **Ursula Schäfer**.

I would like to thank the **DBU** (Deutsche Bundesstiftung Umwelt), which supported me with a doctoral scholarship (Az. 20018/549) and numerous events for doctoral scholarship holders, as well as my supervisor **Dr. Reinhard Stock** and my former supervisor **Dr. Kathrin Schmidt**.

Additionally, I thank **Fabian Hagen** from the Engler-Bunte Institut - Combustion Technology for his help with the TGA measurements.

Finally, I would like to thank my **family**. My **parents**, who have always supported me throughout my school days, studies, and doctoral studies, and my **brother**, with whom I share my dedication for chemistry.

Michael Toni Sturm

Abstract

In the last years, microplastics have been proven to be a ubiquitous environmental contaminant, especially in aquatic environments. Thus, methods and materials for efficient microplastics removal from waters came more and more into the focus of research and engineering. Areas of application are the treatment of municipal- and industrial wastewater as well as urban- or road runoff, to avoid plastic inputs into the environment. Other applications are microplastics sensitive water using processes, such as sea salt extraction or membrane-based seawater desalination. First published in 2017 by Herbort et al., organosilanes could be used successfully to agglomerate and remove microplastics from water. With this novel method, organosilanes can attach to the microplastics surface, collect them in large agglomerates and bind them chemically during a water-induced sol-gel process. The overall aim of this thesis is to further investigate and improve this new process.

The first part of the thesis investigated, which organosilanes are best suitable for microplastics removal. Various alkyltrichlorosilanes with different linear and branched alkyl groups and a chain length between 1 and 18 carbon (C-) atoms were examined for their suitability to agglomerate and fix microplastics (mixtures of polyethylene and polypropylene) from water. The removal efficiency was determined gravimetrically. The reaction behavior during the fixation process were characterized by hydrolysis kinetics. Silicon-29 magic-angle-spinning magnetic resonance (^{29}Si -MAS-NMR) spectroscopy, infrared (IR) spectroscopy, and thermogravimetry (TGA) were used to characterize the chemical composition of the agglomerates. Optical coherence tomography (OCT) allowed the visualization of the agglomerates. The results show that the different alkyl groups have a strong impact on the suitability of the alkyltrichlorosilanes for the agglomeration and fixation, as they influence the hydrolysis- and condensation kinetics, as well as the affinity to the microplastics. Best suited for microplastics removal are intermediate chain lengths between 3 and 5 C-atoms.

As important environmental factors, the effect of water compositions (biologically treated municipal wastewater, salt water, and demineralized water) and temperatures (7.5 °C, 20 °C 40 °C) on the removal process were investigated in part two. The different temperatures and water compositions showed no negative effect on microplastics removal. Additionally, the dissolved organosilane residues after the removal process were quantified comparing inductively coupled plasma atomic emission spectroscopy (ICP-OES) and dissolved organic carbon measurements (DOC) as quantification methods. Here only one of the three organosilanes tested showed no dissolved residues, which makes it suitable for application on a technical scale. As microplastics can consist of numerous different polymers, the process was tested towards five of the most common polymer types with different properties and surface chemistries. Further investigations on the agglomerates were performed using microscopy, infra-red spectroscopy, and thermogravimetric analysis. A strong interaction between the organic group of the organosilane and the surface of the polymer was observed. Increasing polarity of microplastics negatively affects the removal process using organosilanes with non-polar organic groups. By increasing the polarity of the organic group or using higher concentrations of organosilanes, highly polar polymers

can be removed efficiently. This demonstrates that organosilanes can be adapted according to the surface chemistry of certain polymer types to remove them more efficiently.

The previous results show that the removal process strongly depends on the interaction of the organosilane and the surface of the microplastic particles. As microplastics in the environment are commonly covered by biofilms, their influence on removal was analyzed in part three. Common methods for biofilm cultivation on microplastics described in literature need several weeks up to several months. For rapid biofilm cultivation, a packed bed column filled with microplastics and flown through by biologically treated municipal wastewater enriched with glucose was developed and tested. The biofilm was characterized using confocal laser scanning microscopy (CLSM), scanning electron microscopy (SEM), Fourier-Transform infrared spectroscopy (FT-IR), and contact angle measurements. The results show a partial biofilm coverage of the microplastics after 7 days of incubation. Thus, for the first time, a method for fast and standardizable biofilm cultivation on microplastics was developed. To investigate the effect on the microplastics removal, microplastics based on five different polymer types were cultivated in the columns. The removal efficiencies were determined gravimetrically for three different organosilanes. The results confirmed, biofilm coverage affects the removal process and leads to reduced removal efficiencies. Removal of the biofilm using ultrasounds and hydrogen peroxide treatment could improve the removal efficiencies of the microplastics from the water again but did not reach the values of the virgin microplastics. This highlights the importance of simulated environmental exposure in microplastics research and how it can affect surface-active microplastics removal processes

To test the process on a pilot plant scale, a detection method for microplastics in environmental samples is needed. Despite extensive research, there is still no cheap and easily applicable method for microplastics detection available. Staining microplastics with Nile red has great potential, as the only requirement is a device for fluorescent imaging. Previous studies show, that in stained environmental samples, microplastics show stronger fluorescence than natural particles and can be distinguished by their higher fluorescence intensity. To improve the process, Nile red and three newly developed derivatives were tested in part four, to achieve greater selectivity for plastic particles and more intense fluorescence. The investigations were carried out by analyzing solid sample fluorescent spectra of microplastics and natural particles, stained with different organic solvents and water at different pH values. The results show, that the chosen solvent, pH value, plastic- or particle type as well as the modification of the Nile red influence the fluorescence properties of the stained particles. A combination of Nile red and a new Nile red derivative modified with an Ethylhexyl group dissolved in water at pH 2.5 turned out to be the most efficient to distinguish plastics and natural particles. As the selectivity is not yet high enough to avoid false positives by natural polymers like chitin, time-consuming sample preparation is still necessary. Using these findings, the final method was applied for sea salt samples as an example for environmental samples.

Zusammenfassung

In den letzten Jahren hat sich Mikroplastik als allgegenwärtiger Umweltschadstoff erwiesen, insbesondere in der aquatischen Umwelt. So rückten Methoden und Materialien zur effizienten Entfernung von Mikroplastik aus Gewässern immer mehr in den Fokus von Forschung und Ingenieurwesen. Anwendungsgebiete sind die Behandlung von kommunalen und industriellen Abwässern sowie Oberflächenabfluss von Städten oder Straßen, mit dem Ziel Mikroplastikeinträge in die Umwelt zu vermeiden. Weitere Anwendungen sind mikroplastikempfindliche Wassernutzungsprozesse wie Meersalzgewinnung oder membranbasierte Meerwasserentsalzung. Erstmals 2017 von Herbolt et al. veröffentlicht, konnten Organosilane erfolgreich eingesetzt werden, um Mikroplastik zu agglomerieren und aus Wasser zu entfernen. Bei diesem neuartigen Verfahren lagern sich Organosilane an die Mikroplastikoberfläche an und sammeln dieses in großen Agglomeraten, welche in einem wasserinduzierten Sol-Gel-Prozess chemisch gebunden werden. Das übergeordnete Ziel dieser Arbeit ist es, dieses neue Verfahren weiter zu untersuchen und zu verbessern.

Im ersten Teil der Arbeit wurde untersucht, welche Organosilane sich am besten für die Entfernung von Mikroplastik eignen. Verschiedene Alkyltrichlorosilane mit unterschiedlichen linearen und verzweigten Alkylgruppen und einer Kettenlänge zwischen 1 bis 18 C-Atomen wurden auf ihre Eignung untersucht, Mikroplastik (Gemisch aus Polyethylen und Polypropylen) in Wasser zu agglomerieren und zu fixieren. Die Entfernungseffizienz wurde gravimetrisch bestimmt. Das Reaktionsverhalten während des Fixierungsprozesses wurde durch Hydrolysekinetiken untersucht. Zur Charakterisierung der chemischen Zusammensetzung der Agglomerate wurden Silizium-29 Magnetresonanz (^{29}Si -MAS-NMR) Spektroskopie, Infrarot (IR) Spektroskopie und Thermogravimetrie (TGA) verwendet. Optische Kohärenztomographie (OCT) ermöglichte die Visualisierung der Agglomerate. Die Ergebnisse zeigen, dass die unterschiedlichen Alkylgruppen einen starken Einfluss auf die Eignung der Alkyltrichlorosilane zur Agglomeration und Fixierung von Mikroplastik haben, da sie die Hydrolyse- und Kondensationskinetik sowie die Affinität zum Mikroplastik beeinflussen. Am besten geeignet für die Entfernung von Mikroplastik sind Kettenlängen zwischen 3 und 5 C-Atomen.

Als wichtige Umweltfaktoren wurden im zweiten Teil der Einfluss von Wasserzusammensetzungen (biologisch gereinigtes kommunales Abwasser, Salzwasser und demineralisiertes Wasser) und Temperaturen (7,5 °C, 20 °C, 40 °C) auf den Entfernungsprozess untersucht. Die unterschiedlichen Temperaturen und Wasserzusammensetzungen zeigten keinen negativen Einfluss auf die Entfernung von Mikroplastik. Zusätzlich wurden die gelösten Organosilanrückstände nach dem Entfernungsprozess quantifiziert, wobei Atomemissionsspektroskopie mit induktiv gekoppeltem Plasma (ICP-OES) und Messungen des gelösten organischen Kohlenstoffs (DOC) als Quantifizierungsmethoden verglichen wurden. Hier zeigte nur eines der drei getesteten Organosilane keine gelösten Rückstände, wodurch es für eine Anwendung im technischen Maßstab geeignet ist. Da Mikroplastik aus zahlreichen unterschiedlichen Polymeren bestehen kann, wurde das Verfahren an fünf der gängigsten Polymertypen mit unterschiedlichen Eigenschaften und Oberflächenchemie getestet. Untersuchungen der Agglomerate

wurden mittels Mikroskopie, Infrarotspektroskopie und thermogravimetrischer Analyse durchgeführt. Die Ergebnisse zeigen eine starke Wechselwirkung zwischen der organischen Gruppe des Organosilans und der Oberfläche des Polymeren. Eine zunehmende Polarität von Mikroplastik wirkt sich negativ auf den Entfernungprozess mit Organosilanen mit unpolaren organischen Gruppen aus. Durch Erhöhung der Polarität der organischen Gruppe oder Verwendung höherer Konzentrationen von Organosilanen können hochpolare Polymere effizient entfernt werden. Dies zeigt, dass Organosilane an die Oberflächenchemie bestimmter Polymertypen angepasst werden können, um diese effizienter zu entfernen.

Die bisherigen Ergebnisse zeigen, dass der Entfernungprozess stark von der Wechselwirkung des Organosilans mit der Oberfläche der Mikroplastikpartikel abhängt. Da Mikroplastik in der Umwelt häufig von Biofilmen bedeckt ist, wurde dessen Einfluss auf die Entfernung im dritten Teil analysiert. In der Literatur beschriebene gängige Methoden zur Biofilmkultivierung auf Mikroplastik benötigen mehrere Wochen bis mehrere Monate. Für eine beschleunigte Biofilmkultivierung wurde eine mit Mikroplastik gefüllte Festbettsäule entwickelt und getestet, die von biologisch aufbereiteten kommunalen Abwässern, angereichert mit Glucose, durchströmt wurde. Der Biofilm wurde mit konfokaler Laser-Scanning-Mikroskopie (CLSM), Rasterelektronenmikroskopie (REM), Fourier-Transform-Infrarotspektroskopie (FT-IR) und Kontaktwinkelmessungen charakterisiert. Die Ergebnisse zeigen eine partielle Biofilmbedeckung des Mikroplastiks nach 7 Tagen Inkubation. Damit wurde erstmals eine Methode zur schnellen und standardisierbaren Biofilmkultivierung auf Mikroplastik entwickelt. Um anschließend den Effekt von Biofilmbewuchs auf die Mikroplastikentfernung zu untersuchen, wurde in den Säulen Mikroplastik auf Basis von fünf verschiedenen Polymertypen kultiviert. Die Entfernungseffizienzen wurden gravimetrisch für drei verschiedene Organosilane bestimmt. Die Ergebnisse bestätigten, dass der Biofilmbewuchs den Entfernungprozess beeinflusst und zu einer verringerten Entfernungseffizienz führt. Die Entfernung des Biofilms mittels Ultraschall und Wasserstoffperoxidbehandlung könnte die Entfernungseffizienzen des Mikroplastiks aus Wasser wieder verbessern, erreichte jedoch nicht die Effizienzen des fabrikneuen Mikroplastiks. Dies unterstreicht die Bedeutung der simulierten Umweltexposition in der Mikroplastikforschung und wie diese oberflächenaktive Prozesse zur Entfernung von Mikroplastik beeinflussen kann

Um das Verfahren im Technikumsmaßstab zu testen, wird ein Nachweisverfahren für Mikroplastik in Umweltproben benötigt. Trotz umfangreicher Forschung steht noch immer keine kostengünstige und einfach anwendbare Methode zum Nachweis von Mikroplastik zur Verfügung. Das Anfärben von Mikroplastik mit Nilrot hat großes Potenzial, da die einzige Voraussetzung ein Gerät für Fluoreszenzaufnahmen ist. Bisherige Studien zeigen, dass Mikroplastik in gefärbten Umweltproben stärker fluoresziert als natürliche Partikel und somit durch die höhere Fluoreszenzintensität identifiziert werden kann. Zur Verbesserung des Verfahrens wurden im vierten Teil Nilrot und drei neu entwickelte Derivate getestet, mit dem Ziel eine höhere Selektivität für Kunststoffpartikel und eine intensivere Fluoreszenz zu erreichen. Die Untersuchungen wurden durchgeführt, indem Mikroplastik und

verschiedene natürliche Partikel Fluoreszenzspektren mit verschiedenen organischen Lösungsmitteln und Wasser bei verschiedenen pH-Werten gefärbt wurden. Anschließend wurden Feststofffluoreszenzspektren aller Proben aufgenommen und analysiert. Die Ergebnisse zeigen, dass das gewählte Lösungsmittel, pH-Wert, Kunststoff- oder Partikeltyp sowie die Modifizierung des Nilrots die Fluoreszenzeigenschaften der gefärbten Partikel beeinflussen. Eine Kombination aus Nilrot und einem neuen Nilrot-Derivat, modifiziert mit einer Ethylhexylgruppe, gelöst in Wasser bei pH 2,5, erwies sich als am effizientesten zur Unterscheidung von Kunststoffen und natürlichen Partikeln. Da die Selektivität noch nicht hoch genug ist, um falsche Positivbefunde durch natürliche Polymere wie Chitin zu vermeiden, ist weiterhin eine zeitaufwändige Probenvorbereitung erforderlich. Die mit diesen Erkenntnissen entwickelte Methode für Meersalzproben als Beispiel für Umweltproben angewandt.

Publications

Peer-reviewed publications

Sturm, M.T., Herbort, A.F., Horn, H., Schuhen, K., Comparative study of the influence of linear and branched alkyltrichlorosilanes on the removal efficiency of polyethylene and polypropylene-based microplastic particles from water, *Environmental Science and Pollution Research* 27, 10888–10898 (2020)

Sturm, M.T., Horn, H. & Schuhen, K., The potential of fluorescent dyes—comparative study of Nile red and three derivatives for the detection of microplastics. *Anal Bioanal Chem* 413, 1059–1071 (2021).

Sturm, M.T., Horn, H., Schuhen, K., Removal of Microplastics from Waters through Agglomeration-Fixation Using Organosilanes—Effects of Polymer Types, Water Composition and Temperature. *Water*, 13, 675 (2021).

Dwiyitno, D., **Sturm, M.T.**, Januar, H.I, Schuhen, K., Influence of various production methods on the microplastic contamination of sea salt produced in Java, Indonesia. *Environ Sci Pollut Res* 28, 30409–30413 (2021).

Sturm M.T., Schuhen K, Horn H. Method for rapid biofilm cultivation on microplastics and investigation of its effect on the agglomeration and removal of microplastics using organosilanes. *Sci Total Environ*, 151388 (2021).

Book chapters

Schuhen, K., **Sturm, M.T.**, Herbort, A.F., Technological Approaches for the Reduction of Microplastic Pollution in Seawater Desalination Plants and for Sea Salt Extraction, In: *Plastics in the Environment*, Gomiero, A. (Ed.), IntechOpen, London, (2018).

Schuhen K., **Sturm M.T.**, Microplastic Pollution and Reduction Strategies. In: *Handbook of Microplastics in the Environment*, Rocha-Santos T., Costa M., Mouneyrac C. (Eds.), Springer, Cham, (2021).

Conference contributions

Oral presentations

Sturm M. T. & Schuhen K., Development of a novel technological approach for the reduction of microplastic pollution in seawater desalination plants and for sea salt extraction, MICRO 2018 - Fate and Impact of Microplastics: Knowledge, Actions and Solutions, Arrecife, Spanien, (19. – 23.11.2018).

Sturm M. T. & Schuhen K., Development of a novel technological approach for the reduction of microplastic pollution in seawater desalination plants and for sea salt extraction, ICCE 2019, 17th International Conference on Chemistry and the Environment, Thessaloniki, Griechenland, (16. - 20.06.2019).

Sturm M. T. & Schuhen K., Development of a novel technological approach for the reduction of microplastic pollution in seawater desalination plants and for sea salt extraction, μ MED 2019, International Conference on Microplastic Pollution in the Mediterranean Sea, Capri, Italien, (15. - 18.09.2019).

Sturm M. T. & Schuhen K., Novel method for removal of microplastics from sea water using organosilanes, Virtual Symposium on Marine Pollution, Facultad de Ciencias de la Universidad de Granada, Spanien, online Konferenz (18.-19.06.2020).

Sturm M. T. & Schuhen K., Development of a novel technological approach for removal of microplastics from water – comparison of environmental factors and different polymer types, MICRO 2020 - Fate and Impacts of Microplastics: Knowledge and responsibilities, Arrecife, Spanien, online Konferenz (23.-27.11.2020)

Sturm M.T. & Schuhen K., The potential of fluorescence dyes – Comparative study of Nile red and three derivatives for the detection of microplastics, MICRO 2020 - Fate and Impacts of Microplastics: Knowledge and responsibilities, Arrecife, Spanien, online Konferenz (23.-27.11.2020)

Sturm M.T. & Schuhen K., Development of a novel technological approach for the removal of microplastics from water using organosilanes, International Conference for YOUNG Marine Researchers – ICYMARE 2021, Berlin, Germany (21.-24.09.2021)

Poster presentations

Sturm M.T. & Schuhen K., Removal of microplastics from waters using organosilanes, 19th International Symposium on Silicon Chemistry, Toulouse, Frankreich, online Konferenz (18.-19.07.2021).

Table of contents

1	Introduction.....	1
1.1	Microplastics in the environment.....	1
1.1.1	The beginnings of microplastic research.....	1
1.1.2	Definition of microplastics.....	2
1.1.3	Sources, transport and sinks.....	2
1.1.4	Degradation behavior and persistence.....	5
1.1.5	Harmful effects of microplastics in the environment.....	6
1.2	Microplastics removal from water.....	8
1.2.1	Areas of application.....	8
1.2.2	Removal methods.....	10
1.2.3	Microplastics removal using organosilanes.....	11
1.3	Microplastics detection in environmental samples.....	12
1.3.1	Microplastics detection and its challenges.....	12
1.3.2	Fluorescence staining for microplastics detection using Nile red.....	16
1.4	Objectives of the doctoral thesis.....	17
2	Comparative study of the influence of linear and branched alkyltrichlorosilanes on the removal efficiency of polyethylene and polypropylene based microplastic particles from water.....	18
2.1	Introduction.....	18
2.1.1	Microplastics in the aquatic environment.....	18
2.1.2	How does the novel agglomeration-fixation reaction (AFR) work?.....	19
2.1.3	Silicon-based precursors for microplastic reduction (Wasser 3.0 PE-X).....	20
2.2	Materials and Methods.....	21
2.2.1	Chemicals and reagents.....	21
2.2.2	Overview of analytical methods and processes.....	22
2.2.3	Evaluation of polymer removal efficiency from water.....	23
2.2.4	Determination of hydrolysis rates.....	24
2.3	Results and discussion.....	24
2.3.1	Determination of removal efficiencies.....	24

2.3.2 Hydrolysis rates and NMR analytics	27
2.2.3 Characterization of agglomerates by OCT, IR spectroscopy and TGA.....	29
2.4 Conclusion.....	31
3 Removal of Microplastics from waters through Agglomeration-Fixation using Organosilanes – Effects of polymer types, water composition and temperature.....	34
3.1. Introduction	34
3.2. Materials and Methods	36
3.2.1 Used microplastics and chemicals	36
3.2.2 Different water types and temperatures	36
3.2.3 Determination of removal efficiency.....	37
3.2.4 Determination of the organosilane residues dissolved in water.....	37
3.2.5 Additional analytics.....	38
3.3 Results and Discussion	38
3.3.1 Different water types and temperatures.....	38
3.3.2 Comparison of polymer types.....	40
3.3.3 Organosilanes residues dissolved in water	43
3.3.4 Additional analytics.....	45
3.4 Conclusions	47
4 Method for rapid biofilm cultivation on microplastics and investigation of its effect on the agglomeration and removal of microplastics using organosilanes.....	50
4.1 Introduction	50
4.2 Material and Methods	52
4.2.1 Used microplastics and chemicals	52
4.2.2 Biofilm growth on microplastics	53
4.2.3 Biofilm characterization	54
4.2.4 Determination of removal efficiency.....	55
4.2.5 Biofilm removal from microplastics.....	55
4.3 Results and Discussion	56
4.3.1 Biofilm growth and characterization	56
4.3.2 Removal of biofilm-covered microplastics.	61

5	The potential of fluorescent dyes – Comparative study of Nile red and three derivatives for the detection of microplastics	66
5.1	Introduction.....	66
5.1.1	State of the art: Methods for the detection of microplastics in ecosystems	67
5.1.2	Nile red (NR) – A fluorescent dye with high affinity to microplastics but with limitations.....	69
5.2	Material and Methods	71
5.2.1	Nile red, its derivatives	71
5.2.2	Dyeing of samples in water at different pH-values.....	72
5.2.3	Dyeing of microplastics with different NR concentrations.....	72
5.2.3	Dyeing of microplastics with different solvents	72
5.2.4	Acquisition of solid sample fluorescence spectra	72
5.2.5	Fluorescence microscope imaging.....	73
5.2.6	Processing of environmental samples	73
5.3	Results and Discussion	74
5.3.1	Influence of solvent on emission spectra	74
5.3.2	Control of the occurrence of quenching.....	75
5.3.3	Effect of different NR derivatives and pH-value	76
5.3.4	Test of the method on sea salt samples.....	81
5.4	Conclusions.....	81
6	Summary and outlook	84
6.1	Influence of the organic group.....	84
6.2	Influence of water type, temperature, and polymer type.....	84
6.3	Influence of biofilm coverage	85
6.4	Nile red staining for microplastics detection	86
	Appendix.....	88
A1	Supplementary material for chapter 2.....	88
A2	Supplementary material for chapter 3.....	92
A3	Supplementary material for chapter 4.....	103
A4	Supplementary material for chapter 5.....	109
A5	Verification of the contribution from the co-authors	120

List of abbreviations	129
References.....	131

1 Introduction

1.1 Microplastics in the environment

1.1.1 The beginnings of microplastic research

Since the mass production of plastics in the 1950s, it became a part of our everyday life with continuously increasing production amount [1]. Because of its versatile material properties, various applications, and cheap production, modern life without plastics is hardly imaginable. Thereby, it is inevitable that plastic also ends up in the environment, mainly through improper disposal, losses during transport, production or disposal, or the specific form of use such as tire wear [2]. Already in the 1960s and 1970s, researchers identified plastic particles in marine plankton samples, water samples, and guts of sea birds [3–5]. However, the topic of plastics in the environment was largely neglected for a long time, until Richard Thompson drew in 2004 in his Science paper “Lost at Sea: Where Is All the Plastic?”, attention to it. He showed that because of its continuous inputs and high persistence plastic accumulates in the marine environment. Due to environmental influences, it fragments over time into smaller plastic particles, which spread out over the seas and oceans [6]. When smaller than 5 mm, plastic particles are defined as microplastics [6]. Also, Richard Thompson showed that marine organisms and ecosystems are exposed to microplastics, interact with them, and can suffer from harmful effects, which makes them an environmental pollutant. One of the main points of this paper was, how little we know about the entry paths, the degradation- and transport behavior as well as the interaction with the environment of such a commonly used, man-made material, which is foreign to the environment and the ecosystem. This brought a lot of attention to this topic of microplastics in the environment, which rapidly became a trending research topic, identifying it as a global environmental problem (Figure 1-1).

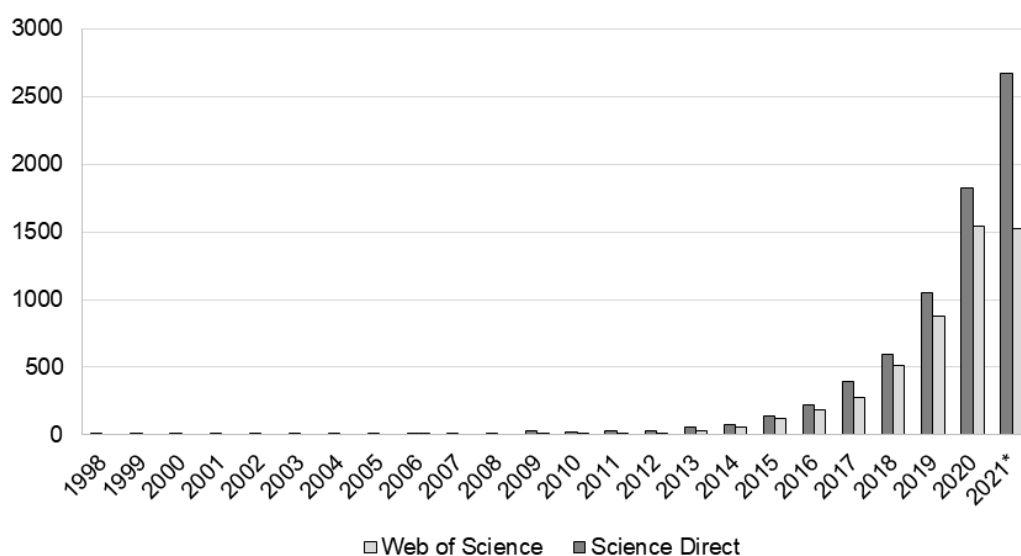


Figure 1-1: Numbers of yearly publications found searching for "microplastics environment" in Web of Science and ScienceDirect. * 2021 data taken on September 15th, 2021.

1.1.2 Definition of microplastics

The among researchers commonly accepted definition is, microplastics are plastic particles smaller than 5 mm [7, 8]. A lower size limit is not given, but microplastics smaller than 1 μm are usually referred to as nanoplastics. Plastics larger than 5 mm are defined as macroplastics (Figure 1-2).



Figure 1-2: Size limits of microplastics, nanoplastics, and macroplastics.

Additionally, microplastics can be classified by their entry paths. Primary microplastics are entering the environment directly as microplastics (Figure 1-3) [9]. They can be produced for intended use as microplastics, e.g. exfoliates in facial cleansers and cosmetics (type A), or result from the breakdown of larger plastics during their usage, e.g. tire wear or fibers of synthetic cloth (type B). Secondary microplastics are microplastics that originate from the breakdown of larger plastics in the environment.

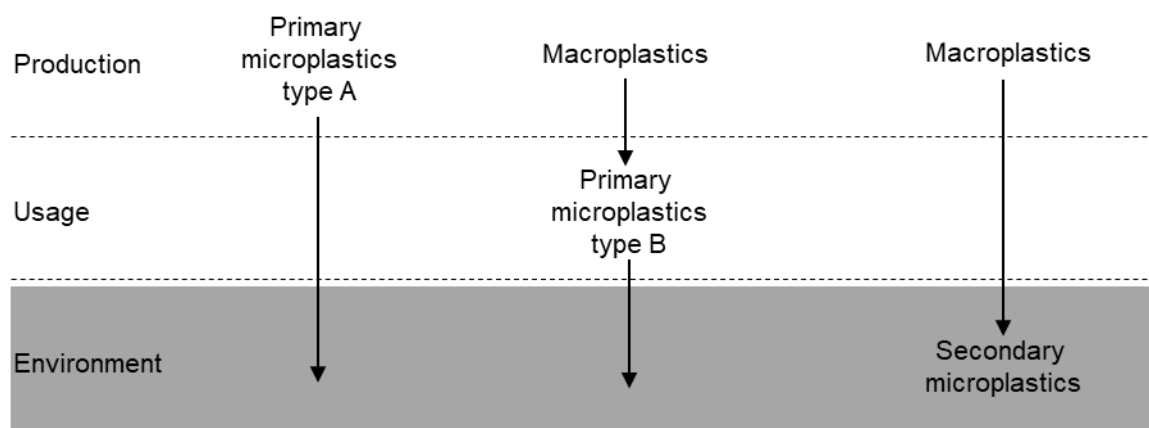


Figure 1-3: Definition of different types of microplastics by entry path into the environment [2].

1.1.3 Sources, transport and sinks

The yearly plastics production is increasing annually since the start of mass production in 1950 with a global production amount of 1.7 Mt reaching 369 Mt in 2020 (Figure 1-4) [1]. The most produced polymer types are polyethylene (PE) and polypropylene (PP) accounting together for 46.8% of the total plastics production. Including polyvinylchloride (PVC), polyurethane (PUR), polyester (PES), and polystyrene (PS) they account for 81.2 % of all produced plastics. Those belong to the polymer types most commonly found in environmental samples [10]. With 44.8 % almost half of the plastic is produced for packaging with an extremely short lifespan [11].

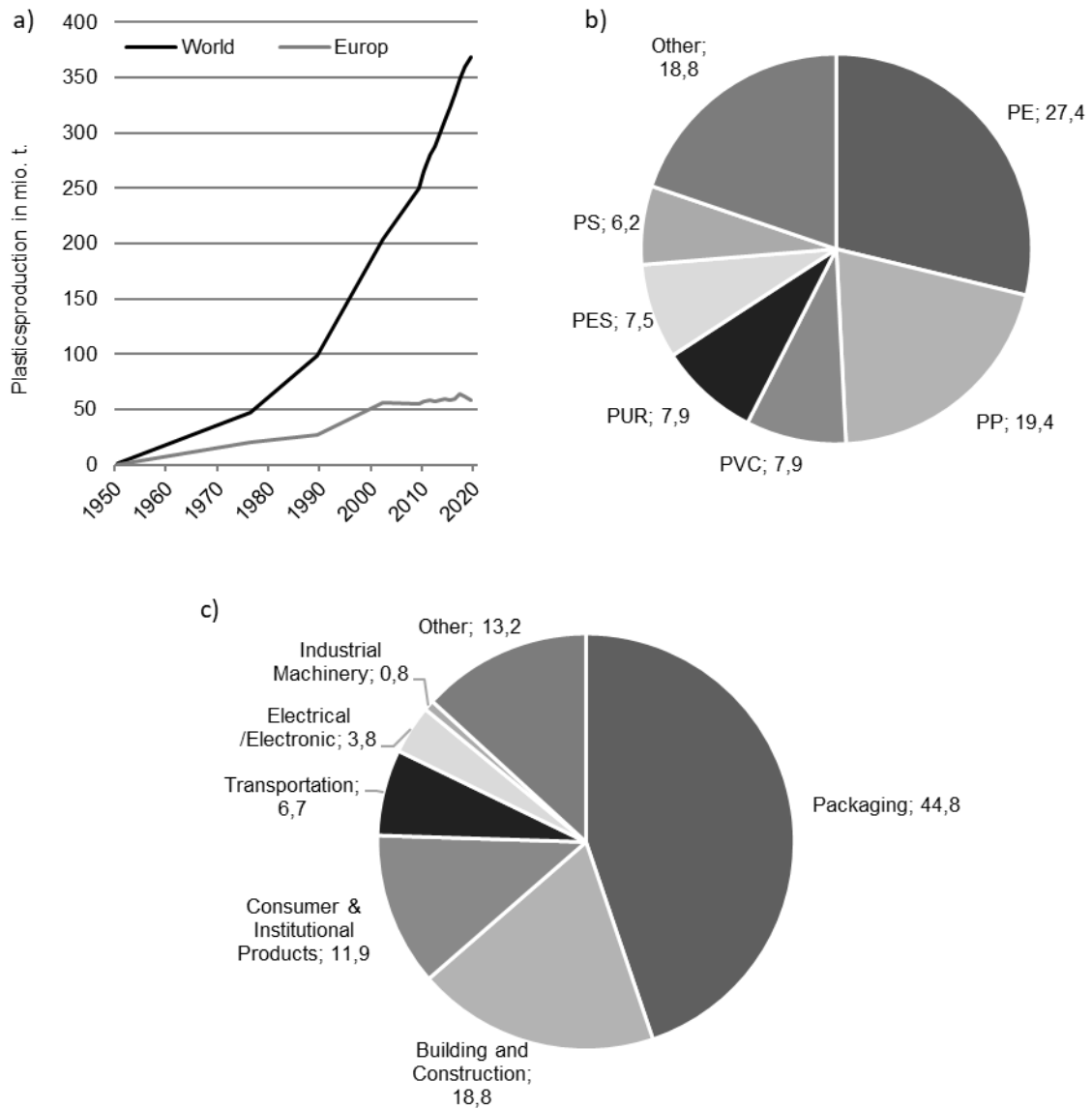


Figure 1-4: a) Annual plastics production worldwide and in Europe, b) polymer composition of produced plastics in 2020 in %, c) use sector of produced plastics in % [1].

Since plastic is broadly available and part of our daily use, it is inevitable that a proportion of the used plastic enters the environment over different pathways. One of the main sources of plastics in the environment is improper waste disposal. Here the driving factors are plastic waste generation, population density, and waste management [12–14]. Especially highly populated areas with poor waste management lead to high inputs of plastic waste into the environment. But also well-developed countries can have high inputs of plastic waste into the environment, also because they commonly export their plastic waste to countries with poor waste management [13]. It is estimated that 19 to 23 Mt, or 11%, of plastic waste generated globally entered the environments due to mismanagement. Because of the continuously increasing plastic production, the amount of plastic waste entering the environment is expected to increase as well [14]. Other sources of macroplastics into the environment are fishing waste

and the loss of shipping containers [15]. Due to different transport and degradation processes, the plastic waste distributes in the environment and fragments over time into smaller particles generating secondary microplastics.

Also, the direct input of primary microplastics into the environment is relevant. This can be shown in the example of Germany, a fully developed industrial country with well-working waste management (Figure 1-5). It is estimated that 1.4 kg/cap a or 26% of the total plastic emission into the environment are caused by mismanaged plastic waste [2]. 4 kg/cap a or 74 % are direct microplastics emissions. This sums up to a total emission of 330 000 t microplastics/a and 115 500 t macroplastics/a for the geographic region of Germany, which accounts for 3.1% of the national plastic usage.

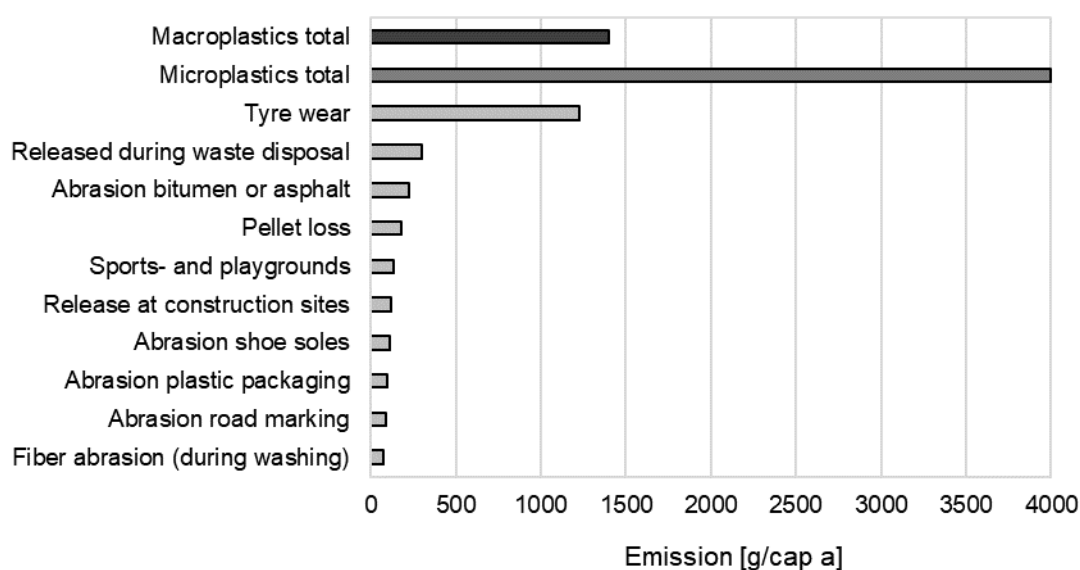


Figure 1-5: Estimated annual release of plastics and microplastics in Germany [2].

Considering transport processes and sinks in the environment, plastics can be released directly into waterbodies or transported by wind and surface runoff into lakes, rivers, or seas and oceans (Table 1-1) [16, 17]. Rivers are important transport pathways from inland into the seas [18]. Therefore it is assumed, that the majority of the plastics end up in the marine environment [16, 19]. There it is transported by wind and currents over long distances what leads to global, ubiquitous distribution. Due to the wind and currents, there are hotspots in the oceans where plastic accumulates and occurs in higher concentrations, the so-called great garbage patches [19, 20]. Nowadays plastic can be found everywhere in the marine environment, in the deep sea, remote unpopulated islands, the Antarctic sea, and also in the majority of living species from sponges over zooplankton to whales [21–26].

Focusing for a long time only on the aquatic environment, around 2016 researchers also started to focus on investigating macro- and microplastics in the terrestrial environment and the air [27, 28]. They could show that microplastics also remain in terrestrial environments and contaminate soils [27, 29]. Also, the

environments and plastic properties, complete degradation by assimilation and mineralization can take hundreds to thousands of years. For larger plastic particles abiotic degradation is the dominant degradation pathway, while small plastic fragments can also be effectively degraded biologically as they are better available to microbes [35]. Because the degradation and fragmentation are taking mainly place at the surface of the plastic, the volume/surface ratio is an important factor for the degradation rate [34].

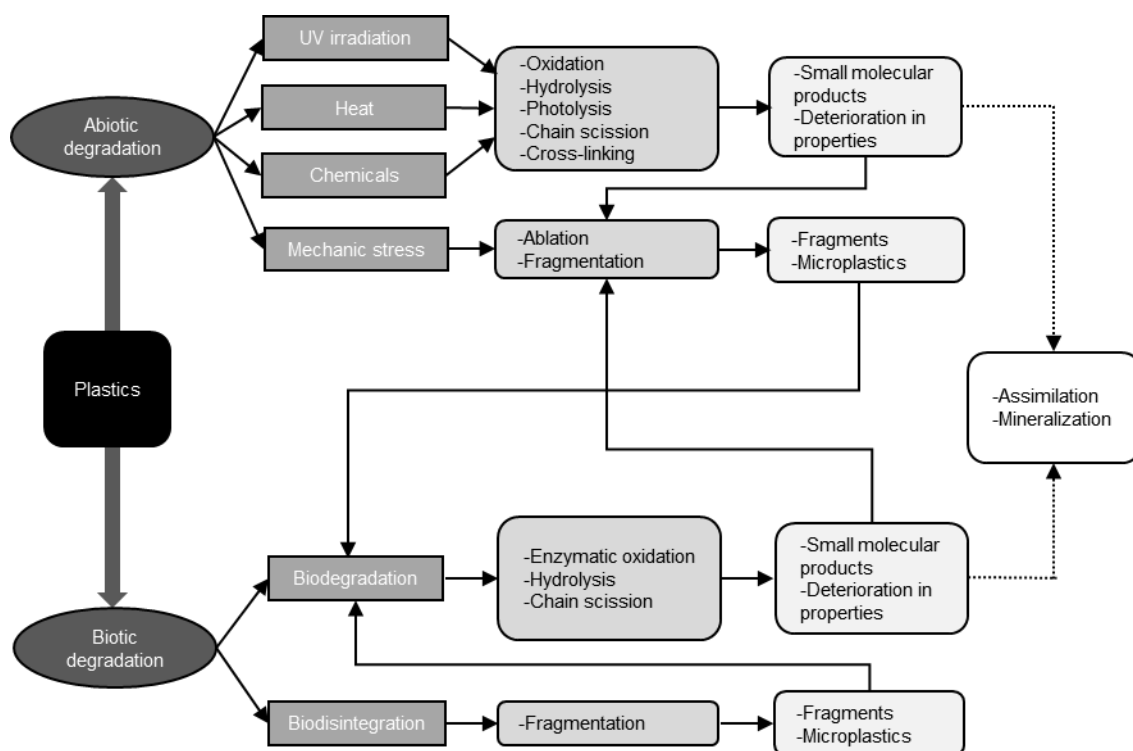


Figure 1-6: Scheme of principal degradation processes of plastics in the environment [33]. Fragmentation and microplastics formation are the dominant processes. Complete assimilation and mineralization take typically hundreds to thousands of years. Abiotic degradation rates exceed biotic degradation rates. Thus, abiotic degradation is predominant in most environments.

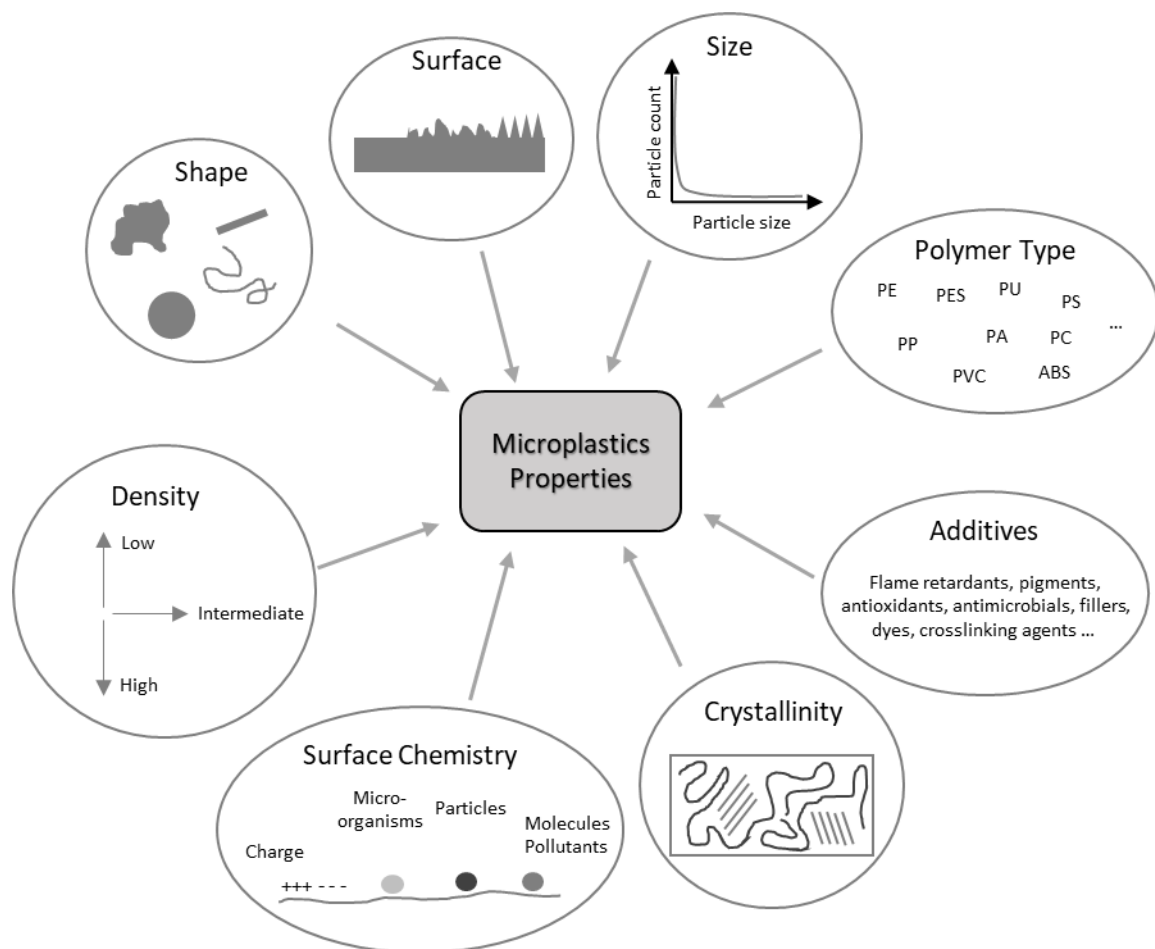
1.1.5 Harmful effects of microplastics in the environment

Its persistence in combination with the continuously increasing inputs of plastics and microplastics into the environment leads to an increased risk potential for ecosystems and organisms [6, 36]. Numerous studies revealed various negative effects of microplastics in the environment (Table 1-2) [37, 38]. It was also shown, that these effects can occur at environmentally relevant concentrations [36]. Due to the increasing concentrations, organisms, communities, and ecosystems will be more and more influenced.

As microplastics are extremely diverse mixtures of different monomers, additives, and adsorbed chemicals with different physical properties as size, density, shape, surface, which all influence their toxicity, the ecotoxicological assessment of microplastics is highly challenging and not yet sufficiently understood (Figure 1-7) [39]. Also, long-term effects are barely explored.

Table 1-2: Harmful effects of microplastics in the environment.

Location	Type of effect	Effekt	Source
Organism	Direct physical harm	Tissue damage	[40]
		Embedding in tissue	[40]
		Reduced food intake	[41]
		Disruption of cell functions	[42]
	Release of contained pollutants	Release of pollutants adsorbed in the environment	[43]
Environment	Microplastics as a transport vector	Release of harmful plastic ingredients	[44]
		Release of harmful plastic ingredients	[45]
		Transport of pollutants	[46]
	Change of environmental properties	Transport of microbial communities	[47]
		Change of soil properties	[48]

**Figure 1-7:** Physicochemical properties of microplastics influencing its toxicity [39, 49].

1.1.6 Human exposure and health risk

Microplastics have also been proven in various groceries and the air we breathe. A first study estimates the intake of 74000 and 211000 microplastics per person and year via food and inhalation, depending on the nutrition and environment they live in [49]. The knowledge about the effects of microplastics in the human body is still very limited. As various studies have already proved the harmful effects of microplastics on organisms in the environment, it is evident that microplastics are also harmful to humans. First studies could already prove harmful effects to humans on a cellular level and due to the leaching of additives into the body [50, 51]. Laboratory experiments have shown that microplastics smaller than 150 μm can get into the surrounding tissue, into the bloodstream, and being transported into internal organs and also into the brain after ingestion [52, 53]. There is a risk of lesions, inflammation, oxidative stress, necrosis, and damage to the DNA. Neurological behavior disorders are also possible [54]. Microplastics have also been detected in the human placenta [55].

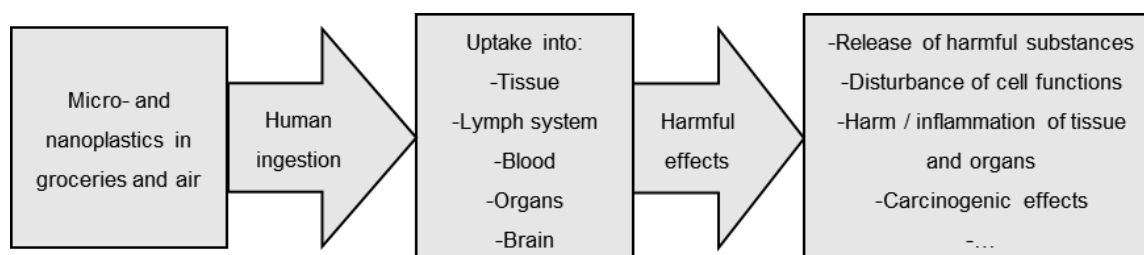


Figure 1-8: Schematic illustration of the risk potential of nano- and microplastics for humans [56].

Thus, it has been proven, that humans are exposed to microplastics, that they can be taken up into the body and can have harmful effects (Figure 1-8). As the knowledge about exposition and uptake as well as the toxic effects is still insufficient, the risk potential can not yet be evaluated [57, 58].

1.2 Microplastics removal from water

1.2.1 Areas of application

Once in the environment, it is extremely difficult and costly to collect macroplastics and almost impossible to remove microplastics. Filtering rivers, oceans, or lakes, removing microplastics from sediments and soils, is not only unrealistic but would also be a huge intervention into ecosystems. Therefore, it is very important to focus on the prevention of macro and microplastics inputs into the environment. Macroplastics inputs can be prevented efficiently by proper waste management. As seen before, in Germany 74 % of the plastic emission are estimated to be microplastics, which are more difficult to avoid [2]. Therefore, it is very important to remove them from point sources [59].

Those are mainly road draining systems, municipal and industrial wastewater treatment plants (Figure 1-9). Wastewater treatment plants can remove 95-99 % of the microplastics from the inflowing water. As the inflowing water is extremely high contaminated, the treated wastewater still accounts as highly contaminated. In combination with the high amounts of wastewater discharge, they are important point sources for microplastics into the environment. Additionally, relief structures and separated sewers can lead to a direct input of untreated wastewater or urban- respective road runoff. Possible soil retention filters in relief structures were found to be inefficient for microplastics removal [60].

Another area of interest for microplastics removal is microplastics sensitive water using processes [59]. Seawater desalination is a process gaining more and more importance in semi-arid coastal regions [61]. The most energy-efficient and therefore favored technique is membrane-based seawater desalination. Here microplastics pose the risk of blocking or fouling the membranes [62]. Facing the increasing microplastics concentrations in seawater, removal of microplastics from the inflowing seawater is of importance for a durable and economical sweater desalination

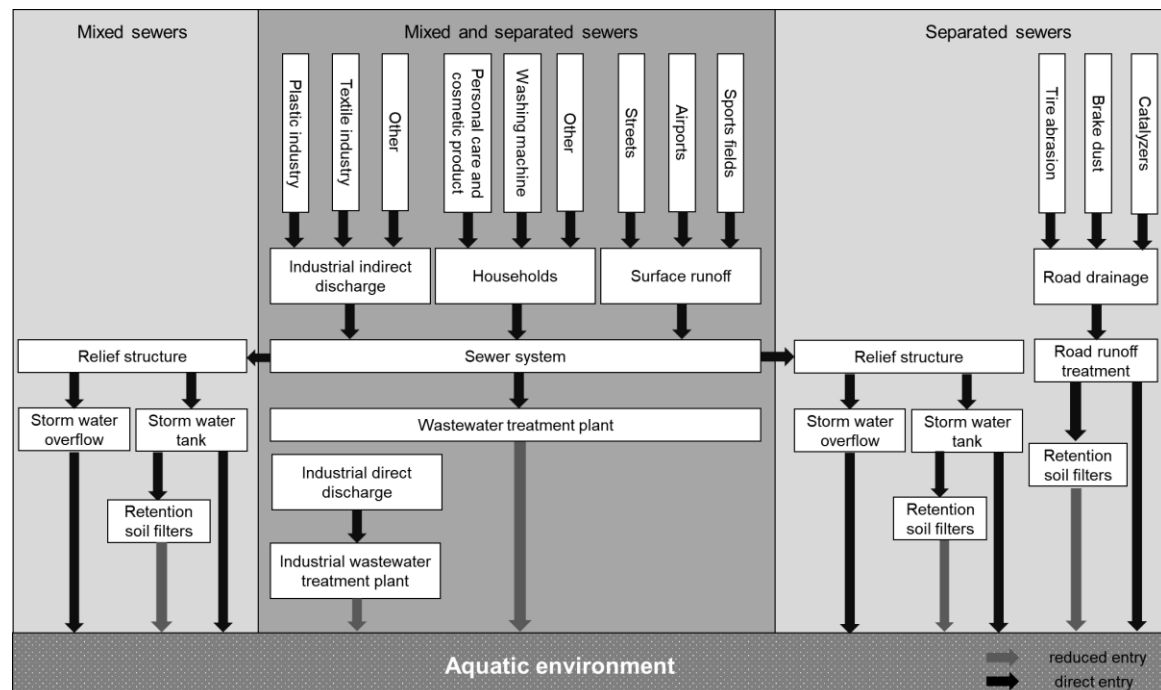


Figure 1-9: Point sources and pathways for microplastics in the environment [59, 63].

To avoid contamination of groceries and transfer them to the human body, it is important to remove microplastics from water used for near food chain processes, [59]. A well-investigated example is sea salt extraction [64]. Sea salt is extracted by filling seawater into basins and letting the water evaporate by sunlight and wind, while the salt remains as solid [65]. The microplastics dispersed in the seawater also remain in the sea salt and, if used for the food industry, are transferred to humans. To avoid this contamination it is important to remove the microplastics from the water flowing into the salt works. Other processes as aquaculture or drinking water treatment can also be of interest when contaminated with microplastics [59].

1.2.2 Removal methods

Due to the need for methods to remove microplastics from water, the test and development of various removal methods came to the focus of scientists and engineers. Existing methods for particle removal were evaluated and new methods were specifically developed to remove microplastics from water (Figure 1-10) [59, 66].

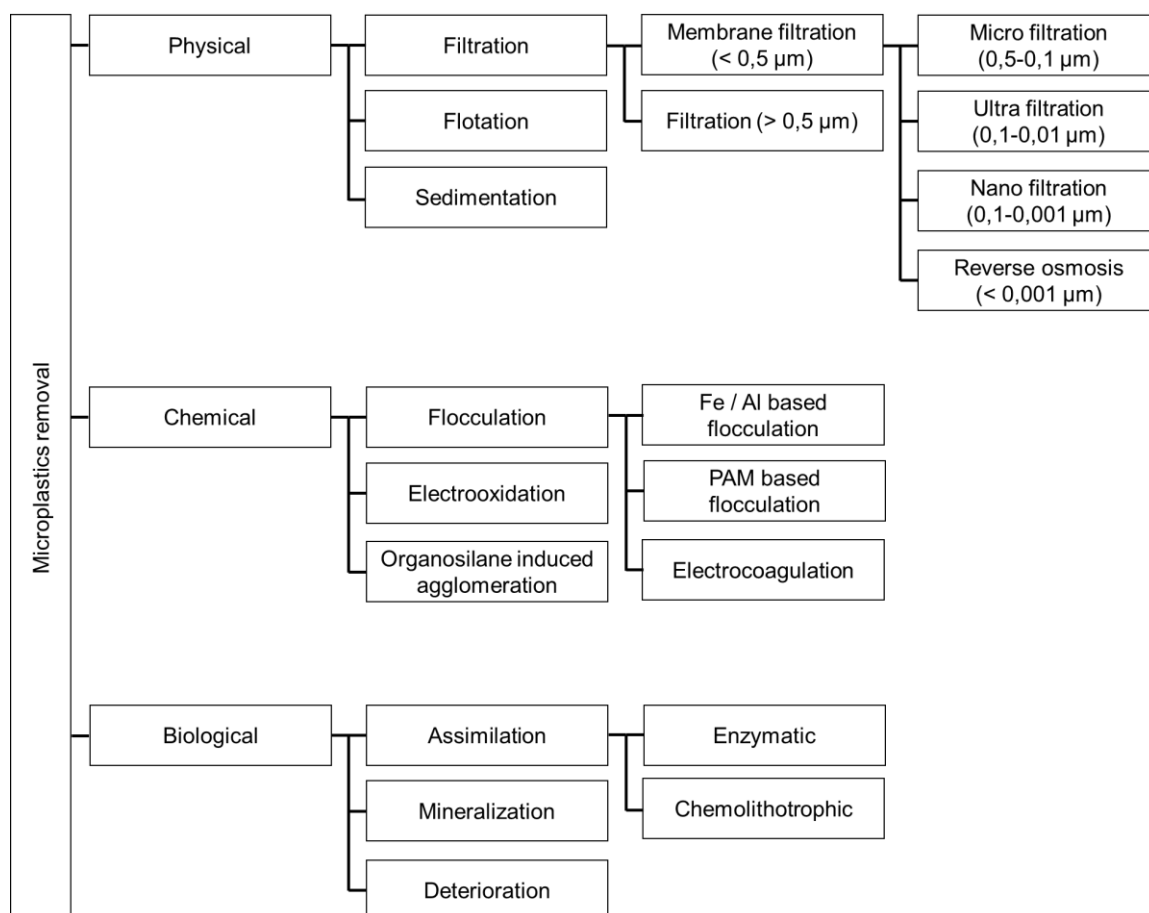


Figure 1-10: Overview of possible removal methods for microplastics from water [59].

Physical methods as flotation and sedimentation are not practical for microplastics, as the latter have a wide range of different densities, which is often close to the density of water. In addition to the small particle size, which leads to a high friction to buoyancy ratio, this results in too slow settling or ascending speeds [59]. Dissolved air flotation can be used to increase the efficiency and speed of the removal process, but has the disadvantage of high energy demand [67, 68]. Also, studies showed insufficient removal efficiencies of 32 – 38 %. Filtration is another very common process to remove microplastics from water. Filtration techniques as sand -, cloth-, disc- and drum filters are only efficient for larger microplastics and suffer from the risk of clogging and biofouling [59, 69–71]. For the removal of small microplastics, membrane filtration is needed, which is a technologically complex process with higher maintenance needs and energy consumption [59, 62, 72]. Additional scaling and fouling of the membranes are problems for membrane-based filtration processes.

To increase the particle size and make physical removal processes more effective, flocculation is applied. The chemical complexity behind the different polymer types summarized by the term microplastics makes finding suitable flocculants challenging, as flocculants need to interact with the surface of the microplastics particles [73, 74]. Aluminum and iron-based flocculants are limited in their adaptability. Polyelectrolyte-based flocculants have a broader variety, but due to their solubility the risk of being discharged into the environment and causing an ecotoxicological impact [75]. Another promising approach is electrocoagulation, which shows good results for certain polymer types as PE or PES [76, 77]. But this method also suffers from limited adaptability and has the disadvantage of additional energy consumption. Electrooxidation as an example of an oxidation process was also tested and found to be inefficient for very small microplastics (26 μm), which makes it even less suitable for larger microplastics [78].

The application of biological degradation of microplastics in a biotechnological process is often discussed in scientific literature, but due to slow degradation rates unsuitable for use on a technical scale [59, 79].

1.2.3 Microplastics removal using organosilanes

The previous chapter showed, up to date, there is no cheap, easy to apply, and sustainable method for effective removal of microplastics on a technical scale. Current methods have drawbacks as low efficiencies or high technical effort and energy demands. Therefore, various new methods were developed and tested for the removal of microplastics from waters [66]. A promising new approach is the microplastics removal by organosilanes, which is based on a physical agglomeration of microplastics followed by chemical fixation, due to a water-induced sol-gel process, which makes the agglomerates stable and easy to remove (Figure 1-11) [80].

Microplastics removal using organosilanes was first conceptualized in 2016 and first successfully tested in 2017 for the agglomeration of microplastics in drinking water spiked with PE and PP-based microplastics by Herbort et al. [80, 81]. The applied organosilanes consist of a silica atom as a core atom connected to an organic group and three reactive groups. The organic group induces the interaction with the surface of the microplastics by van-der-Waals forces. Therefore, when added to water containing microplastics, the organosilane attaches to the microplastic surface and collects it in agglomerates. Due to a water-induced Sol-Gel-Process, the three reactive groups start to form chemical bonds. In the first reaction step, silanols are formed by hydrolysis. The silanols are highly reactive in water and form siloxane bonds by subsequent condensation. Thus, a 3-Dimensional hybrid silica network is formed chemically fixing the agglomerated microplastics, which makes them easy to remove.

An advantage of this new and little researched approach is the high diversity and easy adaptability of the substance class of organosilanes. This gives it the potential to be adapted for application in different environments and to different polymer types.



Figure 1-11: Scheme showing removal of microplastics using organosilanes. 50 mg / l PE and PP (50:50) are removed from 2 m³ drinking water in a model experiment [82].

1.3 Microplastics detection in environmental samples

1.3.1 Microplastics detection and its challenges

To measure the microplastics contamination and evaluate risk potential and transport pathways, it is important to have proper monitoring methods. One of the main challenges of microplastics monitoring in the environment is the high amount of natural particles compared to microplastics particles. Natural particles exceed the number of microplastics in most samples by several orders of magnitude and can have very similar looks and carbon-based chemical structures, which are hard to differentiate from microplastic [8, 83, 84]. Another challenge is the high complexity of the different chemical and structural compositions of different plastic types summarized under microplastics, making the selection of reference material and calibration of the detection method very complex. The microplastics monitoring can be divided into three stages: Sampling, sample preparation, and detection (Figure 1-12).

Water samples are most commonly taken by pulling nets through the water. To prevent clogging, the most common net size is 0.33 mm. A more advanced method, which also enables to sample smaller particles, is pumping water through filters [8, 84]. Sediment samples can be taken by sediment grab samples or shovels [85]. Air samples are taken actively by pumping air through a filter or passive by deposition samples [86]. For biota samples, the animals have to be collected separately. Zooplankton samples are caught with plankton nets [8].

The sample preparation has the aim to reduce the number of natural particles in the sample but preserve the microplastics, to make the detection less prone to false positives [8]. Density separation, as well as

chemical or enzymatic digestion, can be applied. Depending on the methodology chosen, these steps can be very time-consuming.

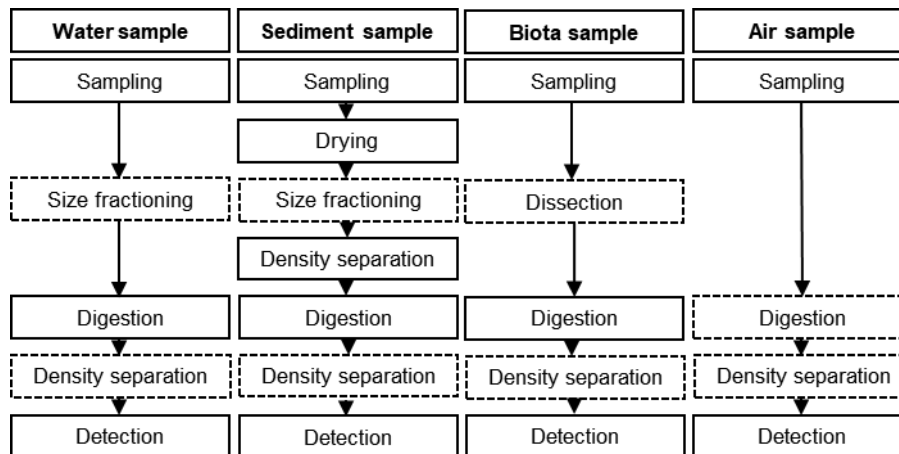


Figure 1-12: Scheme for the proceedings for monitoring microplastics in the environment [86, 87].

For density separation, highly concentrated salt solutions, most commonly NaCl (1.2 kg / l), ZnCl (1.6 kg / l), or NaI (1.8 kg / l), are applied to separate mineral compounds (typical densities around 2.7 kg / l) in sediment and water samples from plastics and natural organic particles. It can be applied in easy setups as separation funnels. For higher separation efficiencies, especially for sediment samples and the analytics of small microplastics, more complex methods are needed. One example is the “Munich Plastic Sediment Separator” applying air bubbles in a stainless steel column equipped with different valves and filters for a more efficient separation [88]. Because of the slow settling speeds of small sediment particles, the time needed for density separation is usually around 12-24 hours [8].

Chemical or enzymatic digestion is used to reduce the amount of natural organic particles in the sample [8]. For chemical digestion most commonly H₂O₂ is applied, as it turned out to be very efficient towards natural organic particles while preserving the microplastics. Less common alternatives are HCl, HNO₃, or KOH, which are more aggressive towards certain polymers [89]. KOH is highly efficient for the digestion of biota samples with high tissue content. Digestion times are commonly between 6 – 24 h. Enzymatic digestion is a very efficient alternative and does not harm any plastics. It is rarely applied because it is a very complex process and with up to 10 days of preparation and digestion time extremely time-consuming [90]. When containing high amounts of digested materials, additional density separation might be necessary after the digestion is completed.

After the sample preparation in the last step, the microplastics are quantified during the detection process. Still widely applied is an optical detection of microplastics using a microscope, due to cost efficiency and low availability of the analytical devices needed for more advanced microplastics detection [83]. Microplastics are identified by their shapes and unnatural colors, but the outcomes are

highly prone to error as microplastics can be easily mixed up with natural particles. Also, the classification of microplastics depends on the evaluation of the operator and therefore is not objective. For more reliable detection, various spectroscopic, thermoanalytical, and chemical methods are available. Table 1-3 summarizes the commonly used methods [8].

From these methods, mostly applied are Attenuated total reflectance Fourier-transform infrared spectroscopy (ATR-FTIR) with a μ -focal plane array (μ -FPA), μ -Raman spectroscopy (μ -Raman), and Pyrolysis–gas chromatography-mass spectrometry (Py-GC/MS). ATR-FTIR + μ -FPA and μ -Raman are examples of spectroscopic methods [8, 83, 91]. Here the samples are prepared on special filters without interfering signals and scanned automatically by the device on a pre-defined grid. Subsequently, a spatial data set is created where every pixel contains a measured spectrum, which needs to be compared to a reference database and assigned to polymer types or non-microplastic substances. Thus, a 2-dimensional image is created and the polymer type, size, and shape can be determined very reliably. The detection limit for ATR-FTIR + μ -FPA is at 10 μ , for μ -Raman at 1 μ m particle size. Disadvantages of this method are high measurement times, which depending on the resolution and measured area are several hours up to days, the sensitive and expensive measurement devices, and the necessity of well-trained staff for the operation and evaluation.

Py-GC/MS is the most commonly used thermoanalytical method [8, 83, 84]. Here, the sample is pyrolyzed under high temperatures, whereby characteristic fragments are formed. These molecular fragments are separated by gas chromatography and detected by mass spectrometry. Thus, mass and respective polymer types contained in the sample can be detected. The advantages of this method are shorter measurement times compared to ATR-FTIR + μ -FPA or μ Raman, automated sample injection, and less extensive sample preparation, as this method is less sensitive to contained natural particles. But also this method needs well-trained staff and a measurement device which is expensive in acquisition and maintenance costs.

Another important point in microplastics monitoring is the avoidance of contamination [8, 83, 84]. For example, a study showed that opening and closing a plastic bottle one time releases an average of 131 microplastics particles [92]. Also, indoor air is usually highly contaminated with microplastics from synthetic textiles, which also deposit on surfaces and samples [93]. Therefore it is important to avoid using plastic equipment, to clean the laboratory regularly, use lint-free clothing, and always measure blank samples for quality assurance.

Table 1-3: Comparison of common detection methods for microplastics in environmental samples. (Attenuated total reflectance = ATR, Fourier-transform infrared spectroscopy = FTIR, Focal Plane Array = FPA, Near-infrared spectroscopy = NIR, Pyrolysis-gas chromatography-mass spectrometry = Py-GC/MS, Thermal extraction and -desorption combined with gas chromatography-mass spectrometry = TED GC/MS, Differential scanning calorimetry = DSC, Inductively coupled plasma mass spectrometry = ICP-MS) [8].

	Spectroscopic				Thermoanalytical				Chemical	
	μ -Raman	ATR-FTIR + μ -FPA	μ -ATR-FTIR	ATR-FTIR	NIR	NIR	Py-GC/MS	TED GC/MS	DSC	ICP-MS
Sample form	Prepared sample on filter	Prepared sample on filter	Prepared sample on filter	Single-particle	Sample	Prepared sample on filter	Prepared sample	Sample	Prepared sample	Sample
Analyzable mass or particles	$10^3 - 10^5$ Particles	$10^3 - 10^5$ Particles	-	-	-	$10^3 - 10^5$ Particles	μ g	mg	mg	μ g
Measurement time	d - h	d - h	min	min	min	h - min	h	h	h	min
Detection limit	1 - 5 μ m	10 μ m	25 - 50 μ m	500 μ m	~ 1 % of mass	50 μ m,	0,01 - 1 μ g	0,5 - 2,4 μ g	50 μ g	
Polymer type detection	Yes	Yes	Yes	Yes	Yes	Yes	Yes	Yes	Only semi crystalline	Only for tire wear
Additives	Yes	No	No	No	No	No	Yes	No	No	No
Aging	Surface oxidation	Surface oxidation	Surface oxidation	Surface oxidation	No	No	Oxidation	No	No	No
Particle count, size, and form	Yes	Yes	Yes	-	No	Yes	No	No	No	No
Plastic content	No	No	No	-	No	No	Yes	Yes	Yes	Yes

1.3.2 Fluorescence staining for microplastics detection using Nile red

The disadvantage of the commonly used methods for microplastics detection is the high cost of the devices, the complex measurement procedures, and the long measurement times. Therefore, there is a need for fast and cheap detection methods. A new cost-effective and promising method for microplastics detection is fluorescent staining using Nile red.

Nile red is a lipophilic fluorescent dye, which is commonly used for the in-situ staining of lipids [94]. Looking for a cheap and easy to apply method for microplastics detection, researchers found Nile red as effective for staining microplastics in environmental samples [95–97]. The idea behind the process is, microplastics show good fluorescence signals and glow brightly when stained with Nile red and investigated under a fluorescent microscope, while natural particles show weak fluorescence and do not glow. But as the method also has several disadvantages, it is a highly discussed method (Table 1-4). One of the biggest critics is the risk of false positives caused by natural polymers which can also have strong fluorescence when stained with Nile red. Another problem are certain polymer types, like PVC, showing weak fluorescence signals or interference of color pigments in microplastics leading to quenching. But as it only needs a fluorescent imaging tool or –microscope and is easy to apply, this method became favored by many scientists and research institutes, especially for low-budget projects.

Table 1-4: Advantages and disadvantages of fluorescence staining for microplastics detection

Advantage	Disadvantage
-Easy applicable, no strong background knowledge necessary	-Risk of false positives from natural polymers
- Cheap, no expensive materials or equipment needed	-Underestimation of polymers with weak fluorescence (e.g. PVC)
-Only requirement fluorescence imaging tools, which are widely available.	- Interference with color pigments
	- No standardized procedure yet (e.g. solvents, times for staining, protocol for evaluation)

Thus, it is already applied in many studies measuring microplastics in the environment or and groceries [98]. Various studies were performed validating and improving the detection process. For example, scripts for automated image processing and microplastics detection for fluorescence images of stained samples have been developed [99]. Also staining or co-staining with other dyes has been evaluated [100]. Nile red has been successfully used to preselect the microplastics for identification by μ Raman, reducing the measurement time and improving the throughput [101]. Additionally, it has been shown, that more advanced fluorescence microscopes, which can perform phasor-analysis, can also determine the polymer type [102]. These examples show the high potential of this method.

1.4 Objectives of the doctoral thesis

Up to date, there is still no cheap, easy to apply, and sustainable method for the removal of microplastics from water. The application of organosilanes for removing microplastics from the aquatic environment has the potential to fulfill these criteria. The broad variety of commercially available organosilanes and their easy adaptability give it a high potential for a successful adaptation to various scenarios. First performed in 2017, it is a relatively new and little researched process. Therefore, the overall objective of this thesis is the further investigation for a better understanding and improvement of the application of this new process.

Firstly, the effect of the organic groups of organosilanes on the removal of microplastics from water should be investigated, to determine which organosilanes are best suitable. For this purpose, methods for the quantification of the removal efficiency, for the investigation of the reaction behavior of organosilanes, and of for the characterization of the formed agglomerates need to be developed.

To ensure that the process can be applied in different aquatic environments, in the second part of the thesis the removal process in different water compositions and at different temperatures needs to be evaluated. In the first step, the focus should be the application in seawater and municipal wastewater treatment. For a risk-free application, the organosilane residues in the water after the removal process need to be measured. Therefore, a quantification method for dissolved organosilanes needs to be developed.

Microplastics can consist of countless different polymer types with different properties and surface chemistries. As for this removal process, the interaction of the organosilanes with the microplastics surface is essential, it has to be tested how different polymer types affect the process and if organosilanes can be adapted to certain polymers.

Additionally, microplastics in the environment are typically covered by biofilms, which as well change their surface properties. To test this effect, a method for biofilm cultivation on microplastics needs to be developed and techniques for evaluation of biofilm growth need to be applied in the third part. Subsequently, the effect of the biofilm coverage on the removal behavior has to be investigated

To evaluate and control the removal process on a technical scale, a monitoring method for microplastics in environmental samples is necessary. Common methods for microplastics detection are highly complex, time-consuming, and need expensive measurement devices. Microplastics detection using Nile red staining and fluorescence microscopy has a big potential for cheap and fast identification of microplastics. Therefore, it should be evaluated and improved by testing various staining procedures and newly developed, chemically modified Nile red derivatives in the fourth part of the thesis.

2 Comparative study of the influence of linear and branched alkyltrichlorosilanes on the removal efficiency of polyethylene and polypropylene based microplastic particles from water

Published as: Sturm MT, Herbort AF, Horn H, Schuhen K. Environmental Science and Pollution Research. 2020;27:10888–98. doi:10.1007/s11356-020-07712-9.

2.1 Introduction

2.1.1 Microplastics in the aquatic environment

Microplastics are currently one of the biggest and most discussed environmental problems. Since the start of mass production of plastic in the 1950s, it has become an integral part of everyday life [6, 11]. By definition, the collective term "plastic" refers to synthetically produced organic chemical polymer compounds of anthropogenic origin. Large quantities of plastic, including plastic waste, are released into the environment because of improper disposal and lack of waste management systems. A particular problem here is the persistence of plastics against environmental influences (Figure 2-1).

Microplastics in the environment	
<i>Properties</i>	<ul style="list-style-type: none"> - Density depended behavior (drifting on the water surface, floating, sinking to the ground) - Chemically inert and hydrophobic - Durable
<i>Degradation</i>	<ul style="list-style-type: none"> - No direct degradation - Fragmentation - Leaching of additives - Surface changes
<i>Transport</i>	<ul style="list-style-type: none"> - Transport through wind, waves and currents - Distribution in water, soil and air - Transport through food chain
<i>Effects</i>	<ul style="list-style-type: none"> -Harmful to organisms -Influence on ecosystems -Leaching of additives and monomers -Transport of organic pollutants

Figure 2-1: Summary of properties, degradation, transport and effects of microplastics in the environment [103].

This results in poor degradability, which means that the plastic remains in the environment for a very long time, fragments over time and forms ever smaller plastic particles (particles < 5 mm are referred to

as microplastics) [6, 104]. Microplastics can also be introduced directly into the environment, e.g. as an ingredient of cosmetics, as textile fibers or tire abrasion [105, 106]. Through transport processes, the plastics or microplastics are distributed in the environment and have already been detected in all parts of the environment. Thus, ecosystems and organisms are exposed to microplastics, which they have a negative effect on [19, 27, 38]. Due to the continuously increasing inputs and constant fragmentation, there is an ever-increasing burden of microplastics on the environment [6].

Due to the heterogeneous distribution of microplastics in the environment and the non-standardized sampling and detection methods, the information on the concentrations of microplastics in the environment shows high variations among different studies. For example, studies in the Mediterranean Sea found values ranging from 0.17 ± 0.32 to 3.13 ± 4.95 microplastic particles / m³ [107].

Different studies showed that industrial and municipal wastewater treatment plants are important point sources for the discharge of microplastics into to the environment [108, 109]. At the sampling of the effluent of 12 municipal wastewater treatment plants in Germany concentrations between 0.26-13.7 microplastic particles / liter (MP / l) were found, while a study in Denmark found 29-447 microplastic particles / l [110, 111].

In order to reduce the input into the environment, it is necessary to remove microplastics from the water of point dischargers, such as municipal and industrial wastewater treatment plants [68]. Due to the fact that microplastics can also be a disruptive factor (fouling, contamination and resulting health risk) in water use processes (e.g. water treatment or sea salt extraction), the particles need to be removed previously (Ma et al. 2019, Amy et al. 2017, Peixoto et al. 2019, Barboza et al. 2018, Iñiguez et al. 2017). Commonly used flocculants turned out to be ineffective and/or cost-intensive for the total sum of microplastic particles, which calls for novel methods for microplastics coagulation [74].

2.1.2 How does the novel agglomeration-fixation reaction (AFR) work?

Inorganic-organic hybrid silica gels are compounds of an inorganic silicon-oxygen compound with one, two or three organic functionalities [112, 113]. In the sol-gel process, an inorganic-organic macromolecule in the form of a highly cross-linked solid is formed by successive hydrolysis and condensation of the precursors (Figure 2-2).

In the first reaction step, leaving groups are hydrolyzed to highly reactive silanol groups, which connect the precursors in the second reaction step to each other by forming siloxane bonds. This leads to the growth of a 3-dimensional network, a so-called hybrid silica. By adjusting the sol-gel conditions such as the proportion of water, the solvent, the temperature, the pH value, the addition of catalysts and the precursor/solvent ratio, the reaction can be controlled in terms of reaction speed and product formation, among other things [113, 114].

The choice of the leaving group (e.g. -Cl, -OR, -OH) is decisive for the consideration of hydrolysis and condensation kinetics [115–118]. Depending on the choice of the leaving group and the influence of the organic part, the reactivity of the precursors and thus the structure of the hybrid silica gel and its inclusion

behavior towards particles, e.g. microplastics, can be influenced [80, 81, 119]. The reason for this behavior lies in steric effects, inductive effects, resonance effects and their polarizability [119, 120]. The organic unit can additionally induce a self-organization process. The pre-organizing function is generated by van der Waals interactions, hydrogen bonds and / or dipole-dipole interactions [121, 122].

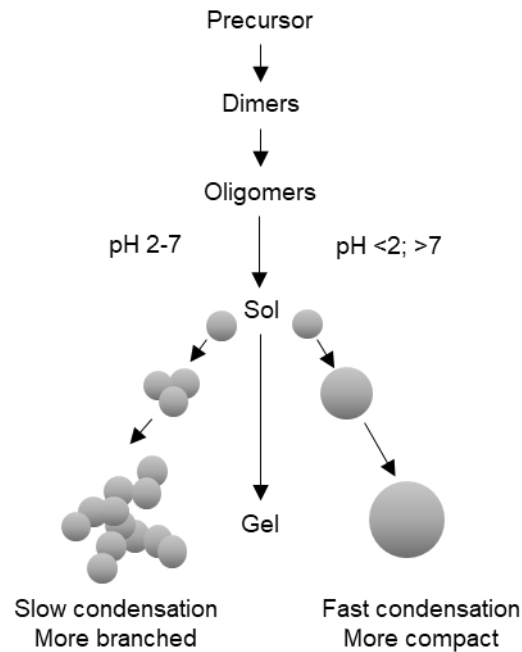


Figure 2-2: Schematic representation of the reaction course of the sol-gel process [123].

2.1.3 Silicon-based precursors for microplastic reduction (Wasser 3.0 PE-X)

A conceptual approach of Herbort and Schuhen from 2016 describes the use of silicon-based precursors for microplastic elimination and was adapted for the technical application in 2018 [80, 81, 124]. The concept consists of two process steps, taking place during the sol-gel process of the silicon-based precursors in water: particle localization and immediate fixation. When added to water the organosilanes attach to the surface of the microplastic particles due to the affinity of their organic groups to the surface of the microplastics by van-der-Waals interactions (self-organization). Subsequently, the water induced sol-gel process described in the previous section leads to the linkage of the silicon-based precursors to each other. Thus, colliding microplastic particles attach to each other and collect in large agglomerates (localization), which are chemically bound by the on-going sol-gel process (fixation). This results in the formation of large agglomerates (>1cm) which can be removed using a simple and, therefore, more cost-effective filtration process (Herbort et al. 2018b). Initially, the precursors were alkoxy-silyl-functionalized derivatives with a large organic-chemical residue containing different heteroatoms (e.g. O, N) (Figure A1-1). In the course of adapting the concept of agglomeration fixation to polymer mixtures, the use of different alkyltrichlorosilanes provides the best results (Scheme 2-1).

Table 2-1 Overview of chemicals used

Name	CAS.no.	Number of carbons
Methyltrichlorosilane	75-79-6	C1
n-Propyltrichlorosilane	141-57-1	C3
Isopropyltrichlorosilane	4170-46-1	C3
n-Butyltrichlorosilane	7521-80-4	C4
Isobutyltrichlorosilane	18169-57-8	C4
t-Butyltrichlorosilane	18171-74-9	C4
Pentyltrichlorosilane (isomers)	107-72-2	C5
n-Hexyltrichlorosilane	928-65-4	C6
Thexyltrichlorosilane	18151-53-6	C6
(3,3-Dimethylbutyl)trichlorosilane	105732-02-3	C6
n-Octyltrichlorosilane	5283-66-9	C8
n-Decyltrichlorosilane	13829-21-5	C10
n-Undecyltrichlorosilane	18052-07-8	C11
n-Dodecyltrichlorosilane	4484-72-4	C12
n-Hexadecyltrichlorosilane	5894-60-0	C16
n-Octadecyltrichlorosilane (5-10% isomers)	112-04-9	C18

2.2.2 Overview of analytical methods and processes

The microplastic-free hybrid silica gel samples used for the analysis were produced analogously to the experimental setup for determining the quantitative determination of polymer removal (2.3) without the addition of polymers.

IR spectra ($4500 - 600 \text{ cm}^{-1}$, resolution 1 cm^{-1}) of the aggregates and hybrid silica gels were recorded with the ATR-FTIR spectrometer Vertex 70, Bruker, Ettlingen, Germany. The aggregates and gels had previously been dried for 24 h at $105 \text{ }^{\circ}\text{C}$.

FK-NMR spectra were recorded with the device Avance 400 WB, Bruker, Ettlingen, Germany. For the ^{29}Si SP MAS measurement, a 4 mm MAS-NMR sample head with 4 mm zirconium dioxide rotors and a rotation frequency of 3 kHz was used. The spectra were obtained at 79.5 MHz and $\pi/2$ pulse (5 ms) and recycle delay of 30 s. Hexamethyldisiloxane was used as the standard. The aggregates and hybrid silica gels had previously been dried for 24 h at $105 \text{ }^{\circ}\text{C}$. The silica was then removed from the silica and dried at 105°C for a further 24 h. The peaks are divided into T-peaks according to the number of siloxane bonds [119, 120].

Images of the formed aggregates (in wet state) were taken by optical coherence tomography (OCT) (GANYMEDE I, Thorlabs GmbH, Lübeck, Germany). An area of 6.5x7x1 mm was scanned with a resolution of 10 μm on the x- and y-axis and 2.08 μm on the z-axis.

Thermogravimetry (TGA) was measured with a Q5000 IR from TA Instruments. Starting temperature at 45 $^{\circ}\text{C}$, purge gas 1: nitrogen 5.0; 25ml/min with a heating rate of 20 $^{\circ}\text{C}/\text{min}$. The gas switching temperature was at 800 $^{\circ}\text{C}$, purge gas 2: oxygen 5.0; 0.25 ml/min with a heating rate of 20 $^{\circ}\text{C}/\text{min}$ and final temperature of 950 $^{\circ}\text{C}$. A platinum crucible was used.

2.2.3 Evaluation of polymer removal efficiency from water

To determine the removal efficiency of the polymers, 1 l of distilled water was placed in a 2 l beaker (high form), mixed with 100 mg polymer (PE, PP) and stirred for 5 min at RT. Then 300 μl of the respective alkyltrichlorosilane were added. After 20 min, the entire contents were filtered through an analysis sieve (stainless steel, mesh size 1 mm, diameter 20 cm) to remove the aggregates >1 mm. All aggregates larger than 1 mm remain in the sieve and are classified as removed polymer agglomerates, as first pilot plant tests showed that particles >1 mm can be removed easily with low technical effort. The filtrate was discharged into a filter crucible (porosity 4, max. pore size 16 μm). Beaker and sieve were thoroughly rinsed with distilled water. The filter crucible was rinsed with isopropanol to dissolve possible organosilicon-based adhesions, and dried for 24 h at 105 $^{\circ}\text{C}$ and weighed. By subtracting the tare weight, the mass of the polymer in the crucible, which is considered as free polymer, can be determined. Figure 2-3 illustrates the test procedure. The experiments were repeated three times. In addition, for economic and ecological reasons, the tests for the alkyltrichlorosilanes with the best removal efficiencies ($>95\%$) were carried out with a reduced application quantity of 100 μl to distinguish which alkyltrichlorosilanes has the best performance at a lower concentration.

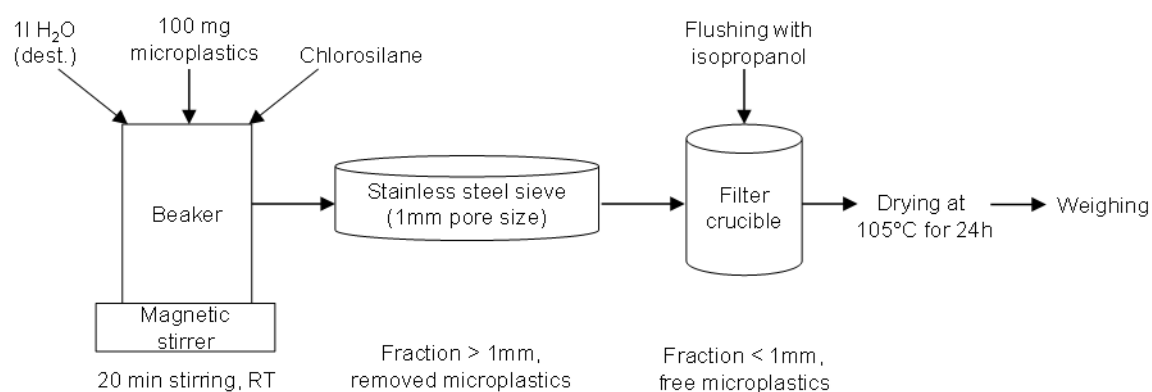


Figure 2-3: Schematic representation of the test sequence for determining the removal efficiency of polymers (PE, PP)

2.2.4 Determination of hydrolysis rates

To determine the hydrolysis rates, 1 l of distilled water was placed in a 2 l beaker (high form), 300 μ l of the respective organosilane added and stirred for 20 min at RT. The conductivity is measured at defined intervals with a WTW Cond 3110, Xylem Analytics Germany Sales GmbH & Co. KG, WTW, Weilheim, Germany. The change in conductivity is due to the HCl formed during the hydrolysis of the chlorosilane groups (Si-Cl). Based on the change in conductivity, a 1st order reaction kinetics can be adapted for hydrolysis and the reaction constant (k) determined (Eq 2-1 – 2-2). The half-life ($t_{1/2}$) was determined according to Eq. 2-2. The experiments were performed simply for all precursors, in addition isobutyltrichlorosilanes and n-octadecyltrichlorosilanes were analyzed three times in order to be able to give an error estimate.

$$c(\text{Si-Cl}) = c_0(\text{Si-Cl}) * e^{(-k*t)} \quad (2-1)$$

$$t_{1/2} = \frac{\ln(2)}{k} \quad (2-2)$$

2.3 Results and discussion

2.3.1 Determination of removal efficiencies

After addition to the water, the hydrophobicity of the alkyl group causes the alkyltrichlorosilanes to adhere to the polymer particles suspended in the water and bond them to agglomerates via self-organization processes (localization). The agglomerates formed are then chemically bound in a water-induced sol-gel process to form an inclusion compound of hybrid silica gels and polymers (fixation).

The starting point of the reaction is the hydrolysis of the chlorosilanes and the formation of silanols with the release of HCl (Scheme 2-1) [80, 125]. The formation of silanols also increases water solubility and supports the agglomeration (localization) of polymer particles [126]. Silanols have a high reactivity and crosslink through condensation, which is additionally catalyzed by the previously formed HCl, to three-dimensional hybrid silica gels, which fix the localized polymer particles.

For optimal removal, the gel formation must take place in a time window that enables a large quantity of polymer particles to be localized in the agglomerates and fixed in the course of gel formation. If the gel formation takes place too quickly, there is not enough time for the localization of the particles. If the gel formation is too slow, the particles cannot be fixed. Both lead to poor removal efficiencies and poor reproducibility. Table 2-2 and Figure A1-2 - A1-3 summarize the measured removal efficiencies.

Table 2-2: Removal efficiency for PE and PP and their standard deviations (S.D.) from water with 300 µl / l alkyltrichlorosilane.

Name	Formula	Branched	PE [%]	S.D. [%]	PE	PP [%]	S.D. [%]	PP
Blank	-	-	0.68	0.46		0.58	0.39	
Methyltrichlorosilane	(C ₁ H ₃)SiCl ₃	-	20.6	15.0		7.7	7.6	
n-Propyltrichlorosilane	(C ₃ H ₇)SiCl ₃	-	95.2	3.2		99.0	0.2	
n-Butyltrichlorosilane	(C ₄ H ₉)SiCl ₃	-	99.1	0.3		98.0	1.1	
Pentyltrichlorosilane (Isomere)	(C ₅ H ₁₁)SiCl ₃	(+)	98.0	1.1		96.6	0.1	
n-Hexyltrichlorosilane	(C ₆ H ₁₃)SiCl ₃	-	64.0	13.7		78.3	19.5	
n-Octyltrichlorosilane	(C ₈ H ₁₇)SiCl ₃	-	29.2	1.8		49.5	9.5	
n-Decyltrichlorosilane	(C ₁₀ H ₂₁)SiCl ₃	-	68.5	7.8		63.7	12.5	
n-Undecyltrichlorosilane	(C ₁₁ H ₂₃)SiCl ₃	-	39.6	16.4				
n-Dodecyltrichlorosilane	(C ₁₂ H ₂₅)SiCl ₃	-	73.2	4.5				
n-Hexadecyltrichlorosilane	(C ₁₆ H ₃₃)SiCl ₃	-	75.0	7.8				
n-Octadecyltrichlorosilane (5-10% Isomere)	(C ₁₈ H ₃₇)SiCl ₃	(-)	58.0	17.5				
Isobutyltrichlorosilane	(C ₄ H ₉)SiCl ₃	+	98.7	0.04		98.9	0.5	
t-Butyltrichlorosilane	(C ₄ H ₉)SiCl ₃	+	13.3	5.0		7.0	6.1	
Thexyltrichlorosilane	(C ₆ H ₁₃)SiCl ₃	+	96.3	0.5		94.1	0.8	
(3,3-Dimethylbutyl)trichlorosilane	(C ₆ H ₁₃)SiCl ₃	(+)	84.1	6.7		84.8	8.2	

Besides the removal efficiencies, also the standard deviation is a good indicator to evaluate the fixation process. The standard deviations are caused by uncontrollable factors of the experiment as attachment of plastic particles to the glass wall and turbulent flow conditions. The turbulent flow conditions cause a random movement and collision of the microplastic particles and agglomerates. Additionally, already formed aggregates are repeatedly drawn into the agitator and broken up. Alkyltrichlorosilanes with suitable reaction kinetics can compensate for these random factors, as they leave enough time for the agglomerates to collect all particles and reunite when broken up. For this reason, alkyltrichlorosilanes with high removal efficiencies show lower standard deviations as the ones with low removal efficiencies. As PE and PP are both completely nonpolar and with a similar density, the differences between both polymers are caused by uncontrollable factors of the experiment.

An optimal reaction process and the best results for polymer elimination (PE, PP) can be observed with n-propyltrichlorosilane, n-butyltrichlorosilane, isobutyltrichlorosilane and pentyltrichlorosilane (isomers). Here, consistently good removal efficiencies are achieved with mean values of more than 95% and with low fluctuations with regard to the reproducibility of the values.

For methyltrichlorosilane, n-octyltrichlorosilane and n-decyltrichlorosilane, n-undecyltrichlorosilane, n-dodecyltrichlorosilane, n-hexadecyltrichlorosilane, n-octadecyltrichlorosilane (experiments at higher concentration (300 $\mu\text{l/l}$)), a rapid gel formation can be observed within 5 to 20 seconds after addition to water. The fast gel formation and fixation does not leave enough time for the microplastics to be localized in the agglomerates. The gel is in the form of white flocks, which float finely distributed in the water and do not interact with microplastic particles after the gelation. This causes an entry of those hybrid silica gel particles smaller than 1 mm into the filter crucible, which cannot be completely removed by rinsing with isopropanol and additionally increases the standard deviations. This leads to poor removal efficiencies, high standard deviations and poor reproducibility. Due to the shortest alkyl residue and the associated lower affinity to the polymer particles used, methyltrichlorosilane shows the lowest removal efficiencies of all alkyltrichlorosilanes in this series with $20.6 \pm 14.9\%$ for PE and $7.7 \pm 7.6\%$ for PP.

Isopropyltrichlorosilane and isobutyltrichlorosilane show worse removal efficiencies as the alkyltrichlorosilanes with respective linear alkylgroups. The stabilizing effects of the branching cause a slower condensation as they stabilize the formed silanols via steric and inductive effects and slow down the condensation process [126]. This leads to incomplete fixation and the formation of soft and unstable aggregates. This can also be observed with n-hexyltrichlorosilane, where the hexylgroups has a stabilizing effect on the silanols.

The effect of too slow fixation is evens stronger with thexyltrichlorosilane and t-butyltrichlorosilane, as they have a stronger branching and the dimethyl group is directly after the silicon atom inhibits the condensation process by steric protection (Hurkes et al. 2014). t-Butyltrichlorosilane dissolves in the water after 1 minute, as it forms a water stable silanol. The formed agglomerates are not stable and disintegrate continuously. Thexyltrichlorosilane remains liquid during the entire reaction and, due to the

strong Si-Si interactions, is deposited on the glass wall, where it collects the polymer particles due to the hydrophobicity of the hexyl group. Thus, it is not detected as a free polymer.

An exception was 3,3-dimethylbutylchlorosilane. Due to its well suitable reaction kinetics, a reasonable agglomeration fixation of PE or PP could be observed. However, due to the high density of the hybrid silica gel formed, the aggregates formed sink and are broken up by the agitator continuously. This leads to a lower removal efficiency and higher standard deviations.

In the experiments with 4 alkyltrichlorosilanes at lower concentrations (Table 2-3, Figure A1-4) only n-butyltrichlorosilane achieves a good removal efficiency of 98.3 ± 1.0 %. It is, therefore, best suited for an economically efficient polymer removal from water. It is followed by isobutyltrichlorosilane with 91.4 ± 1.4 %. This is caused by the stabilizing effect of the branching in the isobutylgroup, which slows down the condensation, respectively the fixation of polymers. n-Propyltrichlorosilane with 47.3 ± 10.1 % and pentyltrichlorosilane(isomers) with 47.3 ± 6.8 % performed significantly worse, as they form unstable and small aggregates at lower concentrations.

Table 2-3: Removal efficiency of PE and PP and their standard deviations (S.D.) from water with 100 μ l / l alkyltrichlorosilane.

Name	Formula	Branched	PE [%]	S.D. PE [%]
n-Propyltrichlorosilane	(C ₃ H ₇)SiCl ₃	-	68,6	10,1
n-Butyltrichlorosilane	(C ₄ H ₉)SiCl ₃	-	98,3	1,0
Isobutyltrichlorosilane	(C ₄ H ₉)SiCl ₃	+	91,4	1,4
Pentyltrichlorosilane (Isomere)	(C ₅ H ₁₁)SiCl ₃	(+)	47,3	6,8

2.3.2 Hydrolysis rates and NMR analytics

When determining the hydrolysis rates, it must be taken into account that the alkyltrichlorosilanes are not water-soluble and are present in the water in drop form. This results in a phase transition which, in addition to the actual reactivity of the alkyltrichlorosilanes, influences the reaction rate [127, 128]. The size of the droplets and thus of the interface depends, on the one hand, on the surface tension of the water, but is also influenced by the addition of the alkyltrichlorosilanes and the flow conditions. Immediately after addition, the droplets retain their size and shape, then unite in the flow after the collision or get into the agitator and are broken up into fine droplets. Some of the droplets remain on the glass wall, where they can form smaller droplets or larger aggregations. The addition by hand and the turbulent flow conditions result in relatively large standard deviations between 21.3% (isobutyltrichlorosilane) and 24.7% (n-octadecyltrichlorosilane). Table A1-1 summarizes the results of the determination of the hydrolysis rates.

The half-lives of the alkyltrichlorosilanes, which show the best removal efficiencies (n-propyltrichlorosilane, n-butyltrichlorosilane, isobutyltrichlorosilane and pentyltrichlorosilane (isomers)), are between 18 and 73 sec. Other alkyltrichlorosilanes also lie in this range, but show worse removal efficiencies (e.g. methyltrichlorosilanes, (3,3-dimethylbutyl)trichlorosilanes or n-

hexadecyltrichlorosilanes). This shows that, in addition to hydrolysis kinetics, condensation kinetics and preorganization also play a decisive role in the fixation process. The hydrolysis rate gives only limited information about the second reaction step in the sol-gel process, condensation [113].

Therefore, the poor fixation of the polymer particles by isopropyltrichlorosilane, n-hexyltrichlorosilane, t-butyltrichlorosilane, with a half-life ranging from 7 and 53 sec, indicates slow condensation and thus slow fixation. This can be explained by the stabilizing effects of the alkyl groups on the formed silanols via steric and inductive effects.

Hexyltrichlorosilane has the longest half-life of 162 minutes. The reason for this is that the strongly branched hexyl residue prevents hydrolysis due to its steric hindrance. Due to the slow hydrolysis, no gelation takes place within the standardized reaction time of 20 minutes selected in our study. This observation explains why in section 2.3.1 no solid agglomerates could be observed.

Since n-undecyltrichlorosilane and n-octadecyltrichlorosilane have a half-life of 493 sec and 798 sec, respectively, the absence of hydrolysis slows down the gelation process. The fact that they form gels within a reaction time of 180 to 600 sec indicates a low stability of the silanols formed and a direct condensation. The large hydrophobic alkyl groups probably leads to low water solubility and strong aggregation of formed silanols. Due to the spatial proximity, condensation can, therefore, take place directly [120]. Despite the slow hydrolysis, this complicates the interaction with the polymers used and their agglomeration.

Table 2-4 summarizes the data of the ^{29}Si -MAS-NMR measurements. Since the signals of the spectra cannot be clearly assigned (wide signals, poor S/N ratio), the range of the peak is also given. All spectra show two wide signals in the range around 50 ppm and 60 ppm. The width can be explained by the fact that the chemical environment of the respective silicon atoms varies greatly due to the heterogeneous gel network. This leads to an overlapping of peaks. The signals at 50 ppm are assigned to the T1 units ($\delta = -48$ to -52 ppm) (Hook 1996, Loy et al. 2000). These can be dimers or simply precursor units connected to the hybrid silica gel network. Since the peaks at 60 ppm are also very wide (10-12 ppm), this is a superposition of the stronger T² units ($\delta = -57$ to -59 ppm) and weaker T³ units ($\delta = -64$ to -67 ppm). This suggests a mixture of less condensed hybrid silica gel with long-chain structural (intramolecular) units or intermolecular aggregation [113].

In the pH range of 3-7, which was present in the investigations, only a small percentage of the silanol groups formed during hydrolysis are protonated. Thus, the catalytic influence of the HCl released during hydrolysis can be classified as weak and the condensation only accelerated marginally. In addition, this supports the formation of long chained oligomers with low surface charge, which promotes the preorganization with the uncharged surfaces of the microplastic particles and the aggregation of formed aggregates. [119, 125, 126, 129].

Table 2-4 Peaks and range of the Peaks of the ^{29}Si -MAS-NMR Spectra. Sample: Hybrid silica based on alkyltrichlorosilanes with respective alkyl group and one agglomerate formed in the fixation process with *n*-butyltrichlorosilane and PE.

Sample (Alkylgroup)	Peak T ¹ [ppm]	Range T ¹ [ppm]	Width T ¹ [ppm]	Peak T ^{2:3} [ppm]	Range T ^{2:3} [ppm]	Width T ^{2:3} [ppm]
Methyl	-48.5	-44.5; -52.2	7.7	60.9	-55.4; -66.8	13.3
<i>n</i> -Propyl	-51.5	-45.8; -55.4	9.6	60.5	-55.6; -66.4	11.4
<i>n</i> -Butyl	-51.6	-45.7; -55.6	9.9	60.7	-55.2; -66.2	10.8
<i>n</i> -Butyl+ PE	-50.8	-45.8; -55.2	9.4	62.3	-56.6; -71.2	11
Isobutyl	-51.8	-47.0; -56.6	9.6	59	-54.6; -64.8	14.6
<i>n</i> -Octyl	-49.0	-44.9; -54.6	9.7	59.7	-54.8; -65.7	10.2
<i>n</i> -Undecyl	-49.3	-44.9; -54.8	9.9	60.2	-55.4; -67.9	10.9
Octadecyl	-50.6	-45.3; -55.4	10.1	60.9	-55.4; -66.8	12.5

2.2.3 Characterization of agglomerates by OCT, IR spectroscopy and TGA

The OCT images in Figure 2-4 illustrate the compact agglomeration of the microplastic. PP particles have a round shape (left), PE particles are irregularly shaped (right). It can be seen that the cavities between the polymer particles are filled with hybrid silica gel, which fixes it.

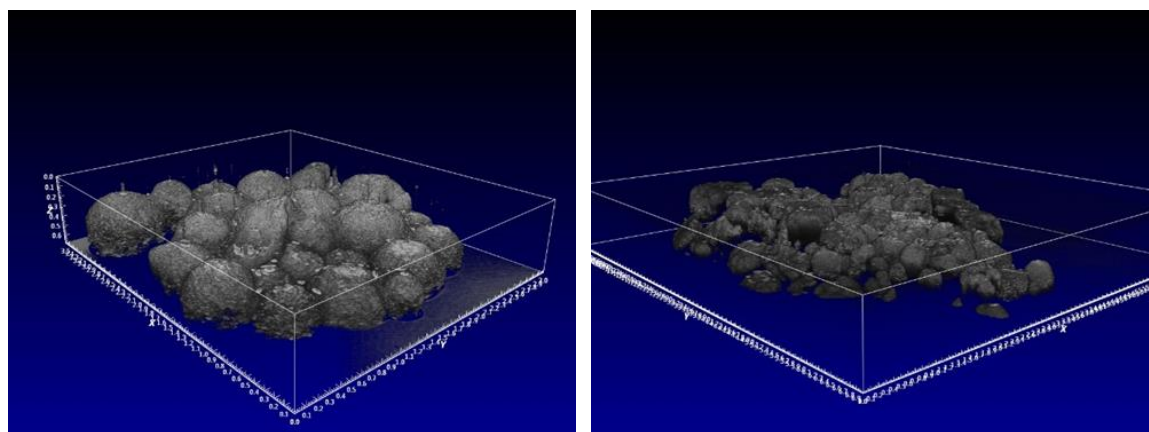


Figure 2-4 OCT Pictures of agglomerate formed with *n*-butyltrichlorosilane and PP (left) and PE (right)

The IR spectra of the hybrid silica gels (Figure 2-5) show the typical peaks for the siloxane bonds at $\nu_{\text{as}}\text{Si-O-Si}$ 1200 cm^{-1} and a wide peak $\nu_{\text{as}}\text{Si-O-Si}$ of 1100-1000 cm^{-1} [130]. The peaks of the silanol groups can be recognized as broad, flat bands at 3500 cm^{-1} due to the hydrogen bonds. The peaks of the

deformation oscillations of the alkyl groups (δ -CH, δ =CH₂) can be seen in the range of 1270-1470 cm⁻¹. The stretching vibrations of the alkyl groups (ν -CH) can be found in the range 2680-2850 cm⁻¹. Compared to pure silica, the agglomerate shows much stronger peaks of the alkyl groups at 1375 cm⁻¹ (δ -CH) 1453 cm⁻¹ (δ -CH) and 2950-2838 cm⁻¹ (ν -CH), induced by the polypropylene contained in the agglomerate. In addition, the Si-O-Si peaks of the hybrid silica are clearly visible in the agglomerate. The IR spectra thus confirm the fixation of the polymer particles (e.g. PP) in the hybrid silica gel network.

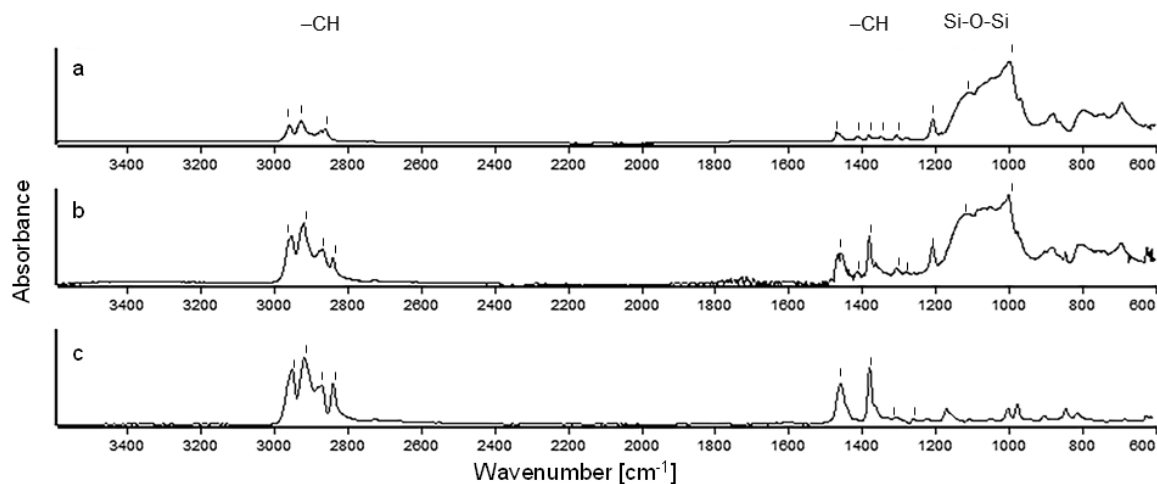


Figure 2-5 IR Spectra of a) *n*-butyltrichlorosilane based hybrid silica, b) Agglomerate of *n*-butyltrichlorosilane based hybrid silica and polypropylene, c) Polypropylene.

Thermogravimetry coupled with differential scanning calorimetry (TGA-DSC) is suitable for characterizing microplastics >12 μ m more closely. For example, the most common plastics PE and PP can be detected accurately. However, it is unsuitable for use in multi-substance wastewater because of strong interference [131].

The TGA analysis of our agglomeration-fixation products compared to starting materials shows a strong weight loss between 380 °C and 500 °C for the pure plastic particles (99.96%, PE) / 99.97%, PP), which consist almost exclusively of organic material. The inorganic component (0.16% (PE) / 0.04% (PP)) due to additives and impurities is negligible (Table 2-5).

Table 2-5: Analysis of TGA data for PE, PP, C1, C4 and C18 and their agglomeration-fixation products.

Sample	Organic ingredient [%]	Inorganic ingredient [%]	Oxidizable ingredient [%]
Reference PE	99.96	0.16	-
Reference PP	99.97	0.04	-
methyltrichlorosilane (C1)	14.35	84.21	1.34
C1 PE	64.57	35.47	0.08
C1 PP	78.53	21.25	0.2
n-butyltrichlorosilane (C4)	43.48	52.86	3.64
C4 PE	96.13	3.99	0.09
C4 PP	94.71	4.94	0.29
n-octadecyltrichlorosilane (C18)	85.76	13.15	1.07
C18 PE	85.00	14.33	0.64
C 18 PP	n.m,	n.m	n.m

* n.m. = not measured

The TGA curve for the hybrid silica (C1, C4, C18) shows a slight decrease with increasing temperatures. The strongest in the range between 500 °C and 625 °C. At these temperatures, the organic ingredient (e.g. 14.35%, C1) of the hybrid silica gel is expelled as CO₂. The remainder (e.g. 84.21%, C1) remains as an inorganic ingredient, which is substantially higher than the organic constituent.

For the products of our agglomeration-fixation process (e.g. C1 PE, C1 PP), the organic constituents are significantly higher than in the hybrid silica gel without microplastic inclusion. Accordingly, the inorganic component is much lower. The TGA analysis finally confirms that a mixed compound of hybrid silica and microplastic was formed.

2.4 Conclusion

In summary, it can be said that there are characteristic differences between the various alkyltrichlorosilanes with respect to their suitability for localization and fixation of polymer particles and their reaction behavior in water. This is due to the influence of the alkyl group on the reaction kinetics in the sol-gel process via steric and inductive effects. Both hydrolysis and condensation kinetics have a decisive influence. Pre-organizing effects of the alkyl groups also have an effect on reaction behavior and the locating of polymer particles.

Particularly well suited for polymer particle fixation are n-propyltrichlorosilane, n-butyltrichlorosilane, isobutyltrichlorosilane and pentyltrichlorosilane (isomers), whereby n-butyltrichlorosilanes provide the best removal efficiencies even at lower alkyltrichlorosilane concentrations.

Branches of the alkyl group show a slowing effect on the hydrolysis and condensation kinetics. This is particularly strong in the case of the strongly branched hexyl and t-butyl groups. Isopropyltrichlorosilane also provides worse results with regard to polymer elimination than n-propyltrichlorosilane due to slower condensation. With n-butyltrichlorosilane and isobutyltrichlorosilane, this effect is also visible at the lower concentration of alkyltrichlorosilane.

Long alkyl groups of 8 or more carbon atoms and the short-chain methyl group proved to be unsuitable because the microplastic particles are not localized sufficiently here, resulting in significantly lower removal efficiencies and high fluctuations within the process. The reasons for this include rapid condensation and the increase in substituent effects.

In future studies (chapter 3) this process is transferred to environmental samples. The first applications are in wastewater and seawater. Simultaneously, a scale up on pilot plant scale is implemented, which allows to run tests at environmental microplastics concentrations and to optimize the process for a large scale applications.

3 Removal of Microplastics from waters through Agglomeration-Fixation using Organosilanes – Effects of polymer types, water composition and temperature.

Published as: Sturm MT, Horn H, Schuhen K. Water. 2021;13:675. doi:10.3390/w13050675.

3.1. Introduction

Microplastics are one of the most complex environmental problems of today. Since the start of mass production in 1950, mismanaged plastic waste has been entering the environment [19, 104]. Over time, the plastic gets brittle and fragments into smaller and smaller plastic particles. From a size of 5 mm and smaller, these plastic fragments are defined as microplastics. Additionally, microplastics can enter the environment directly, e.g. textile fibers released from washing or tire abrasion [132, 133]. Due to their high persistence the microplastics degrade very slowly and can spread over long distances. Nowadays microplastics can be found in all parts of the aquatic and terrestrial environment as well as in the air [19, 27, 134]. Due to a continuously increasing plastic consumption and thus release into the environment, the environment will become increasingly contaminated [12, 14]. This poses a high risk to the environment and ecosystems as well as to human health [38, 135]

Numerous studies identify municipal and industrial wastewater treatment plants as important point sources for microplastics in the environment [59, 136]. Despite reported microplastics removal of 95% to >99% from inflowing wastewater to effluent in tertiary wastewater treatment plants, the level of microplastics contamination in the influent has such a high level, that the effluent still accounts as strongly contaminated. This is especially noticeable, as monitoring of microplastics contamination in the environment show higher contamination levels after wastewater treatment plant effluents. To prevent the release into the environment, there is a need for an improved microplastics removal during the wastewater treatment process.

Additionally, there are several microplastic sensitive seawater using processes. One example is membrane-based seawater desalination, where microplastics pose the risk for membrane fouling [59, 74]. Near food chain processes, such as sea salt production, can transport the microplastics from the environment to human food and therefore pose a risk to human health [64, 135, 137]. To ensure the functionality of microplastic sensitive water using processes there is a need for a method to remove microplastics from water cost effectively and with low technical effort [59, 138, 139].

Filtration is a common method for the removal of solid during water treatment and can also be applied for microplastics removal [59, 72]. But as smaller the particles get, as more complex and expensive the

filtration process gets. Therefore, processes as membrane filtration have disadvantages as high investment costs, high energy consumption and high maintenance, due to processes as scaling and fouling of the membranes. A more easy to use method could be dissolved air flotation (DAF) [59]. But different studies showed insufficient removal efficiencies of microplastics [68]. Even in combination with flocculants and surface modifiers Wang et al 2020 could only reach values between 68.9% and 43.8% for microplastics removal using DAF [67]. Microplastics can consist of a multitude of different types of polymers with different properties and surface chemistries. This can have a strong influence on the interaction of flocculants and microplastics and makes finding suitable flocculants even more challenging [73, 74]. Most commonly used flocculants are based on iron or aluminum and therefore have a limited adaptability [73]. Polyelectrolyte based flocculants are more adaptable, but due to their solubility they remain in the water and can cause harm to aquatic organisms and ecosystems [75, 140].

Facing this challenge, Herbort et al. 2016 developed a new approach to remove microplastics from water using organosilanes (Figure 3-1) [80, 81, 124, 140, 141]. The organosilanes consist of one organic group and three reactive groups. Due to the interaction of the organic group and the surface of the microplastics, the organosilanes attach to the surface of the microplastic and collect it in agglomerates in the first step of the fixation process [80]. In the second step of the fixation, the three reactive groups form a solid hybrid silica gel that includes and fixes the microplastics chemically driven by a water induced sol-gel process. During this sol-gel process, the reactive groups are hydrolyzed to highly reactive silanols, which subsequently condensate and form siloxane bonds [112, 140].

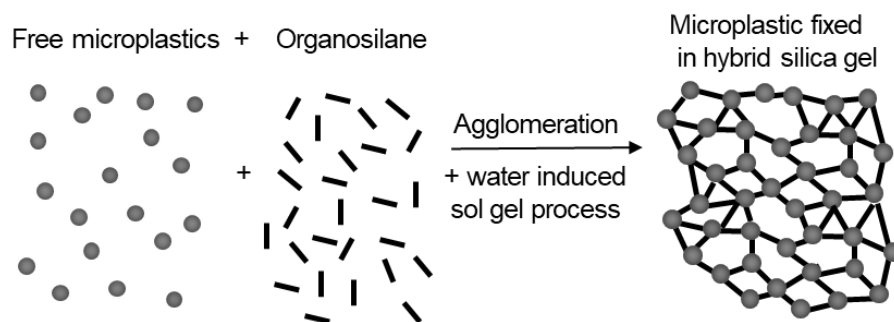


Figure 3-1. Agglomeration-fixation reaction: Removal of microplastics from water using organosilanes. Organosilanes attach to the surface of microplastics, collect it in large agglomerates and chemically fix it by forming a solid hybrid silica in a water induced sol-gel process.

The novelty of this process is the combination of a physical agglomeration process with a water induced chemical fixation process, leading to a strong particle growth and stable agglomerates [80, 124]. Hence, the organic groups can be adapted to different polymer types and surface chemistries. The reactivity of the organosilanes can be adapted to different water compositions by changes in reactive groups and organic groups [124, 140]. The high diversity and adaptability of organosilanes as chemical substance class gives this relatively new and little researched approach a high potential for application in water treatment and microplastics removal.

So far the process has been tested to remove polyethylene and polypropylene based microplastics on lab scale using demineralized water and on pilot plant scale from tap water [80, 140]. To investigate the transferability to processes in sewer and wastewater, it is tested how water compositions affect the removal process, as dissolved ions, natural organic matter or surfactant compounds can affect the sol-gel process and thus the removal process [141]. Also, the influence of water temperatures is tested, as it can vary depending on climatic conditions or wastewater origin. As the formation of silanol groups enhances the water solubility, possible organosilane residues remaining dissolved in the water after the fixation process are monitored. To exclude a potential discharge, no organosilanes must remain dissolved in the water after the process is finished. Additionally, the process was tested for common polymer types with different properties and surface chemistries, to investigate how those affect the interaction with the organosilanes and the agglomerate formation. By the combined investigating of this new and important factors, we want to bring the microplastics removal by organosilanes one step further to the application transfer

3.2. Materials and Methods

3.2.1 Used microplastics and chemicals

Table 3-1 shows the polymer types, mean size and suppliers of the used microplastics (Figure A2-1).

Table 3-1. Overview of microplastics used in the experiments.

Polymer type	Abbreviation	Mean size [μm]	Supplier
Mixture of Polyethylene / Polypropylene (1:1)	PE / PP	318 ± 258	LyondellBasell, Basell Polyolefine GmbH, Germany
Polyamide	PA	357 ± 60	EMS-Grilltech, Switzerland
Polyester	PES	54 ± 87	EMS-Grilltech, Switzerland
Polyvinylchloride	PVC	110 ± 25	Sigma-Adrich, Germany

The organosilanes n-butyltrichlorosilane (CAS 7521-80-4), isooctyltrichlorosilane (CAS 18379-25-4), (3-chloropropyl)trichlorosilane (CAS 2550-06-3) and abcr eco Wasser 3.0 PE-X® (AB930009), a mixture of organosilanes, were provided by abcr GmbH, Karlsruhe, Germany. abcr eco Wasser 3.0 PE-X® is abbreviated as PE-X.

3.2.2 Different water types and temperatures

We compared the removal process in demineralized water, salt water and biologically treated municipal wastewater (secondary clarifier). The salt water was created by dissolving 3.5% by weight of untreated

Atlantic sea salt (Art. No. 8530, Biova, Wildberg, Germany) in demineralized water. The biologically treated wastewater was taken from the sewage treatment plant at Landau i. d. Pfalz, Germany on March 2, 2020 (after several days of rain). The water parameters can be seen in Table A2-1. Both water samples were filtered through a 0.6 µm paper filter (Macherey-Nagel MN 85/70 BF) to remove all solids contained. To compare the influence of different temperatures, the water samples were adjusted to 7.5, 20 and 40 °C using ice bathes or heating plates.

3.2.3 Determination of removal efficiency

The removal efficiency was determined gravimetrically according to Sturm et al. 2020 (chapter 2.2.3) [140]. 1 l of water was filled into a 2 l beaker, the microplastic was added and the suspension was stirred using a magnetic stirrer for 5 minutes with highest speed. Subsequently the stirrer was set to 500 rpm, the organosilane was added and the mixture was stirred 20 minutes to perform the agglomeration process. After 20 min, the contents of the beaker were filtered through an analysis sieve (stainless steel, mesh size 1 mm, diameter 20 cm). Therefore, agglomerates larger than 1 mm remain in the sieve and are classified as removed. The filtrate with the remaining free microplastic was repeatedly filtered through a filter crucible (porosity 4, max. pore size 16 µm) and rinsed with isopropanol to remove possible attached organosilane residues. After drying the sample at 105°C for 24h, the weight of the free microplastic could be determined.

Unless otherwise stated, the organosilane dosage was 100 µl / l and microplastic concentration was 100 mg / l. Performing lab scale experiments using 1 l water, 100mg microplastics per liter was the lowest concentration possible to achieve reliable and reproducible results. An organosilane dosage of 100 µl / l was chosen, as in previous studies it turned out to be the lowest concentration to remove 100 mg PE /PP efficiently (>95%) from water on laboratory scale. The size limit for the agglomerates to be classified as removed was set to 1 mm, as from this size the agglomerates proved to be easy to remove in pilot plant experiments. Microplastics that stick to the wall or the bottom of the beaker and cannot be removed by rinsing thoroughly are also considered as removed.

3.2.4 Determination of the organosilane residues dissolved in water

To measure the dissolved organosilane residues, the standardized removal process was conducted using 100 mg/l of a PE / PP mixture (1:1) as microplastics. After 20 minutes stirring time, a water sample was taken and filtered through a 0.45 µm syringe filter. The silicon concentration of the sample was measured using an ICP-OES spectrometer (Inductive Coupled Plasma Optical Emission Spectroscopy) (Agilent Technologies, ICP-OES 5110). The DOC concentration (dissolved organic carbon) was measured with the Sievers TOC Analyzer 820. Blank values from the respective water samples were subtracted from the measured values.

3.2.5 Additional analytics

To determine the mean size, 20 microplastic particles respectively ten agglomerates were photographed with the stereomicroscope SMT4 from ASKANIA Mikroskop Technik Rathenow GmbH, Rathenow, Germany coupled with a Canon EOS 600D digital camera and subsequently measured.

IR spectra ($4000\text{--}300\text{ cm}^{-1}$, resolution 1 cm^{-1}) of the aggregates and hybrid silica gels, which have been dried previously for 24 h at $105\text{ }^{\circ}\text{C}$, were taken with the ATR-FTIR spectrometer Vertex 70, Bruker, Ettlingen, Germany.

Thermogravimetric analysis (TGA) was conducted using a Q5000 IR from TA Instruments using a platinum crucible. Starting temperature was at $45\text{ }^{\circ}\text{C}$, purge gas 1: nitrogen 5.0; 25 ml/min with a heating rate of $20\text{ }^{\circ}\text{C}/\text{min}$. The gas switching temperature was at $600\text{ }^{\circ}\text{C}$, purge gas 2: oxygen 5.0; 0.25 ml/min with a heating rate of $20\text{ }^{\circ}\text{C}/\text{min}$ and final temperature of $950\text{ }^{\circ}\text{C}$.

3.3 Results and Discussion

3.3.1 Different water types and temperatures

The comparison of the removal efficiencies at different temperatures (Figure 3-2) shows no negative impacts of high or low temperatures on the removal process. Also, between the different organosilanes no significant differences can be seen. All values are within the standard deviations respectively measurement fluctuations. The process should therefore be applicable without problems at high temperatures, such as can occur in industrial wastewaters and at low temperatures, which can occur in the winter months in natural waters or different wastewaters [142, 143].

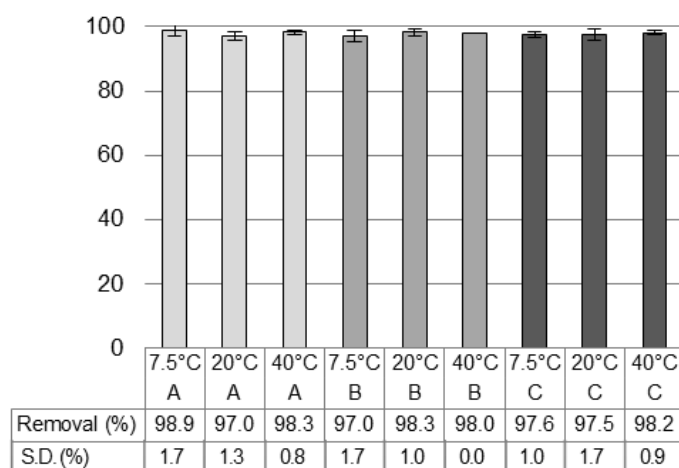


Figure 3-2. Removal efficiency for 100 mg mixture of PE / PP (1:1) from 1l demineralized water at different temperatures using 100 μl organosilane (A = PE-X; B = n-Butyltrichlorosilane; C = Isooctyltrichlorosilane).

This could be shown analogously for different water types. The three different water types show no significant differences regarding the removal process (Figure 3-3). Measurement fluctuations caused the

lower removal efficiency using isooctyltrichlorosilane in salt water, which is also expressed in the higher standard deviation. Due to turbulent flow conditions in the experimental setup, inducing random movement of agglomerates and microplastics, such fluctuations can occur [14]. On pilot plant scale the flow conditions and fluctuations can be controlled better due to advanced steering and mixing mechanisms.

Possible positive impacts of sea- or wastewater could not be examined with the applied parameters, since the combination of 100mg of microplastics in one liter of water with 100 µl of organosilane was selected in such a way, that it had achieved optimum removal (> 95%) with demineralized water as a reference, what leaves no room for measurable improvements.

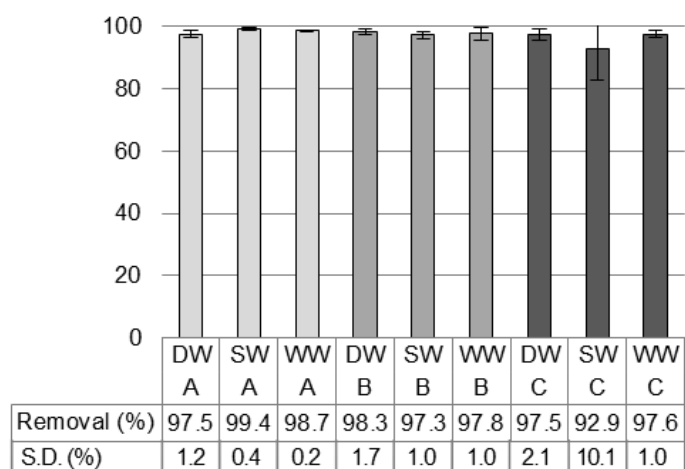


Figure 3-3. Removal efficiency for 100 mg mixture of PE / PP (1:1) from 11 demineralized water (DW), salt water (SW) or biologically treated wastewater (WW) using 100 µl organosilane (A = PE-X; B = n-Butyltrichlorosilane; C = Isooctyltrichlorosilane).

In general, wastewater shows temporal variations on the chemical composition and particle load but also variations depending on the catchment area [144]. In our experiments, we decided to test municipal wastewater, taken during a rainy period, as it contains more microplastic washed from the roads by surface runoff (e.g. tire wear) and poses one of the biggest point sources for microplastics into the environment [145, 146]. Besides, the wastewater is diluted with rainwater and usually contains less nutrients and other chemicals as surfactants. On the day of sampling, the inflow amounted to 38 million L, whereas the average inflow on dry days amounts to 11 million L per day. Although we could not find any negative effect in the wastewater used in our studies, further investigations should focus on the variations of wastewater compositions. Especially industrial wastewater can show strong variations depending on the type of industry [147].

For the salt water, oceans show spatial and temporal variations for the salt concentration and composition [148]. The salt concentration usually varies between 3.2-3.8 %, with an average of 3.5 %, which we choose as the concentration for the experiments. As there is no difference between demineralized water and 3.5 % salt water, the fluctuations of salt concentrations in the oceans should be negligible. Only

saline lakes, which can easily reach salt concentrations >10 % and are often used for salt extraction, could affect the process [149]. Nevertheless, the removal process should be transferable in municipal wastewater and sea water. The functionality of the process in drinking water could already be proven in a previous study [80].

3.3.2 Comparison of polymer types

Comparing the efficiency of the removal process within different types of polymers, clear differences between the types of polymers and the organosilanes used could be determined (Figure 3-4). During the removal process, the organic groups of the organosilanes needs to attach to the surface of the microplastic particles to collect them in agglomerates. Therefore, these differences are caused by the varying interactions of the organic groups and the surface of the different polymer types [140].

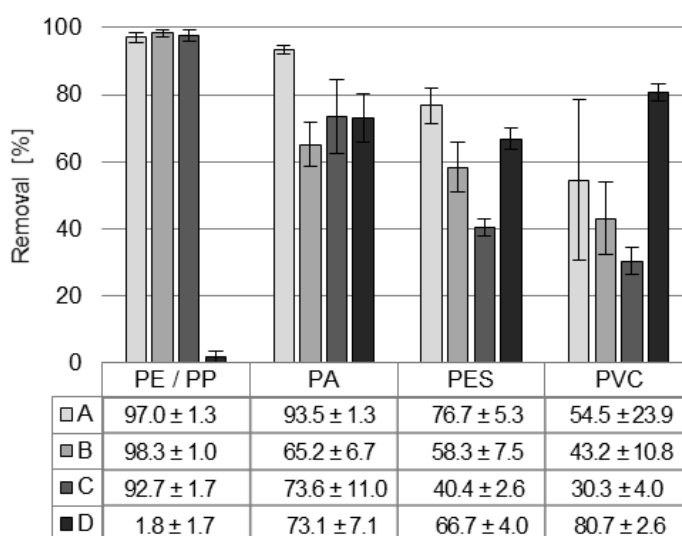


Figure 3-4. Removal efficiency for 100 mg microplastics from 1l demineralized water using 100 µl organosilane (A = PE-X; B = n-Butyltrichlorosilane; C = Isooctyltrichlorosilane; D = (3-Chloropropyl)trichlorosilane).

PE and PP consist of pure alkyl chains, have no heteroatoms and are, therefore, non-polar. PA has nitrogen and oxygen and PES oxygen as heteroatoms, which is why they are more polar. However, since the C-H component predominates, they are classified with medium polarity. PVC results from the crosslinking of vinyl chloride (C₂H₃Cl), which means that it has an extremely high proportion of chlorine atoms and the highest polarity in the polymer series shown.

Among the organosilanes, PE-X, n-butyltrichlorosilane and isooctyltrichlorosilane have non-polar organic groups made of pure hydrocarbons. In the tests with microplastics based on PE and PP, satisfactory removal efficiencies between 97 and 98.3% were consistently reached. But with increasing polarity of the microplastics, the effectiveness decreased, as much smaller agglomerates are formed which partially do not reach the size limit of 1mm (Figure 3-6). With very polar PVC values between

30-55% can be achieved. Another influence factor could be the higher density of the polar polymer types, as it can hinder the accumulation of the microplastics and smaller agglomerates in the vortex by sinking.

In comparison Lapointe et al. 2020 tested aluminum and polyacrylamide based flocculants towards weathered and unweathered PE and could show that the introduction of polar hydroxyl and carboxylic acid groups by weathering could improve the interaction of the flocculants and microplastics leading to an improved removal [73]. This result shows that coagulants with polar sorption sites can lead to enhanced flocculation of polar microplastics.

Therefore, (3-chloropropyl)trichlorosilane was added to the tested organosilanes, which has a higher polarity due to a chlorine substitution at the end of the organic propyl group. This creates an improved interaction with the surface polar polymers. For the highly polar PVC a clear improvement of the removal efficiency is reached. In the case of polymers of medium polarity (PES and PA), which have both polar and non-polar structural units, no clear improvement could be achieved by the chlorine substitution. Using PE / PP, no agglomerate formation was observed, since there was no interaction between the non-polar surface and the polar chloropropyl group. This results in proof of the strong interaction between the organic group of the organosilanes and the surface of the microplastics depending on the polymer type.

Because chlorinated hydrocarbons are generally both ecotoxicologically hazardous and harmful to health, the use of (3-Chloropropyl)trichlorosilane in actual application is unlikely [150]. Due to the good results achieved by the chemical modification of the organic group, future studies should focus on environmentally friendly alternatives for organosilanes with polar organic groups. For this adaptation however, it must also be taken into account that the organic groups can have a strong influence on the reactivity of the organosilanes and thus can negatively influence the fixation process [140]. Therefore, not all organic groups are suitable for this adaptation.

Additionally, a higher dosage or combination of organosilanes was tested for the removal of PVC (Figure 3-5). An increase in the dosage to 300 μ l n-butyltrichlorosilane (84.0 %) and the combination of 100 μ l PE-X with an additional 100 μ l isoctyltrichlorosilane (79.6 %) respectively 100 μ l n-butyltrichlorosilane (77.6 %) show an increase in efficiency comparable to (3-chloropropyl)trichlorosilane (80.7 %). This shows the potential of the combination of organosilanes for microplastic removal and that there is still potential for further improvement of PE-X. Using a dosage of 1 ml n-butyltrichlorosilane, an almost complete removal could be achieved reaching 98.1 %. Studies using aluminum, iron or polyacrylamide based flocculants also showed increased effectivity of higher dosages [73, 74].

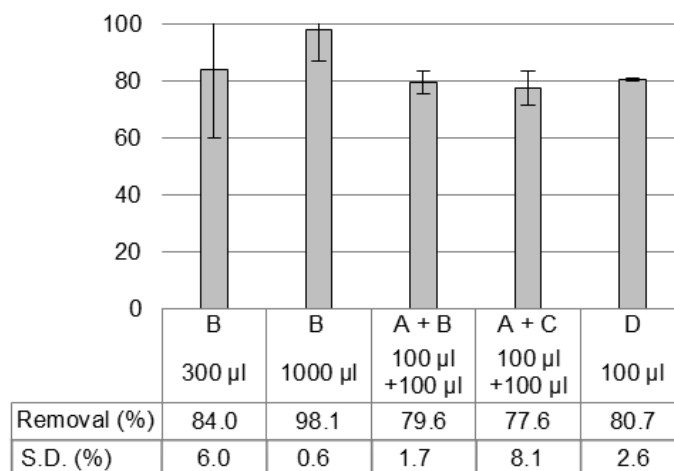


Figure 3-5: Removal efficiency for 100 mg PVC from 1l demineralized water using 100 µl organosilane at different dosages and combinations (A=PE-X; B=n-Butyltrichlorosilane; C=Isocetyltrichlorosilane; D=(3-Chloropropyl)trichlorosilane).

The mean size of the microplastics and the agglomerates is shown in Figure 3-6. It can be seen, that the size composition of the virgin microplastics differs significantly among the polymer types and mixtures. CoPA (\varnothing 357 µm) and PE / PP (\varnothing 318 µm) have a larger starting size than PVC (\varnothing 110 µm) and CoPES (\varnothing 54 µm). Additionally, the standard deviations show that PVC and PA particles have a more even size while the size of PES and PE / PP particles show large deviations. It is currently unclear whether the initial size of the microplastics has an influence on the final size of the agglomerates, as data shows a strong particle growth during the agglomeration process for all polymer types. In previous studies testing flocculation of microplastics with different size compositions using iron, aluminum and polyacrylamide based flocculants, larger microplastic particles showed worse flocculation as they are more difficult to incorporate into the flocks [73, 74].

Ma et al. 2019 reported flock sizes of 258.6 ± 20.8 µm using alumini-based flocculants and 474.8 ± 25.6 for iron-based flocculants for the removal of PE. Lapointe et al. 2020 reported flock diameters of 977 ± 36 µm for the removal of PE < 140 µm and of 504 ± 18 µm for PE > 140 µm applying polyacrylamide-based flocculants. Compared to this, using organosilanes higher agglomerate sizes could be reached for the removal of PE / PP with up to 13130 µm using PE-X. Also it is notable that on pilot plant scale much higher agglomerate sizes can be achieved [80]. This is a big advantage of this method, as larger agglomerates can be removed more easily.

For the determination of the removal efficiency, the limit for agglomerates classified as removed was set at 1 mm, since those could easily be removed in pilot plant tests in a 2 m³ test reactor system [140]. Considering the mean size and standard deviations of the agglomerates, for PA, PES and PVC a proportion of the agglomerates do not reach the size of 1 mm and therefore are classified as free microplastics despite a strong particle growth compared to the initial size. Thus, by optimizing the

agglomerate removal on pilot plant scale and therefore lowering the size limit for the removal, a strong increase in removal efficiency can be expected.

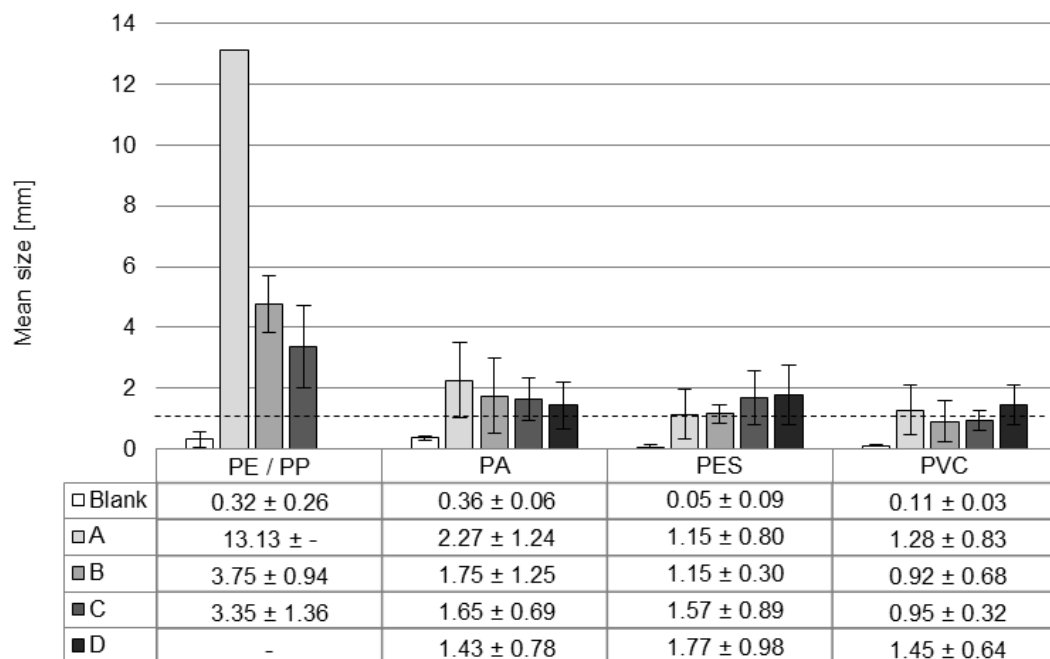


Figure 3-6. Mean size of microplastics and agglomerates. The dashed black line marks the 1 mm limit from which the microplastics is assessed as removed. (A=PE-X; B=n-Butyltrichlorosilane; C = Isooctyltrichlorosilane; D = (3-Chloropropyl) trichlorosilane).

3.3.3 Organosilanes residues dissolved in water

The examination of the organosilane residues dissolved in water (Figure 3-7) shows that for isooctyltrichlorosilane and n-butyltrichlorosilane, between 76.4 and 46.3 % of the added organosilane (calculated based on the Si content) remains in solution. This happens as the silanols formed during the hydrolysis of the chlorine groups increase the water solubility of the organosilanes [126]. During the sol-gel process formed oligomers or dimers with remaining silanol groups can remain in solution and not react completely to solid hybrid-silica gels. This poses a problem for a technical application of the fixation process. However, this effect cannot be seen with PE-X, as no residues could be detected in the water. Therefore, PE-X is suitable for the application.

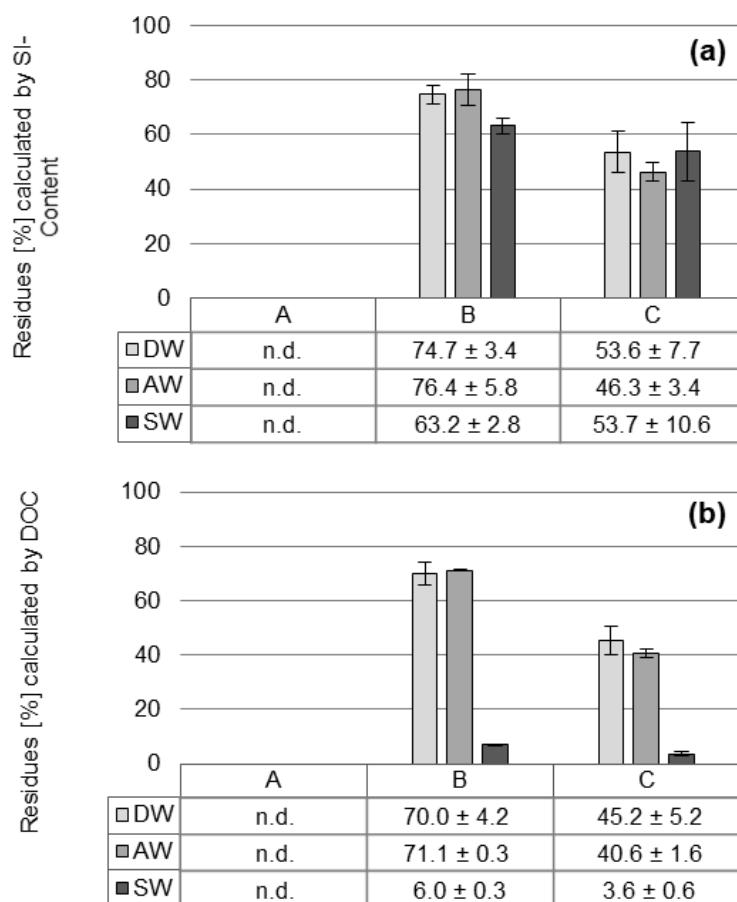


Figure 3-7: Percentage of organosilane residues in the water calculated from the Si content (a) and Table 100. mg PE / PP (50:50) in 1l water adding 100 μ l organosilane and stirring for 20 minutes. (DW = demineralized Water; SW = salt water; WW = biological treated wastewater; A = PE-X; B = n-butyltrichlorosilane; C = isooctyltrichlorosilane). For DOC 100 % correspond to A = 58.7 mg/l, B = 29.1 mg/l and C = 41.8 mg/l. For Si content 100 % correspond to A = 17.2 mg/l, B = 17 mg/l and C = 12.1mg/l.

Comparing the results of the DOC and Silica concentrations, it is noticeable that the residues measured with the ICP-OES (Si content) are always slightly higher than the values measured by DOC. At the start of the DOC measurement, highly concentrated phosphoric acid is added to the sample in order to remove the contained inorganic carbon. This acid catalyzes the sol-gel process, which means that dissolved dimers and oligomers contained in the sample can condense, precipitate and deposit on tubes [112]. This effect is particularly noticeable in salt water, as the combination of acid and dissolved salt additionally intensifies the condensation of the oligomers.

In general, ICP-OES delivers more accurate and reliable measured values, due to the short distance from the intake to the plasma torch and the general robustness of the measuring method. DOC is a good alternative for process control, as it is a cheap and easy to handle method.

3.3.4 Additional analytics

3.3.4.1 Microscope images

The microscope images (Figure 3-8, Figure A2-1) show the formation of stable agglomerates, where the microplastics are held together by the organosilane. As the organosilane forms a thin, transparent to slightly white hybrid silica layer on the microplastics during the formation process, the single microplastics particles can still be recognized. The texture of the agglomerate is tough and viscoelastic, which is typical for hydrogels [151]. In addition, the agglomerates are very sticky and attach to glass, metal, and plastic surfaces.

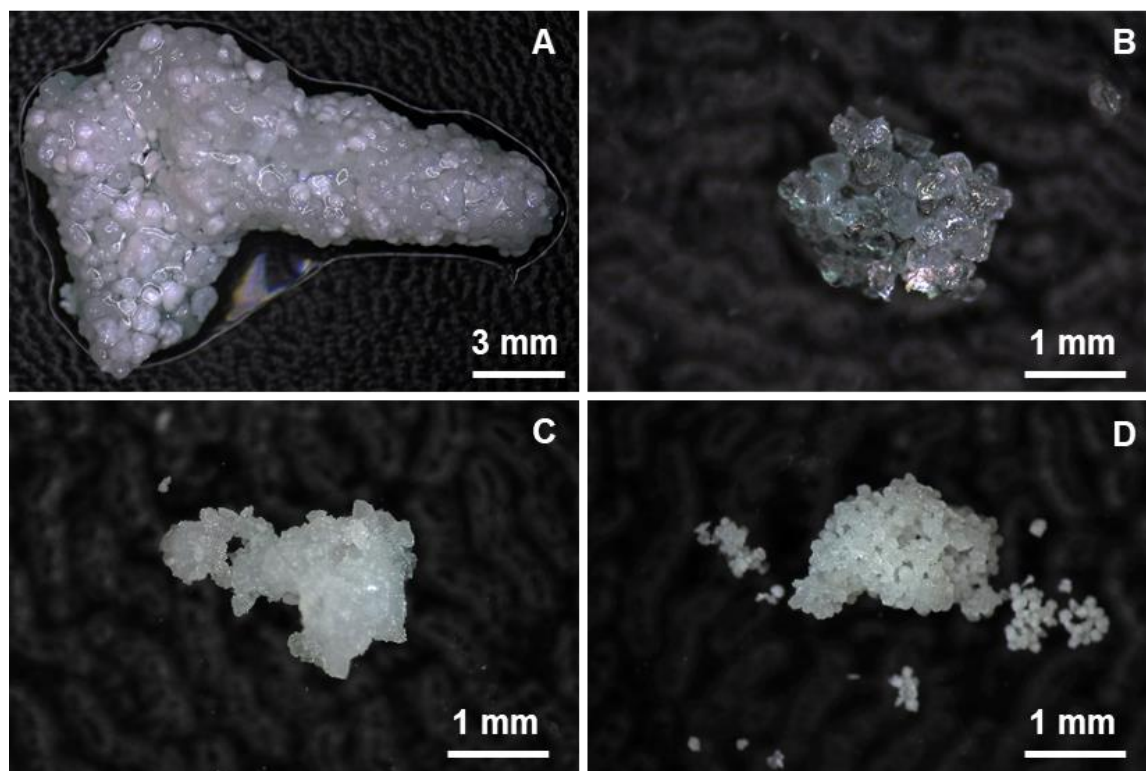


Figure 3-8. Microscope images of wet agglomerates formed during the removal of 100 mg microplastics from 1l demin. water using 100 μ l organosilane. A = PE-X and PE/PP (1:1), B = *n*-Butyltrichlorosilane and PA, C = Isooctyltrichlorosilane and PES, D = (3-Chloropropyl)trichlorosilane and PVC.

3.3.4.2 IR-Spectra

Figures A2-2 – A2-7 show the IR spectra of the different polymers, the hybrid silica resulting from the respective organosilane after 20 min water contact and the agglomerates formed during the removal process. The IR spectra of the hybrid silica gels shows a small peaks for the siloxane bonds at 1200-1240 cm^{-1} ($\nu_{\text{as}}\text{Si-O-Si}$), a wide peak of 1100-1000 cm^{-1} ($\nu_{\text{as}}\text{Si-O-Si}$) and a peak at 390-460 cm^{-1} ($\delta\text{O-Si-O}$) [80, 130]. The deformation oscillations of the alkyl groups ($\delta_{\text{s}}\text{C-H}$, $\delta_{\text{as}}\text{C-H}$, $\delta\text{-CH}_2\text{-}$) can be seen in the range of 1260-1470 cm^{-1} . The stretching vibrations of the alkyl groups ($\nu_{\text{as}}\text{C-H}$, $\nu_{\text{s}}\text{C-H}$) can be found in the range 2850-2970 cm^{-1} .

This peaks for the alkyl groups can also be found in the spectra of the microplastics samples. Therefore, the agglomerates show stronger peaks of the alkyl groups compared to pure silica, caused by the included

microplastics. The presence of PVC in the agglomerate can be confirmed by the peak at $600\text{--}650\text{ cm}^{-1}$ ($\delta\text{C-Cl}$) [152, 153]. PA shows additional peaks at 3290 cm^{-1} ($\nu\text{N-H}$), 1630 cm^{-1} ($\delta\text{C=O}$), 1540 cm^{-1} ($\delta\text{C-N}$, $\nu\text{N-H}$) and 680 cm^{-1} ($\nu\text{N-H}$; $\nu\text{C=O}$). Typical PES peaks are visible at 1710 cm^{-1} ($\nu\text{C=O}$), 1230 cm^{-1} ($\nu\text{C-O}$), 1100 cm^{-1} ($\nu\text{C-O}$), 725 cm^{-1} ($\omega_{\nu,\delta}\text{C-H}$ of aromatic compounds). In addition, the Si–O–Si peaks of the hybrid silica are clearly visible in the agglomerates, which confirms the inclusion of the microplastic in a hybrid silica gel during the fixation process.

3.3.4.3 TGA

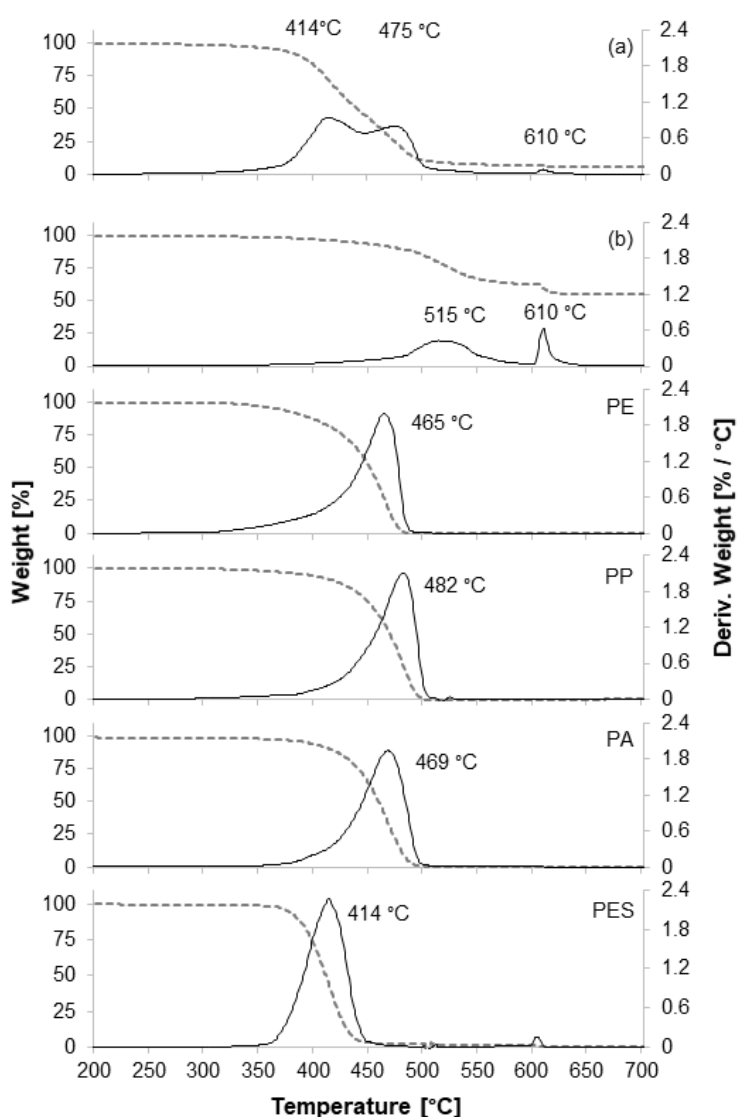


Figure 3-9: TGA curves of (a) agglomerate formed in removal process 100 mg of PE / PP / PA / PES (1:1:1:1) from 1l demineralized water using 100 μl n-Butyltrichlorosilane; (b) hybrid silica formed by adding 100 μl n-Butyltrichlorosilane in 1l demineralized water and different polymer types used in experiments. Grey dashed line = weight in %; black line = derived weight in % / $^{\circ}\text{C}$.

For the TGA measurements, the removal experiments were additionally conducted with mixtures of different polymer types. The data (Figure 3-9, Figures A2-8 – A2-10) show that the agglomerates include the different polymers and the organosilane based hybrid silica formed during the fixation process. Thus, the fixation process is also suitable to remove mixtures of different polymers. The peak at 414 °C can be assigned to PES, the peak at 475 °C results from the overlapping PE, PP and PA peaks and the first peak of the hybrid silica at 515 °C. The peak at 610°C and the continuing weight loss after 505 °C, where the polymers show no weight loss anymore, confirm the presence of the hybrid silica in the agglomerate. Due to the overlapping of the TGA peaks, a quantitative analysis of the composition of the agglomerate was not possible.

3.4 Conclusions

Summarized this study showed, that the novel method of microplastics removal using organosilanes has a huge potential to be applied for microplastics removal on technical scale. Temperature and water type, here salt water and biologically treated municipal wastewater, show no negative effect on microplastic removal with organosilanes, what shows the robustness of the method and should make it easily transferable to processes as advanced wastewater treatment or sea water using processes. As wastewater composition can vary strongly depending on the catchment area, weather and climatic conditions, further investigations are needed to ensure the applicability in different wastewaters. Also, application in highly saline lakes could pose a challenge to the process.

It was also shown, that the chemical composition and surface chemistry of microplastics have a strong influence on the removal process and physical interaction with the organosilanes. The removal efficiency of microplastics based on different polymer types decreases with increasing polarity of the polymer. Highly polar polymers can be removed more efficiently by increasing the polarity of the organic group. However, this leads to a reduced effectiveness towards non-polar polymers. This results show, that the organosilanes can be adapted specifically to improve the removal of certain polymer types by adjusting the organic group to the surface chemistry of the polymer. The high variability and modifiability of organosilanes makes them very promising substance class for this challenge. Another alternative to increase the efficiency is using higher concentrations of organosilanes. Further studies should focus on the combination of different organosilanes for an effective removal of mixtures of polar and non-polar polymers, as they occur in the environment. Also, the effect of biofilm coverage, weathering and NOM adsorption can be taken into consideration (see chapter 4).

The analysis of the size composition of the microplastics and agglomerates shows a strong increase in size during the agglomeration process for all polymer types. However, the limit of 1mm for the agglomerates for efficient removal on pilot plant scale is often not achieved. An improved removal process for the agglomerates with a lower size limit is therefore expected to lead to strongly improved microplastics removal on technical scale.

From the tested organosilanes n-butyltrichlorosilane and isoctyltrichlorosilane both show high quantities of residues dissolved in water after the removal process, ranging from 76.4 to 46.3 %. PE-X shows no dissolved residues and therefore is perfectly suited for the application on technical scale without posing any risk of the introduction of organosilanes into the environment or technical processes, what is a big advantage of this specific organosilane. The tested water compositions show no significant differences on the amount of residues. To control dissolved organosilanes residues, ICP-OES showed more precise and reliable results than DOC measurements. But as cheaper and faster method, DOC is still suitable for an efficient process control in possible technical applications.

Microscope images, IR-spectra and TGA curves confirm the inclusion of the microplastics in a hybrid silica formed by a water induced sol-gel process during the fixation process. The TGA curves can additionally show that it is possible to fix mixtures of different polymers simultaneously in the agglomerates. Therefore, these methods are well suited to investigate the composition of agglomerates and later on to control the process during continuous application.

Due to the limitations of the laboratory scale test setup, 100 mg / l could be selected here as the smallest concentration of microplastics. However, environmental concentrations are usually far below that concentration. Therefore, further pilot-plant studies will focus on a reduction of the microplastics concentrations as well as the function in real applications without microplastics spiking. Also, a broader variety of water compositions is going to be tested. Due to the adaptability of this process to different polymer types and the low technical effort for the application on technical scale we see a high potential for this process to be a cost-effective and easy applicable alternative for standard flocculants.

4 Method for rapid biofilm cultivation on microplastics and investigation of its effect on the agglomeration and removal of microplastics using organosilanes

Published as: Sturm, M.T., Schuhen, K., Horn, H., *Sci Total Environ*, 2021;151388. doi:10.1016/j.scitotenv.2021.151388

4.1 Introduction

Since the early 2000s, the topic of plastics and microplastics in the environment has become of increasing interest in environmental research [6, 104]. Various studies could prove that plastics and microplastics are a global environmental problem. Microplastics, plastics smaller than 5 mm, can originate from direct inputs into the environment or by fragmentation of larger plastics. Due to their high persistence and transport by wind and currents, plastics and microplastics can be found in every part of the environment [19, 154]. Thus, it is inevitable that organisms and ecosystems interact with it, whereby numerous harmful effects have already been proven [36, 38].

To reduce inputs from point sources like municipal and industrial wastewater treatment plants or to ensure the function of water using processes sensitive to microplastics contamination, researchers began to evaluate and develop various methods for the removal of microplastics from water [59, 155]. The challenge is finding a method which can be applied efficiently, economically, and sustainably on a technical scale.

Sedimentation or flotation is difficult to apply for microplastic removal as different plastics can have a high range of densities, often close to the density of water [59]. Small particle sizes leading to slow settling or ascending velocities increase this problem. One of the most common methods for particle removal in water treatment is filtration [72]. For efficient removal of small microplastics, the application of membrane filtration is necessary. Membrane filtration systems have disadvantages such as high investment costs, high energy consumption, and high maintenance, due to fouling of the membranes [62, 156]. Microplastics have a high potential to promote membrane fouling, because of their small size and specific surface properties. Particles larger than the pore size of the membrane can clog the pores or form cake layers which can be easier removed, whereas particles smaller than the pore size of the membrane can cause internal and irreversible fouling [62]. Interactions caused by the surface charge and the hydrophobicity of the membrane and microplastics affect the foiling potential. Opposite charges and similar hydrophobicity increase the attraction between membrane and microplastics and promote the

fouling process. Additionally, microplastics can carry microorganisms and therefore promote biofouling. Easily applicable filtration methods such as sand filtration or cloth filter show insufficient effectiveness, especially for small microplastics (Na et al., 2021; Sembiring et al., 2021; Talvitie et al., 2017). A method to increase the efficiency of filtration, flotation or sedimentation is the application of flocculants, which increase the size of particles by agglomeration [157].

The largest challenge for flocculant optimization is that microplastics include various plastic types with different properties and surface chemistries. These properties affect the interaction of flocculants and microplastics and make finding effective flocculants challenging [73, 74]. Most commonly used flocculants and electrocoagulation are based on iron or aluminum can be efficient for certain polymer types but suffer from limited adaptivity [73, 76, 158]. Polyelectrolyte-based flocculants are more diverse and therefore adaptable but have the drawback of ecotoxicological risk potential when remaining dissolved in water [75, 159]. Despite being commonly used in wastewater treatment, insufficient consideration has been given to their ecotoxicological properties. Due to their high variety and variability, their ecotoxicology is still poorly understood. The toxicity mainly depends on the charge density and hydrophobicity, but also the molecular weight and architecture of the polymer [160]. By binding to cell membranes, Polyelectrolytes can affect cell membrane integrity and nutrient transport [159]. Cationic polyelectrolytes, like polyacrylamides, show the highest risk potentials and can reach toxic effects in concentrations smaller 1 mg/l [75]. Therefore, research has started to focus on alternative flocculants for microplastics removal, like jellyfish mucus, superparamagnetic iron oxides, or protein amyloid fibrils, which are all in an early stage of development [161–163].

Discovered in 2017, the agglomeration and subsequent removal of microplastics via organosilanes is a new and promising approach for sustainable and cost-efficient microplastics removal, as it is applicable with low technical effort and low energy consumption [80]. When added to waters contaminated with microplastics, organosilanes attach to the microplastics surface and collect them in agglomerates [80, 124, 140]. Subsequently, a water-induced sol-gel process, based on hydrolysis and condensation reactions, leads to the formation of siloxane bonds between the organosilanes. In the reaction 3-dimensional networks, hybrid-silica, are formed, which fix the agglomerates chemically and can be easily removed from the water.

An advantage of this process compared to common coagulants is the broad variety and easy customizability of organosilanes, which gives them a high potential to be adapted for the removal of the various polymer types [164]. Also, the chemical fixation, enabling the formation of large agglomerates and the flotation of those agglomerates, which makes them easy to remove, is an advantage [80]. A recent study could prove the higher effectiveness of organosilanes for microplastic removal over common iron and aluminum-based flocculants [158]. Additionally, it was proven that the selection of the right organosilanes leads to a complete reaction into solid hybrid silica during the removal process, which is why they are removed from the water and therefore do not represent any potential risk [164]. Furthermore, the organosilanes are ecotoxicologically tested before testing on a technical scale [124].

The agglomeration process is mainly driven by the interaction of the organic group of the organosilane and the surface of the microplastics [164]. Previous studies showed that the polymer type and therefore surface chemistry can strongly affect the removal behavior. Microplastics in the environment are typically covered with biofilms and various studies showed that biofilm growth changes the properties of microplastics [165]. Therefore, this study investigates how biofilm coverage affects microplastic agglomeration and removal.

Studies investigating biofilm growth on plastics and microplastics usually incubate the plastics in the environment or simulated environmental conditions for several weeks up to several months, which is a time-consuming process [165–169]. The process is strongly dependent on the bacteria in the incubation media, the nutrient availability, the flow conditions, but is also affected by other environmental factors like temperature, pH value, or oxygen availability. Certain bacteria species, e.g. *Bacillus subtilis* which is often used in model experiments investigating biofilm formation, have a higher affinity for biofilm formation than others [166]. High nutrient availability and nutrient exchange by suitable flow conditions promote biofilm growth [171–173]. Flow conditions with too strong shear forces can cause biofilm detachment and be hindering. By optimizing these conditions the biofilm growth can be accelerated. Therefore and to enable biofilm growth under controlled laboratory conditions, a new method for biofilm growth on microplastics in packed bed columns operated with biologically treated municipal wastewater enriched with organic carbon was developed. The collected biofilm-covered microplastics were further tested for removal with organosilanes.

4.2 Material and Methods

4.2.1 Used microplastics and chemicals

The used microplastic samples are a mixture based on fine-grained plastic granulates produced for industrial processing. Five of the most common polymer types were tested (Table 4-1).

The three organosilanes used in this study proved to be the most suitable in previous studies [140, 164]. n-Butyltrichlorosilane (CAS 7521-80-4), (3-Chloropropyl)trichlorosilane (CAS 2550-06-3), and aber eco Wasser 3.0 PE-X® (AB930009), a mixture of organosilanes, were provided by aber GmbH, Karlsruhe, Germany. aber eco Wasser 3.0 PE-X® is abbreviated as PE-X.

Table 4-1: Overview of microplastics (fine-grained plastic granulates) used in the experiments.

Polymer type	Abbreviation	Mean size [μm]	Supplier
Polyethylene	PE	318 ± 258	LyondellBasell, Basell
Polypropylene	PP	(Mixture, 50/50)	Polyolefine GmbH, Frankfurt, Germany
Polyamide	PA	357 ± 60	EMS-Grilltech,
Polyester	PES	54 ± 87	Domat/Ems, Switzerland
Polyvinylchloride	PVC	110 ± 25	Sigma-Adrich, Taufkirchen, Germany

4.2.2 Biofilm growth on microplastics

To avoid clogging of the filters or columns, the respective microplastics were sieved to remove particles smaller than 50 μm . 5 g microplastics were filled into custom-made Plexiglas columns (3,9 x 10 cm) which were closed with nylon filter membranes (pore size 30 μm , diameter 47 mm, Merck Millipore, Germany) on both sides (Figure 4-1). As inoculum and culture medium a sample of biologically treated wastewater was taken from the tertiary clarifier of the municipal wastewater treatment plant Landau, Germany. 2 l of the wastewater was filled into a glass bottle and mixed with 2 g glucose, to ensure high availability of organic carbon for the entire duration of the experiment. The wastewater was stirred slowly and aerated. The bottle with wastewater and the Plexiglas columns were connected using PTFE tubes (1.6 mm inner diameter). The water was pumped through the packed bed column using a peristaltic pump (Ismatec REGLO Analog equipped with PharMed Ismaprene tubes, Cole-Parmer GmbH, Wertheim, Germany). The flow speed was adjusted to reach 1 cm/min in the Plexiglas column. Once per day the column was turned upside down to mix the particles. After 7 days the microplastics were filled into beakers filled with tap water and stored in the fridge at 5 °C for the time they were used for the experiments.

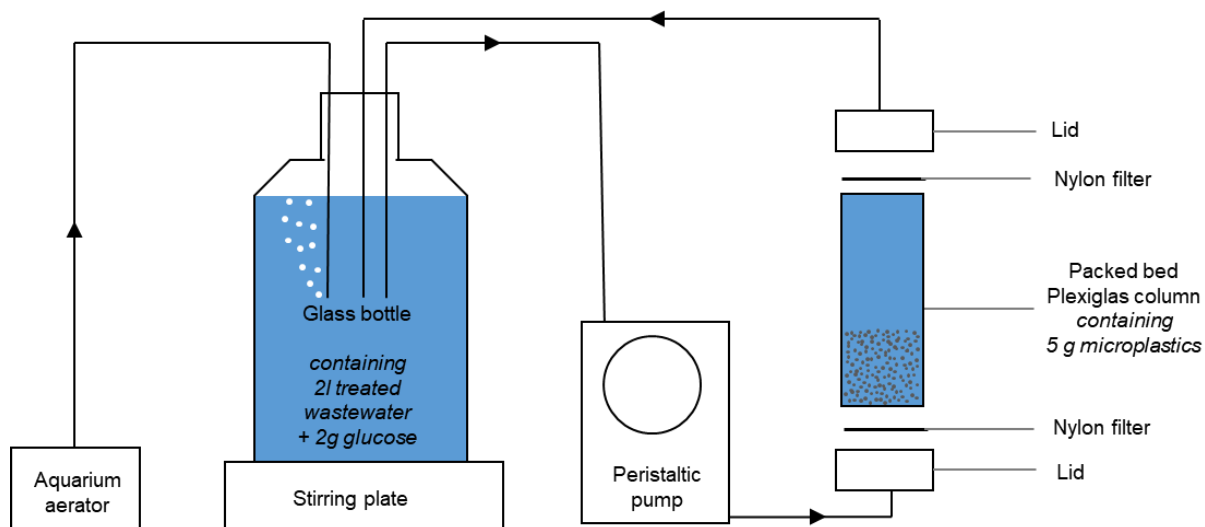


Figure 4-1: Experimental setup for biofilm cultivation on microplastics in packed bed Plexiglas column.

4.2.3 Biofilm characterization

Confocal laser scanning microscopy (CLSM) was performed using a Zeiss LSM700 (Carl Zeiss MicroImaging GmbH, Jena, Germany) equipped with an A-Plan 10x/0.25 M27 objective. Image stacks were recorded for the whole particles and processed using the maximum intensity projection of the Carl Zeiss Zen software (black edition, 2012, version 8.1.2.484). Detailed setting can be found in section S1.

Aleuria aurantia lectin (AAL) Fluorescein isothiocyanate (FITC) (LINARIS Biologische Produkte GmbH, Dossenheim, Germany) was used to stain extracellular polymeric substances (EPS) glycoconjugates according to Staudt et al. (2003). Nucleic acids were stained using SYTO 60 (Thermo Fisher Scientific, Schwerte, Germany). For the staining process wet microplastics were placed on a microscope slide and stained applying 40 μL of SYTO 60 working solution (5 μM) and 40 μL of AAL-FITC working solution (50 μM) for 15 min. After staining, the solution was drained from the slide with a paper towel, and particles were carefully rinsed with tap water. As both dyes showed strong fluorescence signals with virgin PA, PES and PVC particles without biofilms, CLSM images could only be taken for PE and PP, where the stained virgin particles show no signals.

For scanning electron microscopy (SEM) the biofilm covered and virgin samples were dried for 24h at 105°C. Subsequently, they were placed on the sample holder using conductive tape (Plano, Wetzlar, Germany) and sputter coated with an approximately 10 nm layer of Pt using a Leica EM ACE600 (Leica Microsystems, Wetzlar, Germany). The images were recorded with an LEO 1530 (Zeiss, Oberkochen, Germany) under a pressure of 5×10^{-6} mbar using a secondary electron detector with an acceleration voltage of 3 kV.

Contact angle measurements were performed with the sessile drop method using an OCA 20 (DataPhysics Instruments GmbH, Germany) using distilled water with a drop volume of 10-20 μl . The

measure was taken 10 seconds after the drop was applied to the surface. To enable the measurement of microplastic particles, a procedure originally developed for soil samples was applied (Bachmann et al., 2000). Double-sided tape was attached to microscope slides, which were pressed into previously dried (105°C, 24 h) microplastics with and without biofilm coverage. Every sample was measured 10 times, to compensate for measurement fluctuations caused by the uneven surface. The lowest and highest value were removed for each measurement series.

Fourier-transform infrared (FTIR) spectroscopy (4000–300 cm^{-1} , resolution 1 cm^{-1}) was carried out with the ATR-FTIR spectrometer Vertex 70 (Bruker, Ettlingen, Germany) for all biofilm-covered and virgin microplastics. Samples had been dried previously for 24 h at 105 °C. A small spatula of the microplastics was put on the ATR Crystal and pressed down with the pressure applicator.

4.2.4 Determination of removal efficiency

The removal efficiency was determined gravimetrically following Sturm et al. 2020. 1 l tap water was filled into a 2-liter beaker. 100 mg microplastics were added. The biofilm-covered microplastics must be weighed in a wet state. Therefore, it was filtered using a filter crucible (DWK Life Sciences, 30ml, 4, 10 – 16 μm) and weighed wet. The weight loss in the drying process was determined with approximately 100 mg of each polymer in triplicates dried for 24h at 105°C. Thereby, the amount of wet microplastic that must be weighed in to obtain 100 mg dry weight was calculated.

After adding the microplastics, the mixture was stirred for 5 minutes at 500rpm. Subsequently, 100 μl of organosilane were added and stirred for 20 minutes. Everything is filtered through a 1 mm mesh size stainless steel sieve. Agglomerates larger than 1 mm remaining in the sieve are classified as removed, as from this size the agglomerates proved to be easy to remove in pilot plant experiments (WWTP Landau, Germany, results not published). The filtered suspension is filtered again using a filter crucible (DWK Life Sciences, 30ml, 4, 10 – 16 μm), flushed with isopropanol to remove organosilane residues, and dried for 24 h at 105°C. The microplastics in the filter crucible are classified as free microplastics. Microplastics and smaller agglomerates sticking to the wall or the bottom of the beaker, which cannot be removed by rinsing thoroughly with the wash bottle, are considered removed.

4.2.5 Biofilm removal from microplastics

The biofilm-covered microplastics were filled into a 20 ml glass vessel with 10 ml tap water respectively H_2O_2 (35%) and 4-5 grains of $\text{FeSO}_4 \times 7 \text{H}_2\text{O}$. The vessel was placed for 15 minutes in an ultrasound bath (Sonorex Super RK 102 H, Bandelin, Berlin, Germany) at maximum intensity (120 W) then filtered and rinsed with tap water.

4.3 Results and Discussion

4.3.1 Biofilm growth and characterization

4.3.1.1 CLSM images

The CLSM images (Figure 4-2) show attached bacteria and the formation of extracellular polymeric substances (EPS) on the microplastics. Red areas (Syto 60, nucleic acids) are colonized with bacteria, and green areas (AAL-FITC, EPS) are covered by EPS glycoconjugates. It can also be seen that the particles are not evenly covered with biofilms. Some areas are covered more densely than others and some areas are free of biofilm. This indicates a not yet fully developed biofilm after the 7 days of incubation. The biofilm thickness detected with CLSM is below 50 μm , which was analyzed in the 3-D renders of the Zeiss Zen black software. The images, which were taken after stirring in water for 20 minutes, as it takes place during the removal experiments, prove that the biofilm does not completely detach from the plastics and the surface is still covered by biofilm.

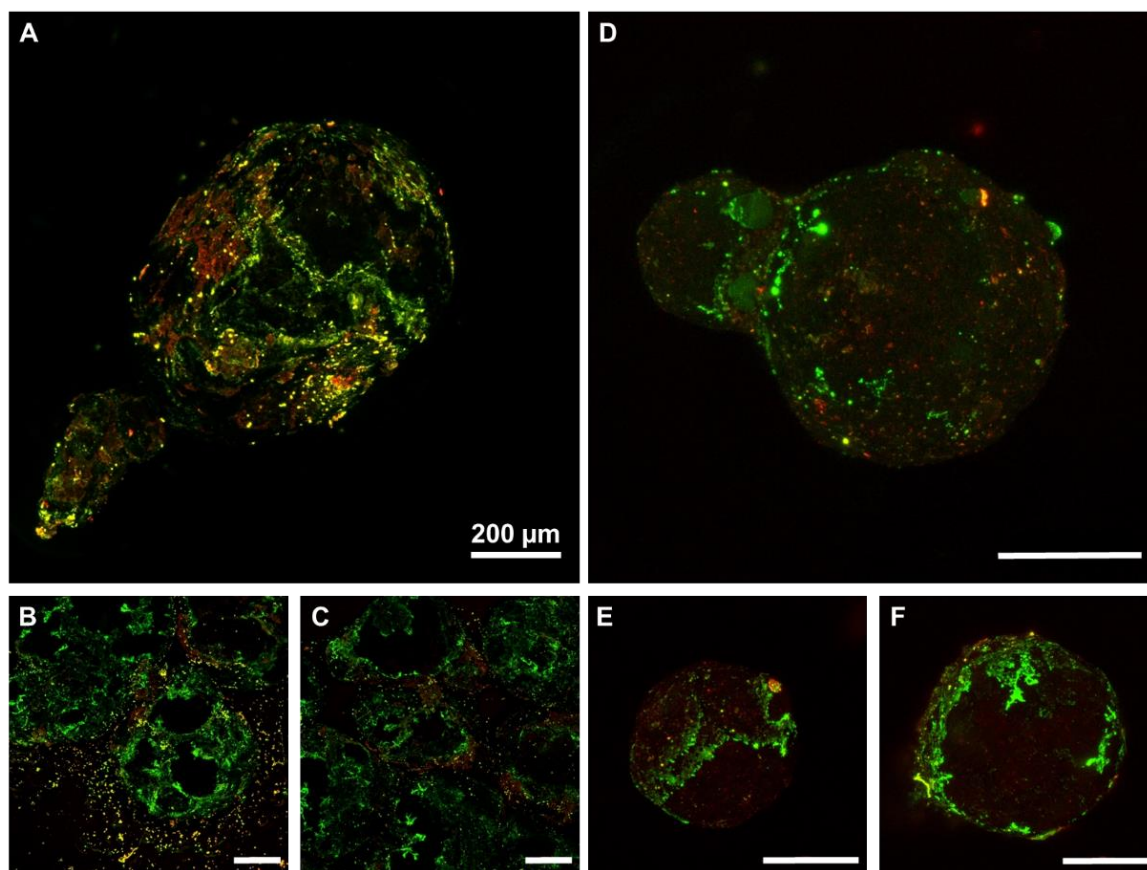


Figure 4-2: CLSM images (maximum intensity projection) of PE and PP based microplastics covered with biofilm. Red areas (Syto 60, nucleic acids) are strongly colonized with bacteria, and green areas (AAL-FITC, EPS) show EPS coverage. A = PE fresh, B+C= PE stirred in water for 20 min, D = PP fresh, E+F = PP stirred in water for 20 minutes.(Figure A3-7 is a version for red-green color blind people).

The CLSM analysis is a well-suited tool for screening the biofilm coverage of microplastics, as the staining provides the possibility to distinguish between different biofilm structures on the microscale. With larger magnification, it is also possible to visualize single bacteria [167, 168]. Unfortunately for AAL-FITC and Syto 60, virgin PA, PES, and PVC showed already strong fluorescence signals. Therefore, for those polymers no CLSM images are available. Fluorescence signals of plastics arising from certain dyes are a known phenomenon and can also be used for microplastic detection [87, 96]. There is a variety of dyes available to visualize additional structures, like structures containing protein, polysaccharide or silica [167, 168].

4.3.1.2 SEM imaging

Another often applied method to investigate biofilm formation on microplastics with a special focus on changes in the surface morphology is SEM [169]. Figure 4-3 compares SEM images of virgin microplastics with biofilm-covered microplastics after the incubation.

For the microplastics used in our study, virgin microplastics already show structures similar to biofilm-covered microplastics or surfaces [170, 171]. In direct comparison of both samples, the attachment of cells and EPS formation can be confirmed. Identifying surface changes by EPS coverage is challenging, as it is difficult to distinguish between EPS-covered surfaces and the rough surface structures of the virgin plastics. For smooth plastic surfaces, this identification is much easier [171, 172]. Due to the applied drying process, some of the cells were conceded or shrunken. This can be avoided by more advanced sample preparation [170–172].

The SEM images indicate partially biofilm-covered microplastics, in an early stage of biofilm formation, where cells attach to the microplastics and start forming communities producing EPS and stretching over the surface [169] This corresponds to the CLSM observation, whereby CLSM shows a clearer differentiation of plastics and biofilm while SEM enables better resolved visualization of the surface morphology.

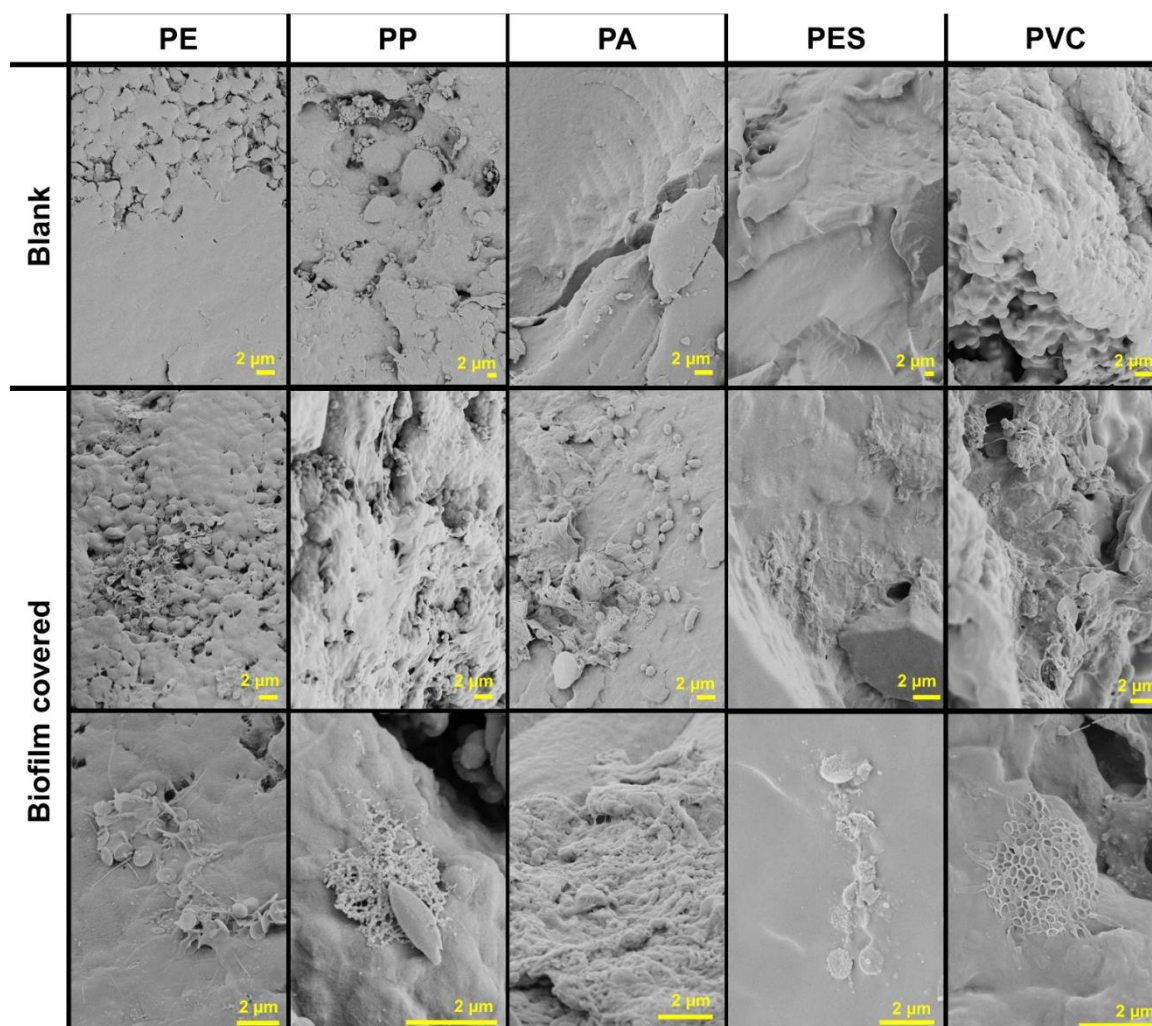


Figure 4-3: SEM images of virgin microplastics in comparison to biofilm-covered microplastics. SEM images indicate an early stage of biofilm formation. Cells are attached to the microplastics and start forming communities producing EPS and stretching over the surface.

4.3.1.3 IR Spectroscopy

A fast and easier to apply method for the identification of biofilm or fouling formation on plastics and microplastics is FTIR spectroscopy, which can be done within a few minutes for each sample [173]. Figure 4-4 shows FTIR spectra of virgin PE, PE covered with biofilm, and pure biofilm grown on the nylon filter during the blank experiment. PE shows the typical bands at 2915 cm^{-1} and 2845 cm^{-1} (C-H stretch), 1472 cm^{-1} and 1462 cm^{-1} ($-\text{CH}_2-$ bend) and 730 and 717 ($-\text{CH}_2-$ rock) [153]. The biofilm shows a broad band from $3600\text{--}3000\text{ cm}^{-1}$ which is a typical area for stretching vibrations of $-\text{OH}$ or $-\text{NH}$ groups. The band from $3000\text{--}2800\text{ cm}^{-1}$ can be assigned to C-H stretching vibrations. From 1750 cm^{-1} to 400 cm^{-1} is an area with various peaks overlapping. This area is typical for numerous chemical groups from biomolecules the biofilm consists of, such as proteins, polysaccharides, and lipids. As those have a very high chemical complexity, it is not possible to assign them.

Comparing the biofilm-covered PE with the virgin PE, the bands of the biofilms are visible at 3600-3000 cm^{-1} , 1550 cm^{-1} , 1250-950 cm^{-1} and 500 cm^{-1} are clearly visible. This enables fast and easy detection of biofilm on microplastics and also shows that due to the biofilm coverage and adsorption of organic matter, the chemical composition of the microplastic surface changes [165, 173]. A disadvantage of this method is, that biofilm heterogeneity, structure or coverage can not be measured with this method. More advanced spectroscopic methods, as Raman microscopy, could give more information about these aspects and the chemical modification of the surface [174, 175].

Checking the FTIR spectra of the other polymer types (Fig A3-1 – A3-4), for PP also a clear signal is visible for biofilm-covered microplastics. For PA and PVC, it is more difficult to distinguish the changes in the spectra caused by biofilms, as they have more bands overlapping with the biofilm spectra. For biofilm-covered PES the biofilm could not be observed in the IR spectra, as the biofilm signal is too weak in comparison to the PES signal and there are too many overlapping bands. Therefore, IR spectroscopy is fast and easy to apply, but not suitable to detect biofilms for all polymer types.

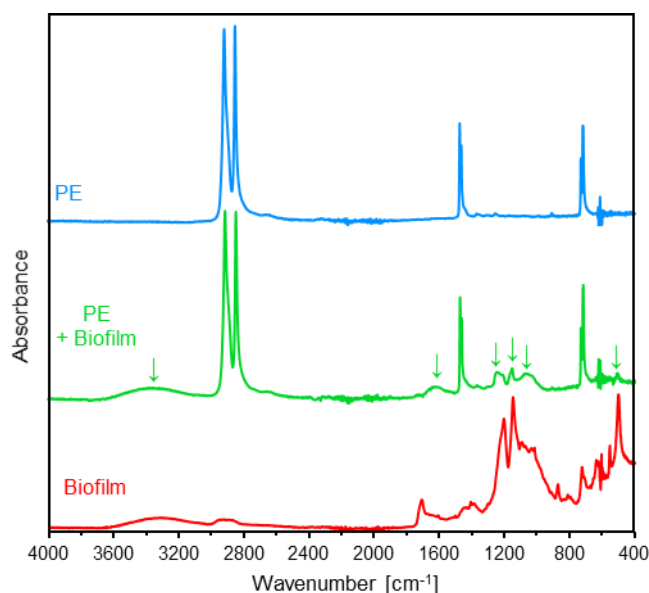


Figure 4-4: FTIR spectra of virgin PE, a pure biofilm sample, and PE covered with biofilm. Both signals can be seen in the sample of PE with biofilm, the biofilm signals are marked with green arrows.

4.3.1.4 Contact angle measurement

To investigate the changes of hydrophilicity on the surface, a helpful method is contact angle measurement (Table 4-2). The only hydrophilic virgin polymer in this series with a contact angle under 90° is PVC. PE, PP, PES, and PA are hydrophobic. For those, biofilm coverage causes a reduced contact angle, whereas biofilm-covered PE and PP are still in the hydrophobic area. Biofilm-covered PA and PES show stronger changes and enter the hydrophilic area. For PVC it is the other way around and the contact angle increases into the hydrophobic area for the biofilm-covered PVC. This might be caused

by biological degradation processes like dechlorination or the degradation of additives contained in the PVC [176–178]. This changes can not be detected in the FTIR measurements, as it is not sensitive enough. The chemical transformation only happens in a thin surface layer but the IR-beam penetrates the sample and reaches chemically unaltered areas [33, 34].

The surface roughness of the microplastic particles as well as the roughness caused by the particles themselves changes the measured contact angles [179, 180]. As the microplastics used in these experiments have different particle size compositions and surface roughness, they can not be directly compared among each other. However, the comparison of virgin microplastics and biofilm-covered microplastics can show that the biofilms change the polarity and wettability of the microplastic surfaces, which should also affect the interaction of the organosilanes with the surface during the removal process [73, 164].

Table 4-2: Contact angles measured for microplastics with and without biofilm. Ten measurement replicates per sample, lowest and highest value were removed.

Polymer	Sample	Mean	S.D.
PE	Virgin	128.8	2.9
	With biofilm	110.1	5.0
PP	Virgin	135.8	8.2
	With biofilm	113.9	4.7
PA	Virgin	132.9	1.1
	With biofilm	86.2	5.7
PES	Virgin	112.5	6.5
	With biofilm	78.0	4.5
PVC	Virgin	76.0	3.0
	With biofilm	108.3	1.4

3.1.5 Evaluation of biofilm growth and its method

Summarized the CLSM- and SEM images show that after 7 days of incubation in the packed bed column the microplastics were partially covered by a biofilm in an early stage of development, forming an EPS-matrix and starting to spread over the entire microplastic surface. The FTIR-Spectroscopy and contact

angle measurements can be used to prove and partly quantify (contact angle) the biofilm formation [181]. Therefore, the applied methods are well suited to investigate the effect of biofilm formation on microplastic removal.

Biofilm growth on plastic and microplastic surfaces can also be performed by incubating the plastics directly in the environment or simulated environmental conditions for several weeks up to several months [165, 167, 170, 182, 183]. The method presented here provides a possibility to grow a biofilm on microplastic with clearly defined conditions. The fast development in biofilm formation is caused by the high nutrient content in the water. Moreover, the flow conditions with optimized mass transfer trigger a high nutrient availability [184–186]. By further optimization of the process, especially flow conditions (e.g., flow velocity, shear stress) and nutrient availability (e.g., optimized culture medium by adding specific nutrients, self-created culture media), a faster biofilm formation should be feasible. Additionally, sterilized culture media could be inoculated with biofilm-forming bacteria, as *Bacillus subtilis* [166]. Also, different environments (e.g. saltwater, freshwater) or environmental conditions (oxic, anoxic) can be simulated, to check their influence on the biofilms. The main purpose of the presented method is then the delivery of biofilm-covered microplastic for further experiments.

4.3.2 Removal of biofilm-covered microplastics.

4.3.2.1 Effect of biofilm on microplastic removal

Figure 4-5 shows the removal efficiencies of microplastics covered with biofilm in comparison to virgin microplastics (data for virgin microplastics originate from Sturm et al., 2021). It can be seen that for the combinations of polymers and organosilanes tested in this study, the biofilm coverage decreases the removal efficiencies. Biofilm-covered PP and silane A (PE-X) is the only combination reaching a considerably high removal of 92.8%. The next highest removals are achieved by biofilm-covered PE removed with silane A (71.9%) and biofilm-covered PP removed with n-butyltrichlorosilane (64%) (silane B). All other combinations reach low removal efficiencies between 32.3% and 3.8%.

Previous studies showed that the interaction of the polymer surface and the organic group of the organosilane are essential for the agglomeration process, as they cause adsorption of the organosilanes onto the microplastics surface and the collection of those in agglomerates [164]. Nonpolar polymers, such as PP and PE, were removed well using non-polar organosilanes, such as silane A and silane B. Polar polymers, such as PVC, were removed better using polar organosilanes, such as chloropropyltrichlorosilane (silane C). For polymers with intermediate polarity, here PA and PES, both types of organosilanes had similar removal efficiencies.

As the biofilm coverage, as well as adsorption of organic molecules and possible biodegradation processes, change the surface properties of the microplastics, also the interaction with the organosilanes, and therefore the agglomeration and removal behavior is affected [73, 187–189]. Especially the EPS with its gel-like structures can affect this process strongly. The better removal of biofilm covered PE

with silane A and the biofilm covered PP with silane A and B compared to the other combination is caused by parts of its surface staying uncovered from biofilm, which still can interact well with the silanes A and B. The worse removal of biofilm-covered PE compared to PP might be due to stronger biofilm coverage of PE. Polar silane C shows a poor interaction with the non-polar virgin PE and PP [164]. Biofilm coverage does not change this performance.

Considering the removal efficiencies of the intermediate polar polymers PA, PES, and the polar polymer PVC, all of the silanes tested reached low removal efficiency under 32.3% for the biofilm-covered microplastics. This is caused by the fact, that the tested silanes interact worse with these virgin polymers than with the non-polar PE and PP. Therefore the parts of the surface which are uncovered from biofilm interact worse and the lower removal efficiency is reached. Also, there are no consistent differences between the use of polar and non-polar organosilanes. Therefore, the higher polarity of silane C does not lead to a better interaction and removal performance for biofilm-covered microplastics.

Lapointe et al. 2020 investigated the effect of weathering and natural organic matter (NOM) adsorption on the coagulation of PE with an aluminum-based coagulant. Here the weathering and NOM adoption led to improved coagulation, as the introduction of new chemical groups improved the interaction with the coagulant. Biofilm coverage was not considered. But these results also demonstrate the importance of environmental exposure for coagulation experiments with microplastics, as the properties can be affected strongly.

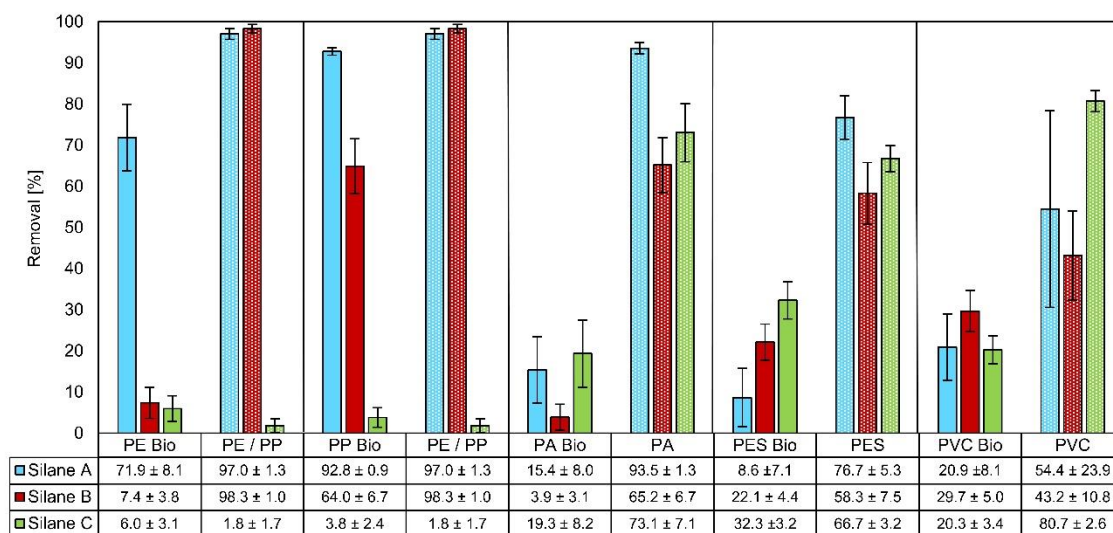


Figure 4-5: Comparison of removal efficiency of microplastics with and without biofilm. 100 mg microplastics were removed from 1l tap water using 100 µl organosilanes. Silane A = PE-X; Silane B = n-Butyltrichlorosilane; Silane C = Chloropropyltrichlorosilane, Bio = biofilm covered. Data for virgin microplastics originate from [164], where the same microplastics and organosilanes were used. For virgin microplastics, PE and PP were combined as they showed the same removal behavior.

3.2.2 Biofilm removal using ultrasound and H₂O₂.

To check whether a mechanical or chemical treatment could remove the biofilm from microplastics and lead to better removal, biofilm-covered PE and PA were treated with ultrasound and a combination of ultrasound and H₂O₂. The data (Figure 4-6) shows that biofilm removal using ultrasound and ultrasound combined with H₂O₂ treatment increase the removal efficiency of the biofilm-covered microplastics from water. Biofilm removal could be confirmed using CLSM imaging (Figure A3-5 – A3-6). As the ultrasound treatment removes the biofilm efficiently, the additional H₂O₂ treatment does not lead to any improvement. Differences in the removal efficiencies are within the standard deviation. The values of virgin PE and PA (Figure 5) could not be reached after the biofilm removal. This is probably due to chemical transformation processes of the plastic surface by degradation and biodegradation processes, leading to worse interaction with the organosilane [73, 187, 188].

Ultrasound treatment is also applicable on a technical scale. As it would add additional complexity and energy consumption to the process, an adaptation of the organosilanes would be the preferred option. Improved chemical characterization of the changes in the surface, for example by Raman microscopy or mass spectrometry-based techniques, could be helpful to enable more targeted interactions [175, 189].

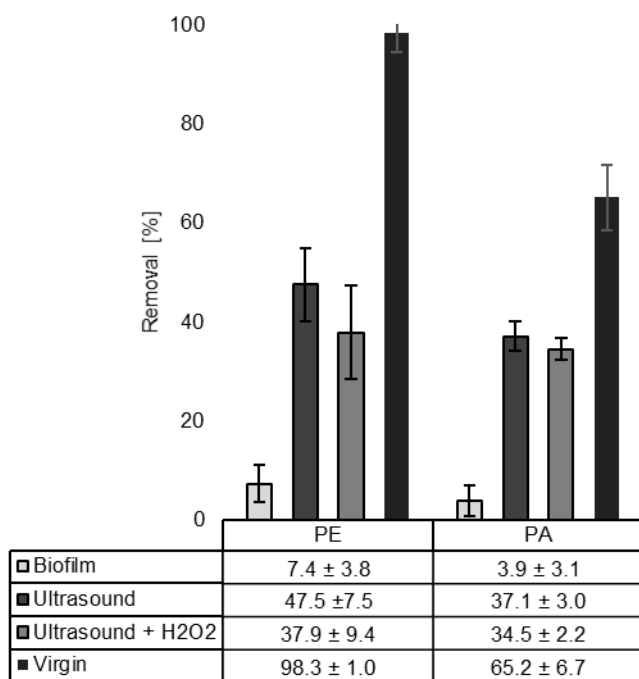


Figure 4-6: Comparison of biofilm-covered microplastics and biofilm-covered microplastics after biofilm removal with ultrasound or a combination of ultrasound and H₂O₂. 100 mg microplastics were removed from 1 l water using 100 µl silane B (n-butyltrichlorosilane).

4 Conclusions

With the here presented packed bed column, a biofilm could be cultivated on the surface of microplastics within 7 days. The growth conditions are optimized with a constant flow of water and continuous nutrient supply. This leads to faster biofilm formation compared to studies placing the samples in the environment or simulated environments. Optimization of this method is expected to lead to faster biofilm growth. Also, the effects of different types of waters should be tested and investigated, to get biofilms representative to different environments. As simulated environmental exposure is essential to get representative results in microplastics research, this method could lay the foundation for a standardized, fast, and well controllable method to cultivate biofilms on microplastic samples.

To characterize the biofilms on microplastics, CLSM imaging was well suited to visualize the distribution of the biofilm on the surface of the PE- and PP-based plastic particles to distinguish different structures. The dyes chosen dyed the other virgin polymers (PES, PA, PVC), which prevented biofilm detection for those. Application of other fluorescent dyes might be suitable for those polymers. SEM works well to visualize the surface morphology of the plastic particles and the changes caused by biofilms. However, some structures of virgin microplastics are very similar to biofilm structures, which makes it challenging to detect biofilms on plastics without a reference sample for comparison. FTIR spectroscopy is a well-suited method for rapid detection of biofilms on microplastics, but for more chemically complex polymers it is more difficult to apply, as bands of the polymers and biofilm can overlap. Contact angle measurement is a good method to investigate the change of hydrophilicity caused by the biofilm coverage.

As the biofilm coverage changes the surface chemistry and deteriorates the interaction with the silanes, biofilm coverage leads to worse removal efficiencies for the combinations of the polymers and silanes tested in this study. Biofilm removal by ultrasound could improve the removal efficiencies of the microplastics from water, whereby the values of virgin polymers could not be reached after biofilm removal. This is probably due to biochemical degradation processes chemically modifying the polymer surface, affecting the interaction with the organosilanes. As ultrasound treatment adds more complexity to the process, it is more favorable to adapt the organosilanes for better interaction with biofilm-covered or chemically transformed microplastics. First discovered in 2017, the topic of organosilanes for microplastic removal is still little researched. Organosilanes are a big chemical class and easily chemically modifiable. Therefore, they have high adaptability and in further studies, different organosilanes could be tested and specifically modified for this purpose.

5 The potential of fluorescent dyes – Comparative study of Nile red and three derivatives for the detection of microplastics

Published as: Sturm MT, Horn H, Schuhen K. *Anal Bioanal Chem.* 2021;413:1059–71. doi:10.1007/s00216-020-03066-w.

5.1 Introduction

Plastic litter, on macro, micro and nano scales, is widespread and has accumulated worldwide in our environment [6, 36, 190]. In 2010 alone, the amount of plastic waste discharged into the oceans was estimated at up to 12.7 million tons [12]. Due to ultraviolet (UV) radiation, oxidation and mechanical forces, plastic items break down into increasingly smaller microplastic fragments, below 5 mm in diameter [19]. These are then located in the water column, sink to the bottom or are distributed over long distances by air and land [27, 191].

Micro-sized fragments such as synthetic fibers from textiles, facial cleansers and many other products also introduce microplastics via the direct path (primary microplastics) [191]. This has led to a build-up of microplastics of varying sizes, composed of different polymer types, across a wide array of marine habitats. Because of their size, microplastics are available and ingested by a broad range of organisms, possibly threatening ecosystems and even human health. [19, 135, 192, 193]

The risks that microplastics pose to marine life and humans are widely recognized and have been included in national and international marine protection strategies, policies and legislation (e.g. EU Marine Strategy Framework Directive) [38]. Knowledge of plastic concentrations, spatial and temporal changes, sizes, polymer distributions and fragmentation dynamics are a prerequisite for understanding the fate and impact of microplastics (Figure 5-1) [194]. To monitor spatial and temporal trends of microplastics, simple, cost-effective and standardized protocols, capable of efficiently and accurately enumerating microplastics in a wide variety of environmental matrices, need to be developed. However, efficient identification and quantification of microplastic contamination is a major challenge, because as the size of the particles decreases, it becomes increasingly difficult to detect them and distinguish them from natural particles.

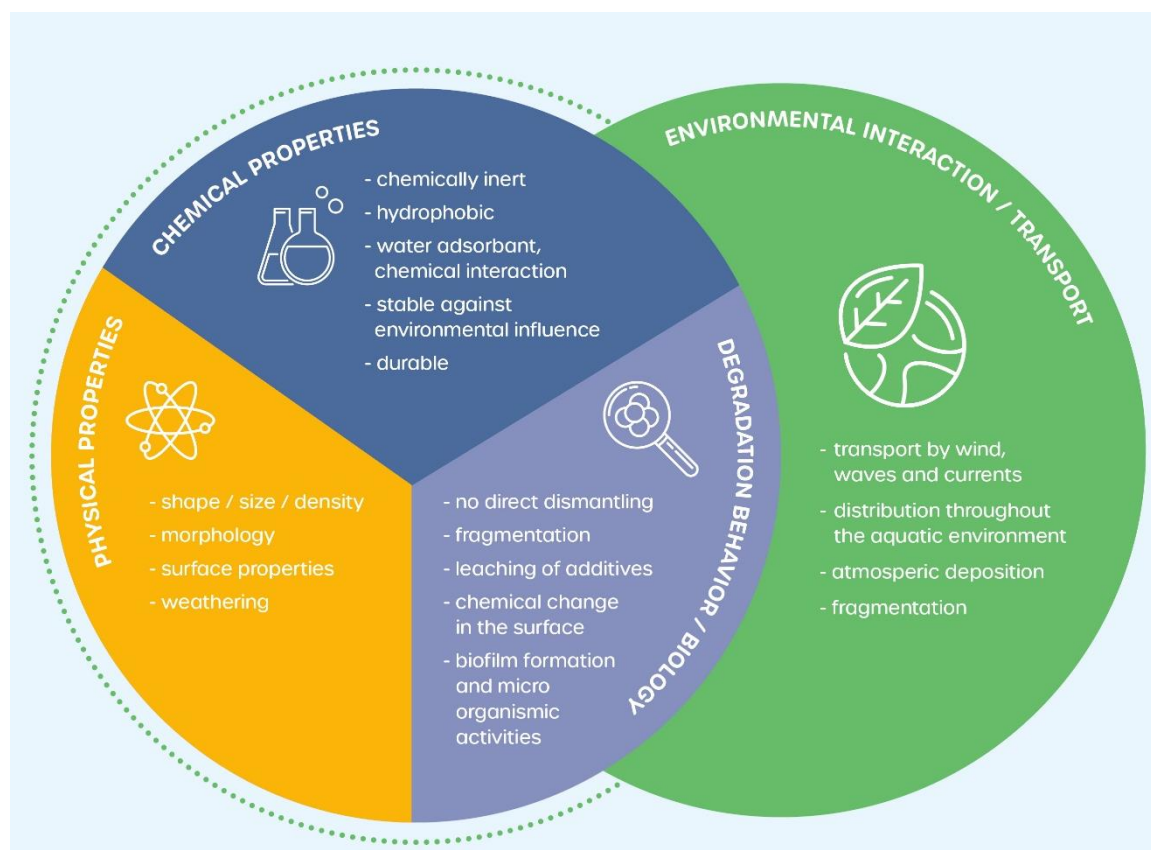


Figure 5-1: Chemical, physical and biological influence on microplastics in environmental samples [196–198].

5.1.1 State of the art: Methods for the detection of microplastics in ecosystems

The monitoring of microplastics is divided into sampling, sample preparation and detection [83]. So far, all analytical methods need time-consuming and complex extraction and sample preparation before the microplastics can be detected. In most water studies, microplastics are sampled using plankton nets with a mesh size of about 0.33 mm [83, 195]. Smaller mesh sizes lead to clogging after only a short time. In sediment samples, a density separation with highly concentrated salt solutions separates floating microplastics from sinking mineral components.

To reduce the quantity of natural particles and potential false positives, natural organic substances are decomposed chemically, most commonly by using hydrogen peroxide (H₂O₂) or potassium hydroxide (KOH) solutions or less aggressively using specific enzymes (e.g. cellulase, protease, chitinase). In this process, it is important to find a method that does not damage the microplastics in the sample. Figure 5-2 shows a schematic representation of the proposed approach for sample preparation, which was developed for the isolation of microplastics.

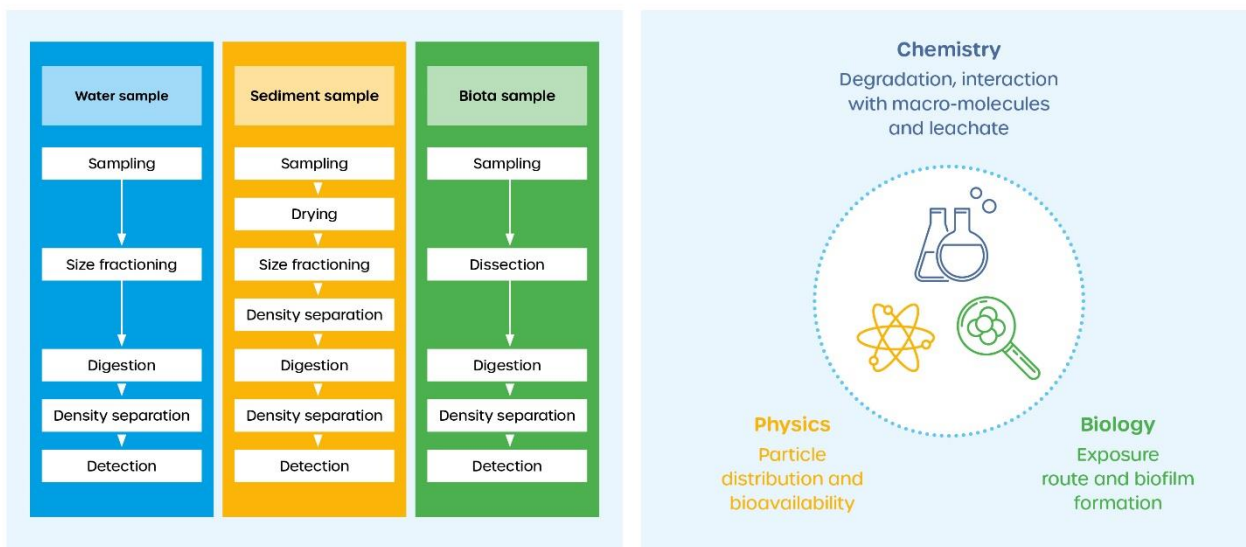


Figure 5-2: Process of microplastic detection in environmental samples (left) and overview of existing requirements on experimental design based on chemical, physical and biological effects (right) [196–198].

Despite the complex processing, not all natural organic particles can be separated from the microplastic. Renner and his colleagues have reviewed more than 170 peer-reviewed research papers published between 2015 and 2017 and have been working on the analysis of microplastics to find out how the identification of microplastics is currently performed [199]. The detection, identification, sizing and quantification of microplastics is performed by visualization (with the naked eye or using a microscope) in 79% of the cases examined.

Microplastic particles are identified by their unnatural coloring (e.g. light blue and multicolor) and/or unnatural shape (e.g. fragments with sharp edges, perfectly spherical). but can easily be confused with other anthropogenic or natural particles (fly ash, particles of street paint, metal vapor, fish scales, ceramic flakes, etc.) [133, 199]. The error rate is estimated between 20 and 70% [83]. Thus, a more selective method is necessary to avoid false positives and get precise data.

Addressing this challenge, recent studies have applied chemical analytics to determine polymer types of the processed samples to reduce the risk of false positive / negative misidentification and to introduce automated routines (Figure 5-3, Table A4-1) [84, 89]. The most commonly used methods are vibrational spectroscopy or gas chromatography coupled with mass spectrometry (GC-MS). Fourier transform infrared (FTIR) and Raman spectroscopy can be used to determine exact polymer types of particles larger than approximately 300 μm . Coupled with microscopy these two techniques allow polymer identification of particles down to a few μm . Despite current research attempts on automating IR or Raman microscopy procedures for microplastic identification to make it less time-consuming and more precise, the techniques are not routinely applied for monitoring, because they are still limited by long measurement times, high cost and poor spectral resolution, which makes the processing of larger sample

sets by micro-spectroscopy challenging [200, 201]. Pyrolysis (Pyr) GC-MS can be used to characterize the chemical composition of the microplastics contained in whole samples. As with this method mass balances are measured, there is no information about the size distribution of the microplastics in the sample which is of high interest for the eco toxicological evaluation [39]. In addition, FTIR or Raman microscopes and Pyr GC-MS are rare, expensive and need trained personnel for operation.

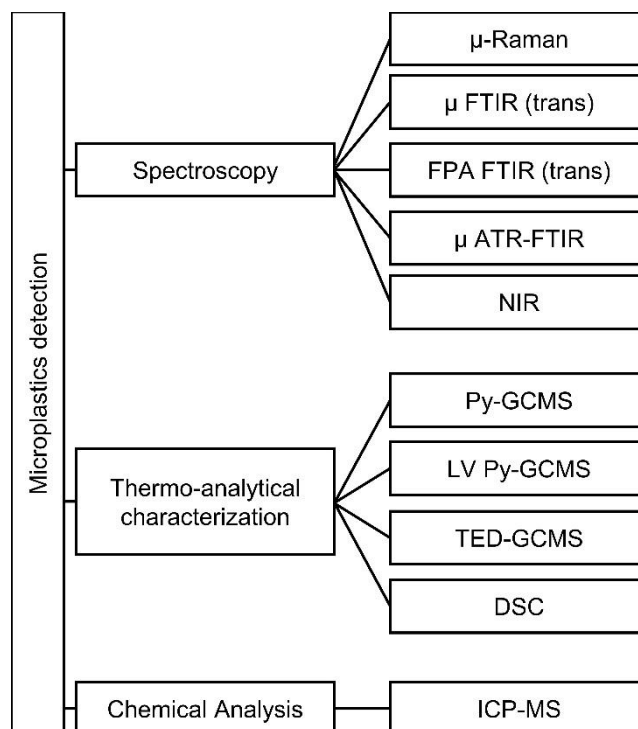


Figure 5-3: Overview of methods used for microplastic detection.

A promising approach for a more rapid and easily applicable detection of microplastics is fluorescent staining. Andradý proposed the use of the lipophilic fluorescent dye NR to stain microplastics in environmental samples, facilitating visualization under a fluorescence microscope [202]. In 2016, Shim et al. evaluated this method for the first time for environmental samples and found out that most polymer types can be selectively distinguished from natural particles [96]. The staining allows for a more selective detection of the microplastics compared with optical microscopy and the only technical device needed is a device for fluorescence imaging such as a fluorescence microscope, which is available at many research institutes, easy to handle and has comparatively cheap acquisition costs. Additionally, there are small and portable or even hand-held versions of fluorescence imaging tools available that could be used directly on site for microplastic detection [203].

5.1.2 Nile red (NR) – A fluorescent dye with high affinity to microplastics but with limitations

NR is a lipophilic fluorescent dye, which allows the in-situ staining of lipids. It has been frequently employed to evaluate the lipid content of animal cells and microorganisms, such as mammalian cells, bacteria, yeasts and microalgae [94]. More recently it has also been used for staining and detecting

microplastics [96, 204, 205]. It is a phenoxazinone dye with low molecular mass and can be present in locally excited (LE), twisted intermolecular charge transfer (TICT) or planar intermolecular charge transfer (PICT) form, the latter two forms having intramolecular charge transfer mechanisms [206]. Despite extensive work on NR photophysics, it is still not fully understood. Various studies in solvents with different polarities suggest that the TICT state is not relevant for the photophysics of NR [207]. Dual emission or strongly quenched emission in either non-polar or polar solvents, which would be caused by an emissive or non-emissive TICT state, is not seen for NR. The major emissive state is supposed to be a planar excited state with a charge transfer character, because of a merocyanine-type chromophore structure [208]. This leads to high fluorescence quantum yields in non-protic solvents [209]. In aqueous environment, hydrogen bonding has to be considered, presumably associated with the quinonimine-zwitterion equilibrium in indoaniline dyes. Additionally, protonation must also be considered.

To detect microplastics in environmental samples, the samples are stained with NR dissolved in an organic solvent in accordance with the microplastic extraction and sample preparation described in the previous section. NR mainly binds to the polymer surfaces via Van-der-Waal interactions with additional dipole interactions in polar polymer types [97]. The recommended digestion method is hydrogen peroxide treatment, after which natural organic substances stained with NR show a significantly weaker fluorescence than microplastics, which gives the method increased selectivity for plastics [205]. Thus, microplastics can then be detected under a fluorescence microscope or by fluorescence imaging, due to their more intense fluorescence. NR could already be used for the effective identification of PE (polyethylene), PP (polypropylene), EPS (expanded polystyrene), HDPE (high-density polyethylene), PC (polycarbonate), PUR (polyurethane) and PEVA (polyethylene vinyl acetate) [96].

The most used wavelengths for microplastic particle detection are at green-yellow fluorescence at an excitation wavelength of 450 to 490 and emission wavelengths from 515 to 565 nm [204]. In addition, Maes et al. showed that the maximum emission wavelengths shift towards longer wavelengths with increasing polarity of the polymers [97]. This behavior might allow microplastics to be categorized into types based on their general hydrophobicity e.g. polyolefin, polyaromatic, polar (polyesters/nylons), or it could provide a useful indicator to evaluate residence time via temporal changes in surface properties due to oxidation or biofouling in the environment. This can be explained by the solvatochromism of NR, meaning its fluorescence emission spectrum shifts depending on the polarity of its environment [97, 210].

There are already attempts to substitute NR with different functional groups in order to achieve better water solubility while maintaining the good fluorescence properties [211]. The NR derivatives have carboxylic acid groups, making them water soluble and enables a possible dissociation depending on the solvent and pH-value.

In our research, the attempt was made to improve the interaction between the microplastic surface and NR by adapting the functional groups with the aim of achieving greater selectivity for plastic particles and more intense fluorescence (Figure 5-4). Furthermore, the influence of using different solvents and different pH-values in water as solvent on the fluorescence properties was investigated.

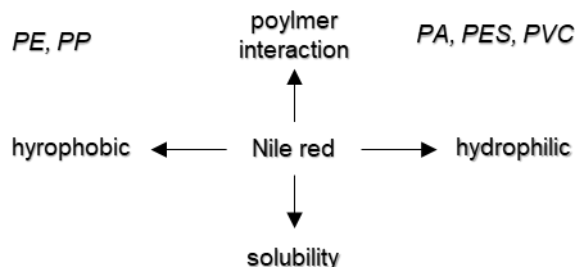
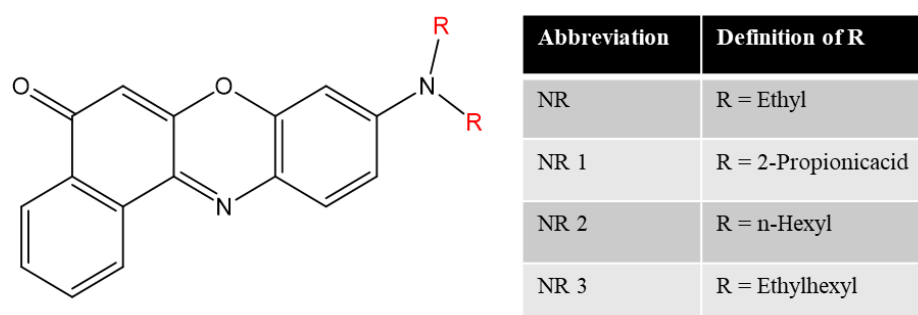


Figure 5-4: NR properties relevant for microplastic detection.

5.2 Material and Methods

5.2.1 Nile red, its derivatives

Nile red (NR, AB139346) and its derivatives (NR1, AB 534698; NR2, AB 534699 and NR3, AB534700) were purchased from abcr GmbH, Karlsruhe, Germany.



Scheme 5-1: Structure of Nile red and newly developed Nile red derivatives.

The ethyl substituents present in NR were replaced with a longer unbranched n-hexyl group (NR2) or branched ethylhexyl group (NR3) in order to increase the lipophilicity and thus the affinity for microplastics. In the case of NR 1, it was investigated whether the substitution by a propionic acid group could increase the affinity for polar polymer types such as PVC.

Microplastic and natural particles

Table 5-1 shows the list of the used microplastics and natural particles. As they are considered as particularly resistant against most digestion methods and present in most samples, as natural particles chitin, wood and chalk, respectively seashell were chosen.

Table 5-1: Microplastics and natural particles used for the experiments

Polymer	Abbreviation	Supplier / Preparation
Polyethylene	PE	LyondellBasell, Basell Polyolefine GmbH, Frankfurt, Germany
Polypropylene	PP	LyondellBasell, Basell Polyolefine GmbH, Frankfurt, Germany
Copolyamide	PA	EMS-Grilltech, Switzerland
Copolyester	PES	EMS-Grilltech, Switzerland
Polyvinylchloride	PVC	Sigma-Aldrich, Germany
Wood	-	Fine shavings of Quercus spec.
Chalk	-	Ground shell of Mytilidae
Chitin	-	Ground exoskeleton of <i>Pandalus borealis</i>

5.2.2 Dyeing of samples in water at different pH-values

Stock solutions of the dyes (1 mg / ml) were prepared for NR, NR2 and NR3 in acetone and for NR1 in isopropanol / acetone (mixture 1:1). 30 ml distilled water respectively 29 ml distilled water and 1 ml 0.1 M HCl- or 1M NaOH-solution were added to an Erlenmeyer flask. Subsequently 0.15 ml stock solution were added and the resulting solution (end concentration 5 mg / l) was stirred mechanically. Subsequently, 3g of polymer or natural particles were added and stirred for 24 h, filtered, washed with 20 ml distilled water and dried for 24 h at 50 °C.

5.2.3 Dyeing of microplastics with different NR concentrations

To check for the occurrence of quenching, dyeing was conducted analogue to the previous step with NR concentration of 5 to 0.005 mg /l.

5.2.3 Dyeing of microplastics with different solvents

60 ml of solvent were mixed with 300 µl of NR stock solution (1 mg / ml in isopropanol; c = 5 mg / l). This solution was mixed with 3 g of microplastics and stirred for 2 h to avoid damage to the polymers through dissolving by the organic solvents. The microplastic was then filtered off and dried at r.t. for 24 h on a dark shelf.

5.2.4 Acquisition of solid sample fluorescence spectra

The spectra were taken with a Horiba Aqualog® (Horiba Jobin Yvon GmbH, Bensheim, Germany). For the measurements, the samples were filled into quartz cuvettes and mounted at a 1933 Solid-Sample-Holder at 55° shift to measure front-face fluorescence. As blanks, unstained microplastics and natural particles were used. Excitation was set to 240-800 nm with 2 nm increment, detection to 245-828 nm with 0.58 nm increment and a integration time of 0.01 s. Post processing: Using the software Aqualog 3.6.11.20 a 1st and 2nd order Rayleigh masking with sum of slit width of 10 nm was applied.

5.2.5 Fluorescence microscope imaging

The images were taken with the fluorescence microscope Zeiss Imager Z.1 (Carl Zeiss Microscopy GmbH, Jena, Germany) in epifluorescence mode using a 10x objective and a mercury vapor lamp as the light source. The used filter sets and exposure times can be seen in Table 5-2.

Table 5-2: Specifications of the used filter sets and exposure times for fluorescence imaging.

Fluorescence color	Filter Name	Zeiss filter set No.	Excitation [nm]	Emission [nm]	Beam Splitter [nm]	Exposure time
Green	FTIC	44	BP 475/40	BP 530/50	FT 500	10 sec
Orange	DsRed	43	BP 550/25	BP 605/70	FT 570	0.5 sec
Red	Alexa Flour 660	26	BP 600/50	BP 685/50	FT 645	0.5 sec

5.2.6 Processing of environmental samples

As an example, for environmental and industrial samples, we used processed and unprocessed sea salt, which is basically only evaporated sea water (Table 5-4). A certain amount of sea salt was dissolved in water to a concentration of 350g/l in a separation funnel. After 24 h, precipitated particles, including hardly soluble sulfates, were separated. Subsequently the sample was filtered through a black filter membrane (Metricel® Black PES, pores: 0.45 µm, diameter 47 mm). The filter was transferred to an Erlenmeyer flask, boiled up once with 20 ml of 35% H₂O₂ and then stored at 60-70 °C for 6 h. After filtering over the black filter membrane (Metricel® Black PES, pores: 0.45 µm, diameter 25 mm), the samples were stained by dropping an aqueous solution of 0.5 mg / l NR and 0.5 mg / l NR3 acidified with HCl (pH = 2.5) on the filter. After 24 h at r.t., the filter was then investigated under the fluorescence microscope using green fluorescence. The lower size limit for microplastics was set to 50 µm.

For samples with a high chitin content, treatment with chitinase is necessary before H₂O₂ treatment. To test this process according to da Costa et al, 20 ml PBS solution (phosphate-buffered saline) and 20 ml chitinase (EC 3.2.1.14, ASA Spezialenzyme GmbH, Wolfenbüttel, Germany) were added to a chitin sample [14].

In order to obtain reliable measured values, the prevention of contamination of the sample with plastic particles from the laboratory environment is necessary. This contamination occurs primarily through plastic particles from house dust and clothing as well as through plastic abrasion from laboratory equipment [30, 83]. Therefore, only materials and vessels made of metal and / or glass are used in sampling and sample treatment. To protect against contamination from dust, sample processing is carried out in a separate laboratory, which is only used for processing MP samples, has a dust protection door and is cleaned with low-lint cotton cloths before each use. In addition, a low-lint protective suit (4510M, 3M Deutschland GmbH, Ness, Germany) is worn, cleaned with a lint brush before entering the laboratory to prevent the entry of clothing fibers. In preliminary tests with blanks, contamination of only

1-3 particles per sample was achieved and the average of two particles per sample was removed from the MP count of the sample.

5.3 Results and Discussion

5.3.1 Influence of solvent on emission spectra

As seen in Figure 5-5, the choice of the solvent influences the emission spectra in their intensity and also in the shift of their band maximum. This can be explained due to the solvatochromism of NR and the incorporation of into the polymeric network by swelling [205, 213–216]. For both, PE and PES, the use of water shows the highest emission intensities. This could be caused by the fact that in the polar solvent water the lipophilic NR sorbs more strongly on the non-polar plastic than in the less polar organic solvents. The solvatochromic effect causes a shift of the emission spectra towards higher wavelengths with increasing polarity of the solvents. Due to swelling, small amounts of the solvent enter the microplastics, a change in polarity is the consequence [212, 213]. The degree of swelling depends on the respective combination of the polymer and solvent. It is to be expected that the organic solution will be absorbed more than water. Another possible effect of the swelling could be the transport of the NR into the polymeric structure. This causes a stronger binding which hinders rotational and vibrational movement of the NR molecule changing the intensity of the emission bands and their ratios [214–217]. As the polymers are non-transparent, the absorption of NR by swelling could also cause a weakening of the signal, as the NR inside the particles is not detected. The shift of the band maximum is more present for PES than for PE, which indicates that there is a stronger swelling for the PES than for the PE.

Nevertheless, the shift caused by the polymer type itself is notably stronger than the shift caused by the solvent. The strong influence of the polymer type on the spectra indicates a strong interaction between the polymer and NR due to the adsorption to the surface or incorporation into to polymeric network by swelling.

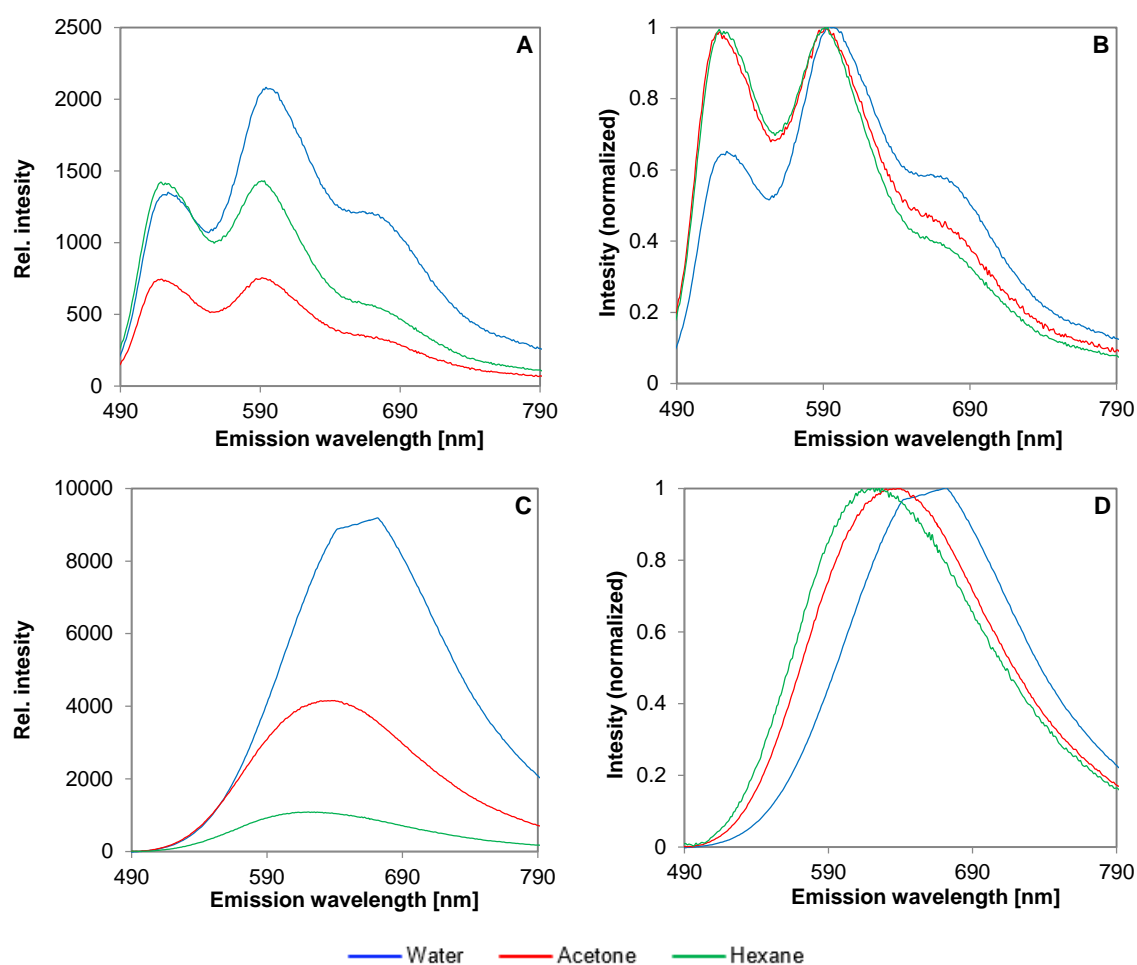


Figure 5-5: Fluorescence emission spectra (excitation at 488 nm) from PE and PES based microplastics dyed with NR in different solvents with different polarities. A = PE; B=PE normalized; C = PES; D =PES normalized. Normalization was conducted via the maximum intensity of the respective spectra. Water = polar, acetone = intermediate polarity, hexane = nonpolar.

5.3.2 Control of the occurrence of quenching

Previous studies reported the occurrence of quenching at higher concentrations of NR [100, 205]. While Erni-Cassola et al. 2017 recommends a concentration of 10 $\mu\text{g} / \text{l}$ to avoid quenching, Shim et al. 2015 used a concentration of 5 mg / l [96, 205]. Hence, the occurrence of quenching was checked by dyeing PE with NR at concentrations from 5 $\mu\text{g} / \text{l}$ to 5 mg / l (Figure 5-6). Here we can see three vibronic bands at 545, 580 and 630 nm. For the band at 580 nm there is a steady increase in the intensity of the fluorescence signal up to the concentration of 5 mg / l . The fitting of a power function shows an average increase of the fluorescence signal by a factor of 3.1 at an increase of the NR concentration by the factor 10. This difference could be caused by slight quenching, which does not yet cause an overall decrease of the signal. For the concentration of 5 mg / l the ratio of the bands changes, as the band at 545 nm shows a reduced increase. This can be caused by as the fact that the adsorbed or embedded NR molecules cannot freely move during the lifetime of the excited state changing the emission intensity of these

vibronic bands and their ratio [214–217]. Due to the good signal at 580 nm, the concentration of 5 mg / l was maintained for the further experiments

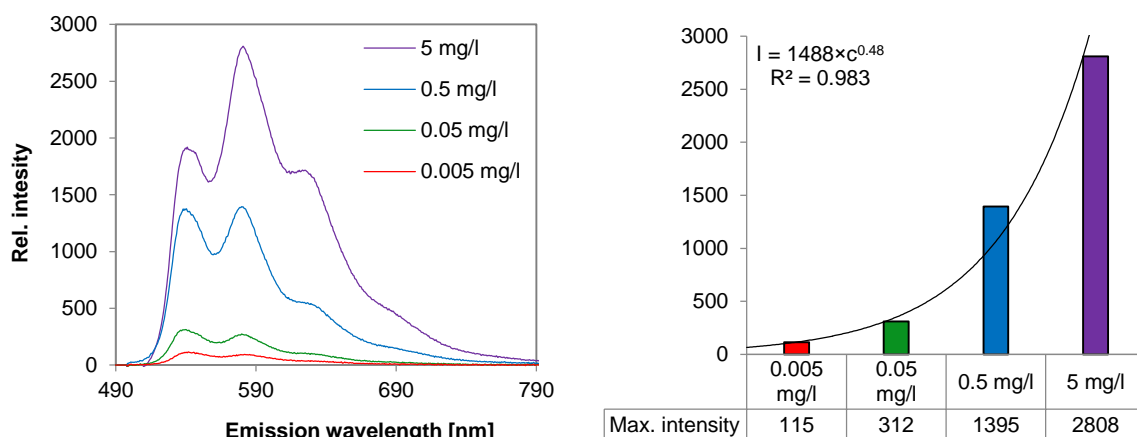


Figure 5-6: Fluorescence emission spectra (excitation at 488 nm) and maximum emission intensity at 580 nm (I) of PE dyed with different concentrations (c) of NR in water.

5.3.3 Effect of different NR derivatives and pH-value

As explained before, the solvatochromic effect of NR causes a shift of the fluorescence towards higher wavelengths with increasing polarity of the polymers and particles, due to the binding to the particle surface or incorporate into the polymeric network (Figure 5-5 - 5-7; A4-1). Also, the previously discussed strong adsorption on and into the polymeric network can hinder molecule movement and therefore change the vibrational bands. The strongest shift can be seen for the highly polar PVC. Also, wood and chitin show strong shifts due to the high polarity of their polymeric compounds. The 3-D-fluorescence spectra (Figure A4-1) show that also the respective excitation is shifted towards higher wavelength with increasing polarity.

Orange fluorescence (typical excitation at 560 nm) and red (typical excitation at 630 nm) fluorescence are unsuited to differentiate between natural particles and plastics, as non-polar polymers have signals weaker than natural particles (Figure A4-4 - A4-5).

Green fluorescence (typical excitation at 488 nm) can be used to distinguish between natural particles and plastics (Figure 5-7). In the transmissive area of the FTIC emission filter used here, non-polar plastics as PE and PP have a good emission signal. Due to their shift for intermediate polar plastics, such as PES and PA, the emission signal starts to rise in the transmissive area of the filter, which also makes them visible. For highly polar plastics such as PVC and natural particles the emission signals are weaker and more shifted towards long wavelength which excludes them in the used filter

Comparing the samples dyed at different pH-values (Figure 5-7, A4-2 – A4-3), this effect is the strongest using acidified water, as the overall signal of the intermediate polar polymers PA and PES is stronger here than using neutral or basic water. Therefore, also the signal in the transmissive area of the emission filter gets intensified. Those differences are caused by protonation or deprotonation of the different

organic groups of NR and also at the surface of the different plastics and natural particles. This causes a changed charge of the molecules and the particle surface, by which the sorption kinetics are changed and more NR can be adsorbed [217, 218]. Due to the carboxyl-group, which deprotonates at neutral and basic pH-Value, NR1 shows the overall strong loss in signal intensity at basic and neutral pH. For the other derivatives, mainly the protonation of the dialkylamine group will cause changes in charge. Previous studies described that the pH values between 4-9 have no effect on the quantum yield of NR itself [217, 219]. Only in very acidic environments is NR protonated, which causes a shift towards red fluorescence [220]. Therefore, we assume the changed adsorption kinetics are mainly caused by the changed surface charges of the polymers. However, it is unclear whether this is also the case for NR1 or if the deprotonation of the carboxyl groups can lead to the strongly quenched emission.

Between NR and its derivate, there are clear differences between the intensities for the combinations with the different plastic and natural particles (Figure 5-7). These intensities vary between the respective combinations. For detecting certain polymer types, this could be useful. However, no consistently positive effect of the functionalization of the NR derivatives, which would lead to an increased signal intensity for plastic particles and / or reduced signal intensity for natural particles and, therefore, an increased distinction between both particle types, can be seen here.

When it comes to the choice for the stain used in actual samples, NR1 and NR2 show too strong a signal for PP, which would disturb the identification of other polymers (Table 5-3). In addition, wood (NR1) and chitin (NR2) have signals ranging into the transmissive area of the emission filter. Thus, a combination of NR and NR3 in acidic water is the best choice to differentiate between microplastics and natural particles and are combined in further experiments.

Table 5-3: Expected fluorescence intensity for green fluorescence of different polymers dyed with the NR derivatives at acidic pH-value (pH = 2.5) predicted from emission fluorescence spectra (excitation at 488 nm) and use of the FTIC filter set (green fluorescence). Green = strong, yellow = intermediate, orange= weak, red= none.

	NR	NR1	NR2	NR3
PE	yellow	orange	orange	yellow
PP	yellow	green	green	red
PA	orange	orange	orange	orange
PES	orange	orange	orange	orange
PVC	red	red	red	red
Chitin	red	orange	orange	red
Wood	red	orange	red	red
Chalk	red	red	red	red

In Figure 5-8 the fluorescence microscope images of microplastics and natural particles dyed with a mixture of NR and NR3 (1:1) in water at pH 2.5 taken with common filters for green, orange and red

fluorescence are shown. It can be seen that orange and red fluorescence do not lead to the intended selectivity between natural and plastic particles. The polar plastic types, chitin and wood all show strong signals for orange and besides chitin also for red fluorescence. The non-polar PE and PP and chalk only show very weak signals for red and orange fluorescence.

Therefore, the fluorescence images confirm that green fluorescence is best suited to detect microplastics and distinguish them from natural polymers. Despite the lower fluorescence intensity, which makes a long exposure time necessary, here we have the best distinction between natural particles and plastic particles. Of the plastic particles, the non-polar PE and PP have the strongest signal, followed by the intermediate polar PES and PA. The highly polar PVC, only shows a very weak green fluorescence, which is one drawback of this method [205]. This corresponds to the observations of the emission spectra (Figure 5-7), where the emission non polar PE and PP is in the transmissive area of the filter, the rising emission of the intermediate polar PA and PES also ranges in the transmissive area of the filter, but the strongly shifted emission of the PVC is excluded by the filter. By changing the transmissive area of the used emission filter towards higher wavelengths, the signal of PA and PES would be intensified and possibly PVC could also be detected. However, there is a risk that the signal from natural particles would also be amplified, by shifting the transmissive area too far.

For the natural particles, wood and chalk show a very weak signal, as the emission is strongly shifted towards longer wavelength and therefore excluded by the emission filter. Therefore, they do not cause false positives. Contrary to the expectation from analyzing the emission spectra (see Table 5-3) predicting the emission outside of the transmissive area of the filter, chitin shows a very strong signal at green fluorescence. This problem was described before by Erni-Casolla et al. 2017, who solved it by applying a hydrogen peroxide treatment, which weakens fluorescence intransitive strongly and reduces the risk of false positives (Figure 5-9). For samples containing large quantities of chitin, it is additionally recommended to remove the chitin completely using chitinase. [90]

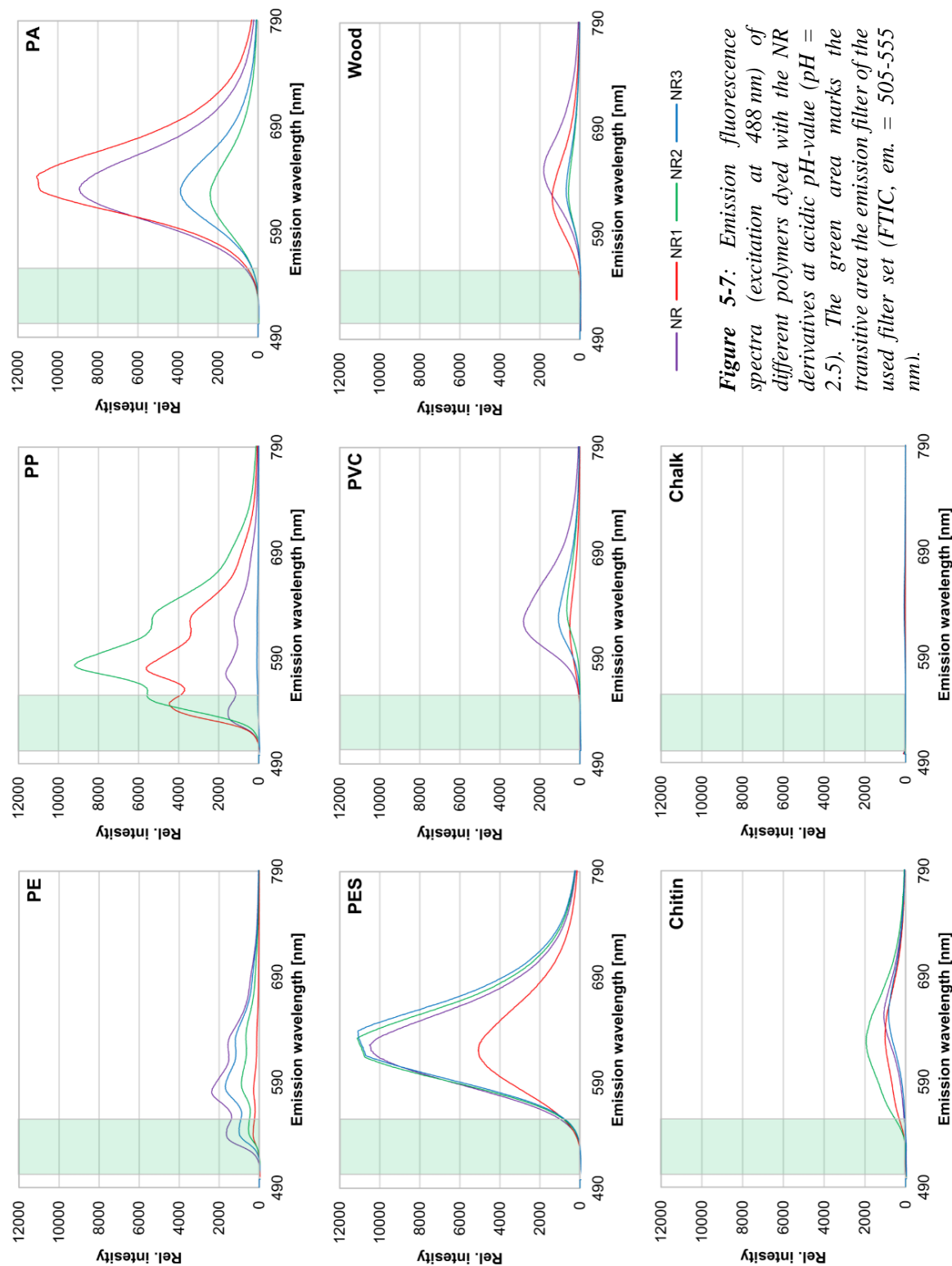


Figure 5-7: Emission fluorescence spectra (excitation at 488 nm) of different polymers dyed with the NR derivatives at acidic pH-value (pH = 2.5). The green area marks the transitive area the emission filter of the used filter set (FTIC, em. = 505-555 nm).

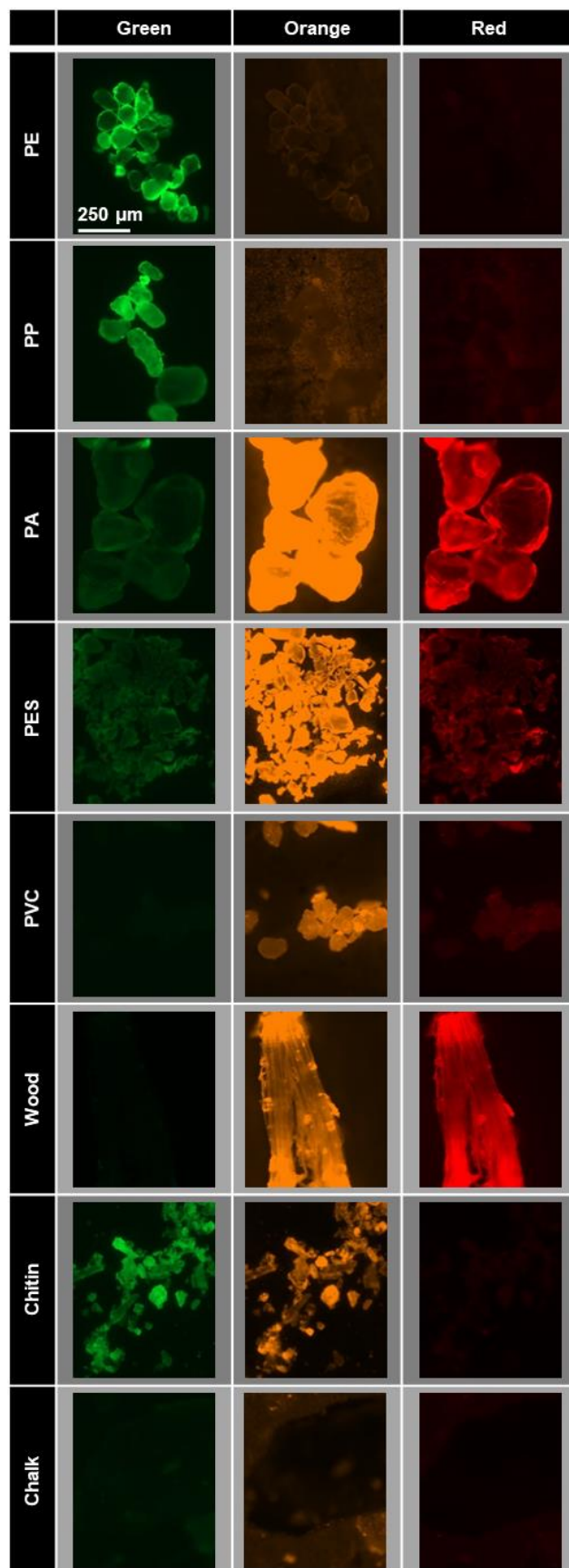


Figure 5-8: Fluorescence microscope images of microplastics and natural particles dyed with NR and NR3 (1:1) in water at pH 2.5. Used optical filters: Green - ex. = 455-495 nm, em. = 505-555 nm; orange - ex. = 533-558 nm, em. = 570-640; red - ex. = 575-635 nm, em. = 660-710 nm.

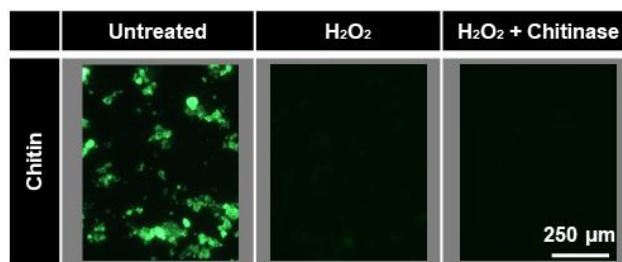


Figure 5-9: Fluorescence microscope images of treated and untreated chitin particles dyed with a mixture of NR and NR3 (1:1) in water at acidic pH-value (2.5). Used optical filter: Green fluorescence - ex. = 455-495 nm, em. = 505-555 nm

5.3.4 Test of the method on sea salt samples

Compared to the literature, our results ranging from 33- 688 MP / kg (Table 5-4) are in a reasonable range for microplastic contamination in sea salt, which is usually in the area between 0-1300 MP / kg, in extreme cases up to 19800 MP / kg [64]. In many cases, the plastic particles emitted a clear green fluorescence signal and were easy to identify (Figure A4-6). The green fluorescence helped a lot to distinguish particles in which no difference was visible using epiluminescence mode. In some cases, the green fluorescence made particles visible that were not visible at all using normal epiluminescence microscopy (Figure A4-6). However, in some cases, the fluorescence signal was of intermediate strength, which made it difficult to say whether it comes from a natural polymer or plastic (Figure A4-6). As these cases mostly occurred at size ranges below 50 µm, we set the lower size limit for the microplastics to this size to reduce the uncertainties in this method.

To avoid this uncertainty, protocols for image evaluation with pre-defined thresholds for fluorescence intensity can also be used [99, 205]. Another advantage of using these protocols is automated particle measurement and counting. However, the camera of the used microscope could only capture an area of 890 x 660 µm, which is only 0.11% of the total filter area. This small proportion cannot capture the number of MP particles on the whole filter, ranging from 6 to 77, representatively. Thus, the entire filter was evaluated with the naked eye.

Table 5-4: Results of the microplastic identification in sea salt samples

ID	Origin	Refined	Dissolved amount	Particle count	MP / kg
Salt A	Atlantic, France	yes	122 g	4	33
Salt B	Atlantic, France	no	72 g	35	486
Salt C	Baltic Sea, Germany	no	109 g	75	688

5.4 Conclusions

The results show that the choice of the solvent for staining affects the fluorescence spectra. Reasons can be changed sorption kinetics depending on the polarity of the solvent. Another reason is swelling, as

swelling can change the polarity of the microplastics causing a shift of the emission by solvatochromism or transport NR into the polymeric network of the particle including it in the polymeric network hindering the molecule movement and thus weakening the emission bands. A higher polarity of the solvent causes a shift towards higher wavelengths. The use of water leads to the strongest fluorescence signals. By staining microplastics with NR in water, up to a concentration of 5 mg / l no quenching could be observed, while on average an increase of the NR concentration by the factor 10 leads to an increase of the fluorescence intensity by a factor of 3.1.

Analyzing the solid sample fluorescence spectra, the solvatochromism of NR causes a shift of the spectra induced by the different polarities of plastic types and natural particles. In addition, the incorporation of NR in the polymeric network changing the ratio between the emission bands plays an important role in this shift. This allows the distinction of non-polar and intermediate polar plastic particles from natural particles using green fluorescence. A drawback of this method is, that highly polar polymers such as PVC cannot be detected, as the signals they show are too weak.

Due to a change in the charge of the NR molecules and the particle surfaces, the pH-value influences the sorption of NR and thus the fluorescence intensity of the stained particles, whereby the change of the charge of the particle surface has a much higher influence. The derivatization of NR did not show the intended increased selectivity for all plastic types. For staining of samples, a mixture of NR and NR3 in water at pH 2.5 turned out to be most efficient. To avoid false positives by polymers like chitin, a time-consuming sample preparation is still necessary for processing environmental samples

The tests of the final method using sea salt samples led to reasonable results. Using green fluorescence, natural particles could be well distinguished from plastics particles in most cases down to a size limit of 50 μm . In some cases, the intermediate fluorescence signal makes it hard to distinguish between natural particles and plastics. These uncertainties can be avoided by automated image processing. Furthermore, a better adjustment of custom-made imaging tools could improve the detection process. An optimization of the sample preparation and dyeing process should also significantly shorten the overall time required for sample measurement. Summarized, the method is well suited to measure an approximate level of MP contamination in environmental samples with low costs and low technical effort.

6 Summary and outlook

Concluding, the findings of this thesis helped to gain a better understanding of the physical and chemical processes behind the removal of microplastics by organosilanes. Thereby the process could be improved and optimized towards an application transfer. Additionally, a fast and cheap detection method for microplastics in environmental samples, based on Nile red staining, was developed, to enable the evaluation and control of the removal process on a pilot plant scale.

6.1 Influence of the organic group

The first important finding of the thesis is, that the organic groups of the organosilanes are not only important for the interaction with the plastic surface and therefore the agglomeration, they also have a high impact on the reaction behavior of the organosilanes in the water-induced sol-gel process and therefore the chemical fixation of the agglomerate. For too slow reaction velocities the organosilanes do not become solid hybrid silicas, do not fix the agglomerates, and the agglomerates disintegrate again. If the reaction happens too fast, the organosilanes harden fast and do not have enough time to agglomerate the microplastics. For the comparison of linear and branched alkyl trichlorosilane with a chain length from 1-18 carbon atoms, organosilanes with small and large organic groups showed too fast reaction velocities. Organosilanes with branched alkyl groups close to the silica atom showed too slow reactions, due to a steric hindering of the reaction. Intermediate chain length between 3-5 carbon atoms leads to the best reaction kinetics and best removal efficiencies. Thus, when choosing organosilanes it is very important to consider the effect of the organic group on the reaction behavior. Reaction kinetics should allow an efficient removal process, which depends on the chain length of the organic group in the organosilanes.

6.2 Influence of water type, temperature, and polymer type

After finding the best working organosilanes, the process could be successfully tested in treated municipal wastewater and seawater on a laboratory scale. Both water compositions showed no negative effect on the microplastics removal compared to experiments in demineralized water. Thus, the removal process should work well in these applications. As natural waters and different wastewaters can strongly differ in their composition, more tests are needed to ensure a wider applicability. Additionally, the removal was performed successfully at different temperatures. Tested were 7.5°C, which can occur in winter months in the environment, 20°C, as average room temperature, and 40°C, which can occur in industrial wastewaters. To quantify possible dissolved organosilane residues in the water after the removal process, DOC measurement and ICP-OES could be applied successfully. Both are suitable for process control in possible applications of the removal process. From the tested organosilanes only eco abcr Wasser 3.0 PE-X ® showed no residues in the water, which makes it suited for an application transfer.

As the removal process strongly depends on the interaction of the organosilanes with the surface of the microplastics, five different polymer types (PE, PP, PA, PES, and PVC) with different surface

chemistries and properties were tested. The results showed non-polar organosilanes work less efficiently with increasing polarity of the microplastics surface. Adapting the organosilanes to the polar polymers by adding a more polar organic group led to an improvement in the removal efficiency. The more polar organosilane did not form agglomerates at all with the non-polar polymers, due to a missing interaction. These results show, that the organosilanes can be specifically designed and adapted to improve the interaction with certain polymer types. During the thesis, it was only possible to test a very limited amount of organosilanes and polymer types. The high variability and easy chemical adaptivity of organosilanes give them a big potential to be adapted to remove different polymer types from water. The final goal would be creating a mixture of different organosilanes for the specific removal of polymer mixtures from water.

6.3 Influence of biofilm coverage

Microplastics in the environment are typically covered by biofilms, which change their surface chemistry and therefore the interaction with the organosilanes. To test the effect on the microplastics removal, a new method was developed to cultivate biofilms fast and standardized under laboratory conditions. This method uses a packed bed column filled with microplastics and flown through by water. For a fast growth biologically treated municipal wastewater enriched with glucose was used, as it contains high amounts of bacterias for inoculation and has high availability of nutrients. After 7 days the microplastics were partially covered by biofilms. This method can be further optimized by enhancing the nutrient composition or improving the flow conditions. Also, it can be adapted for a controlled simulation of different environments as saltwater or freshwater. Further, it can be used in other fields of microplastics research, as ecotoxicology or transport processes, where biofilm coverage also influences the results.

Using this method, biofilms were cultivated on PE, PP, PA, PES, and PVC-based microplastics. The result shows, that the biofilm coverage negatively affects the microplastic removal for the tested organosilanes. Only combinations, where the organosilanes interact very well with the microplastics, they could still be removed, as the biofilm did not cover the whole microplastics surface. The organosilane still attaches to free spots on the surface and agglomerates the microplastics. Additionally, removal of the biofilm from the microplastics using H_2O_2 and ultrasound was conducted. After this process, the microplastics removal efficiencies were improved again, but removal efficiencies from the virgin microplastics were not reached. This is caused by degradation and transformation processes of the microplastics surface as well as the attachment of natural organic matter. These results show the importance of simulated environmental exposure for conducting experiments with microplastics. As only a limited amount of organosilanes could be tested in this study, an adaptation of the organic group to biofilm-covered microplastics was not possible. Further experiments should focus on finding suitable organosilanes with good interactions with biofilms.

6.4 Nile red staining for microplastics detection

To test the pilot plant without additional microplastics spiking, a method for microplastics detection in environmental samples is necessary. Compared to common methods for microplastics detection, fluorescent staining using Nile red is very simple, cheap, and fast, but has disadvantages as low sensitivity for some polymer types as PVC or the risk of false positives due to natural polymers. By chemically modifying the Nile red and testing various approaches for the staining process using different solvents and water at different pH values, the sensitivity and selectivity of the detection process could be improved. Nile red combined with a new derivative modified with an Ethylhexyl group dissolved in water at pH 2.5 turned out to be the best approach for staining the samples. The application of the method was fast and uncomplicated. A big disadvantage is still the complicated and time-consuming sample preparation, which is necessary before applying the detection method. By further improvement of the selectivity, it might be possible to reduce the sample preparation necessary. Also, the detection of highly polar polymers like PVC can still be improved, by modifying the Nile red for more targeted interaction or testing more solvents.

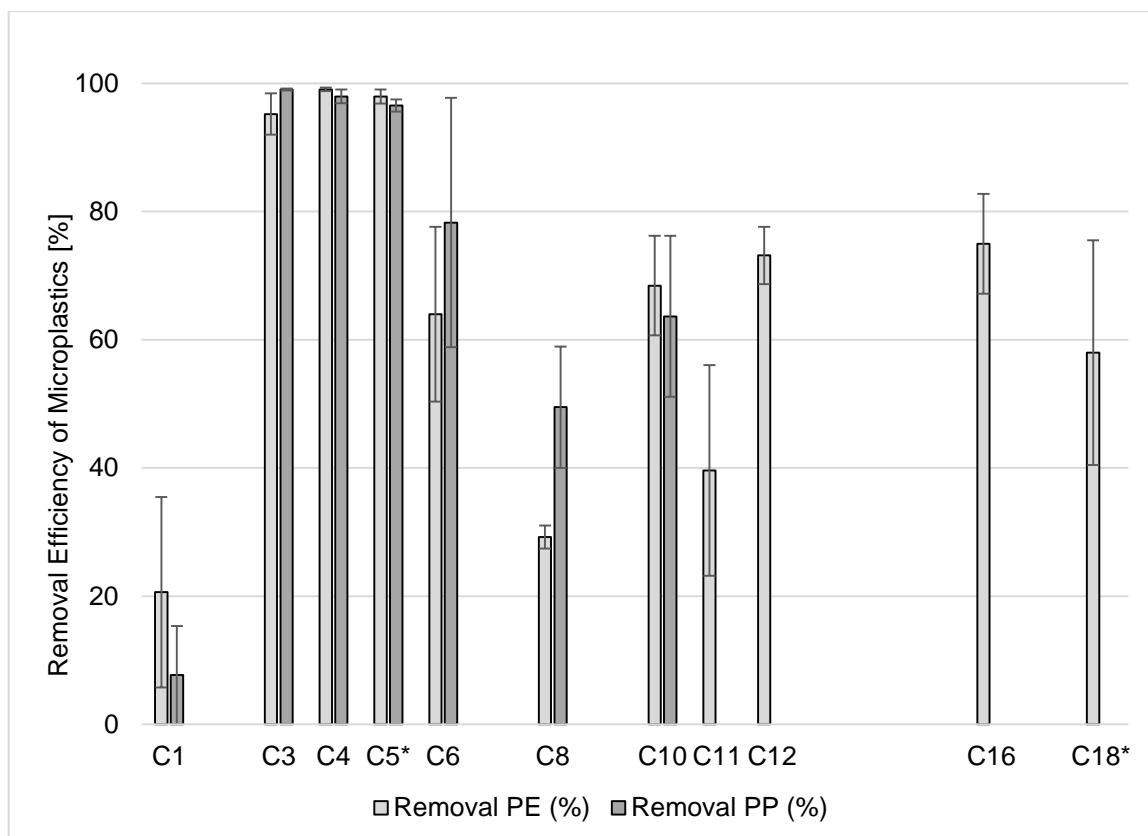


Figure A1-2 Removal efficiency of PE and PP from water for the tested linear alkyl substituted trichlorosilanes (300 μl / l) with the respective alkyl group.* C5- and C18-alkyltrichlorosilane were only available as mixtures of isomers.

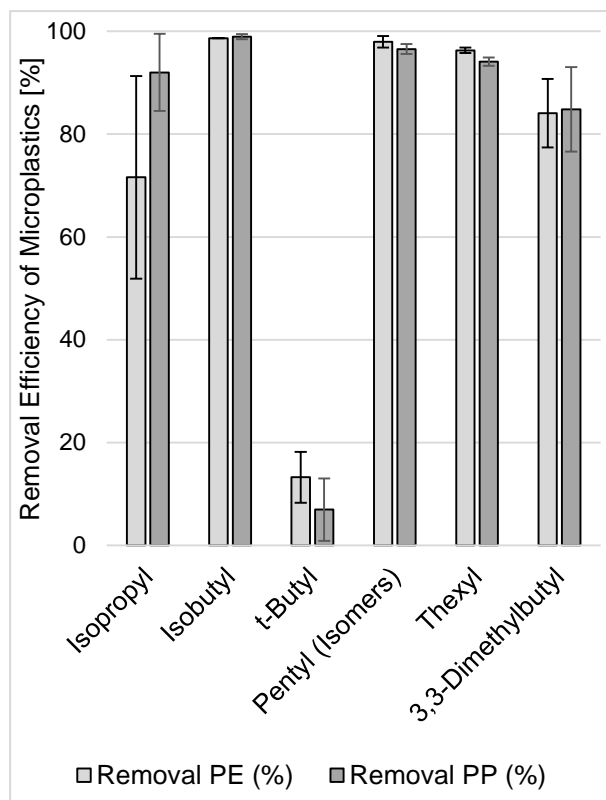


Figure A1-3 Removal efficiency of PE and PP from water for the tested branched alkyl substituted trichlorosilanes (300 µl / l) with the respective alkyl group

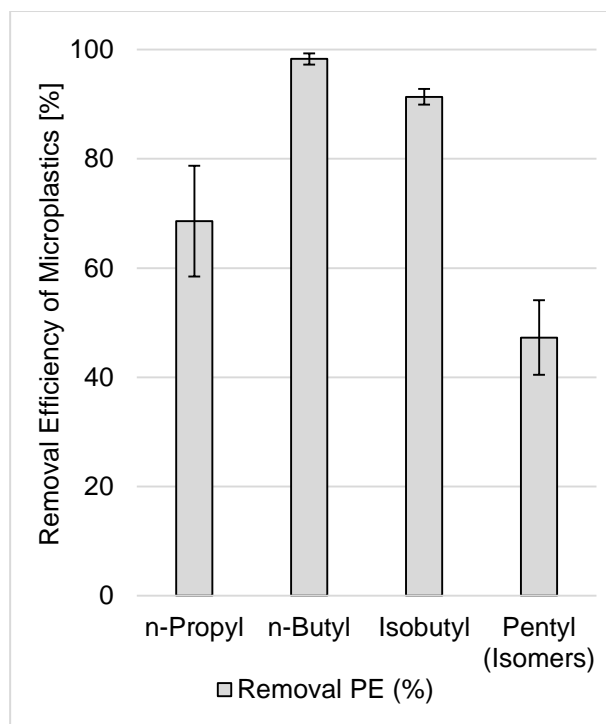


Figure A1-4 Removal efficiency of PE from water for the alkyl substituted trichlorosilanes (100 µl / l) with the respective alkyl group

Table A1-1: Reaction rate constant (k), half lifetime ($t_{1/2}$) and correlation coefficient (r) for reaction kinetics fitting of the alkyltrichlorosilanes in water

Precursor	k [1/s]	$t_{1/2}$ [s]	r	R.S.D (k; $t_{1/2}$)
Methyltrichlorosilane	3.31E-02	21	0.985	-
n-Propyltrichlorosilane	3.55E-02	20	0.996	-
n-Butyltrichlorosilane	9.47E-03	73	0.992	-
Pentyltrichlorosilane (Isomere)	3.96E-02	18	0.992	-
n-Hexyltrichlorosilane	1.03E-01	7	0.947	-
n-Octyltrichlorosilane	8.86E-02	8	0.987	-
n-Decyltrichlorosilane	4.27E-02	16	0.997	-
n-Undecyltrichlorosilane	1.40E-03	493	0.828	-
n-Dodecyltrichlorosilane	5.22E-03	133	0.998	-
n-Hexadecyltrichlorosilane	1.05E-02	66	0.977	-
n-Octadecyltrichlorosilane	9.25E-04	798	0.980	24.7 %
Isopropyltrichlorosilane	2.08E-02	33	0.996	-
Isobutyltrichlorosilane	1.28E-03	57	0.998	21.3 %
t-Butyltrichlorosilane	7.80E-03	89	0.999	-
Thexyltrichlorosilane	7.95E-05	8718	0.996	-
(3,3-Dimethylbutyl)trichlorosilane	2.08E-02	33	0.996	-

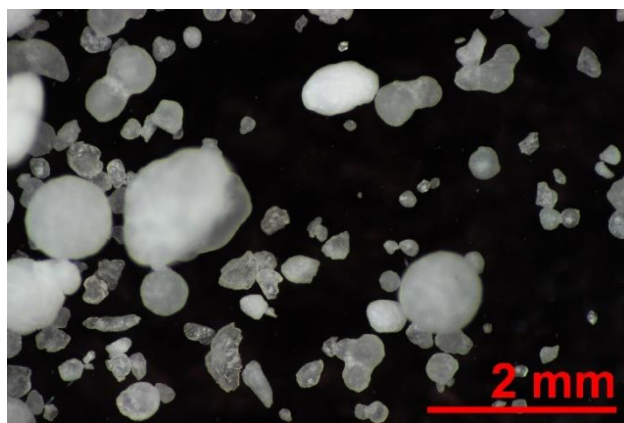
A2 Supplementary material for chapter 3

Supplementary materials: Influences of polymer types, water composition and temperature on the removal of microplastic particles from waters using organosilanes

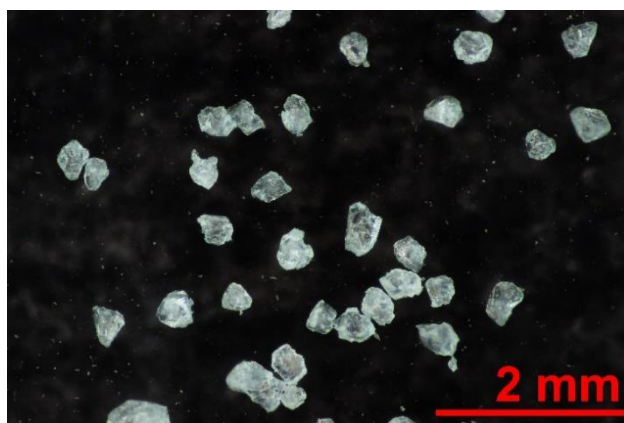
Table A2-1: Water parameters of a 24 h composite sample taken at 2nd march 2020 at the effluent of the sewage treatment plant Landau i. d. Pfalz, Germany. The values were provided by the operators of the sewage treatment plant, Entsorgungs- und Wirtschaftsbetrieb Landau.

Turbidity	Total suspended solids	Chemical oxygen demand	Ammonia	Total nitrogen	Nitrate	Total Phosphorous
[TEF]	[ml/l]	[mg/l]	[mg/l]	[mg/l]	[mg/l]	[mg/l]
0.0	0.00	14.90	0.50	5.69	4.98	0.15

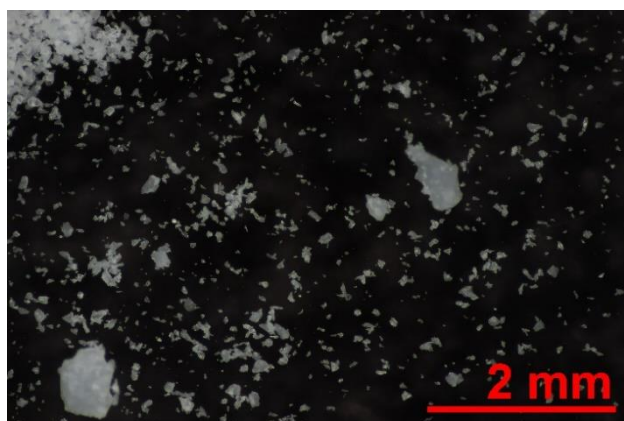
PP/PE



CoPA



CoPES



PVC

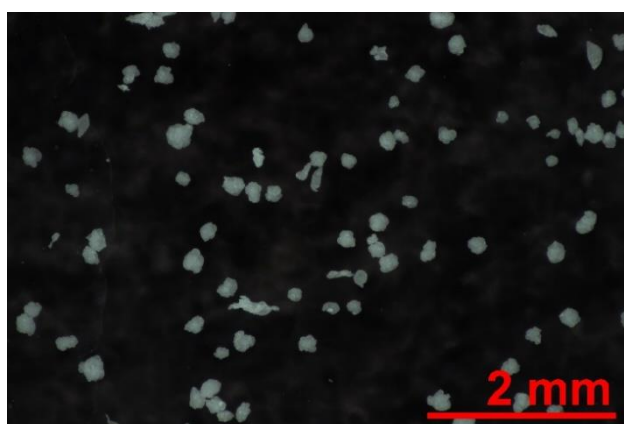


Figure A2-1: Stereomicroscope images of raw microplastics used for the fixation experiments

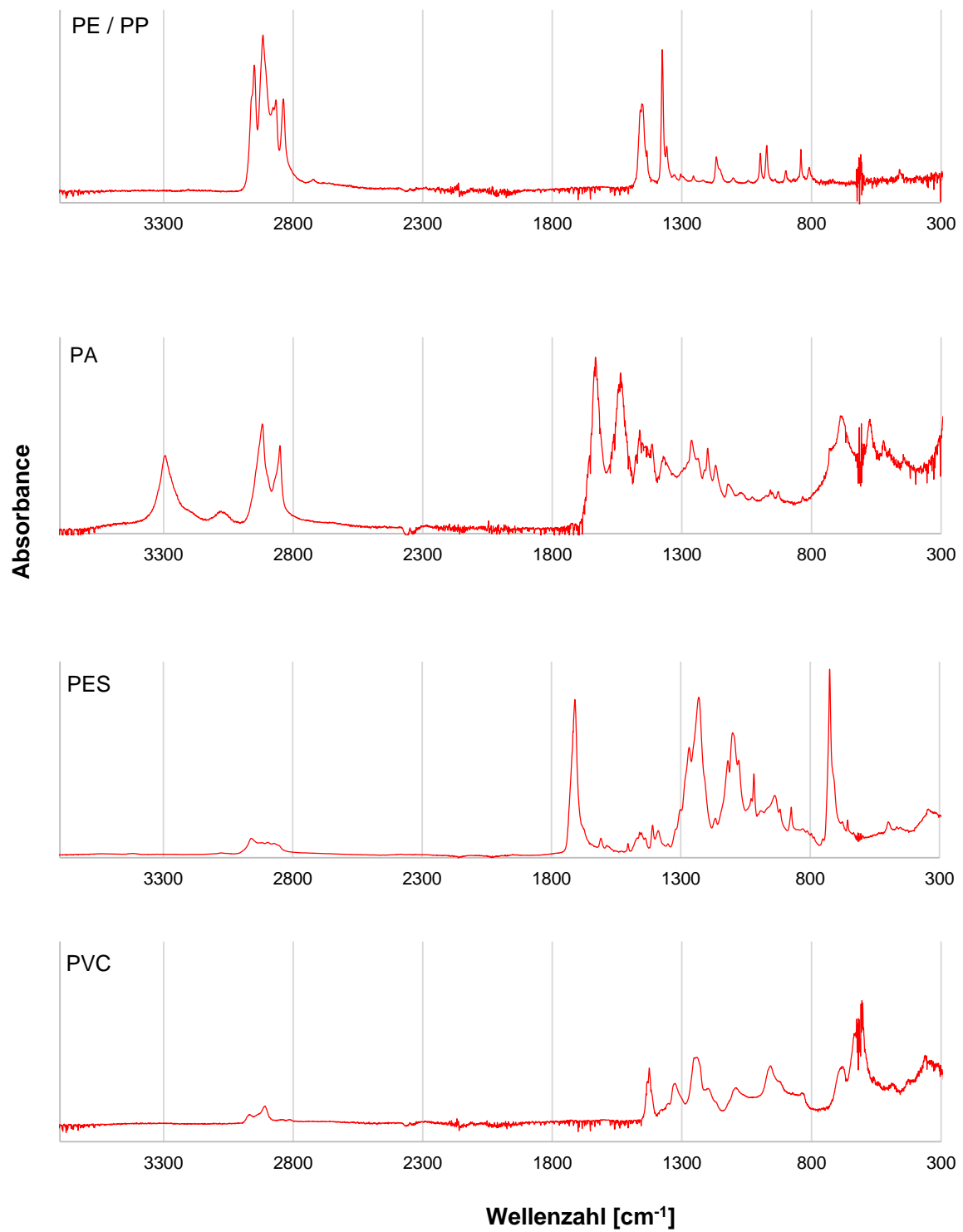


Figure A2-2: FTIR-Spectra of the microplastics used in the fixation experiments.

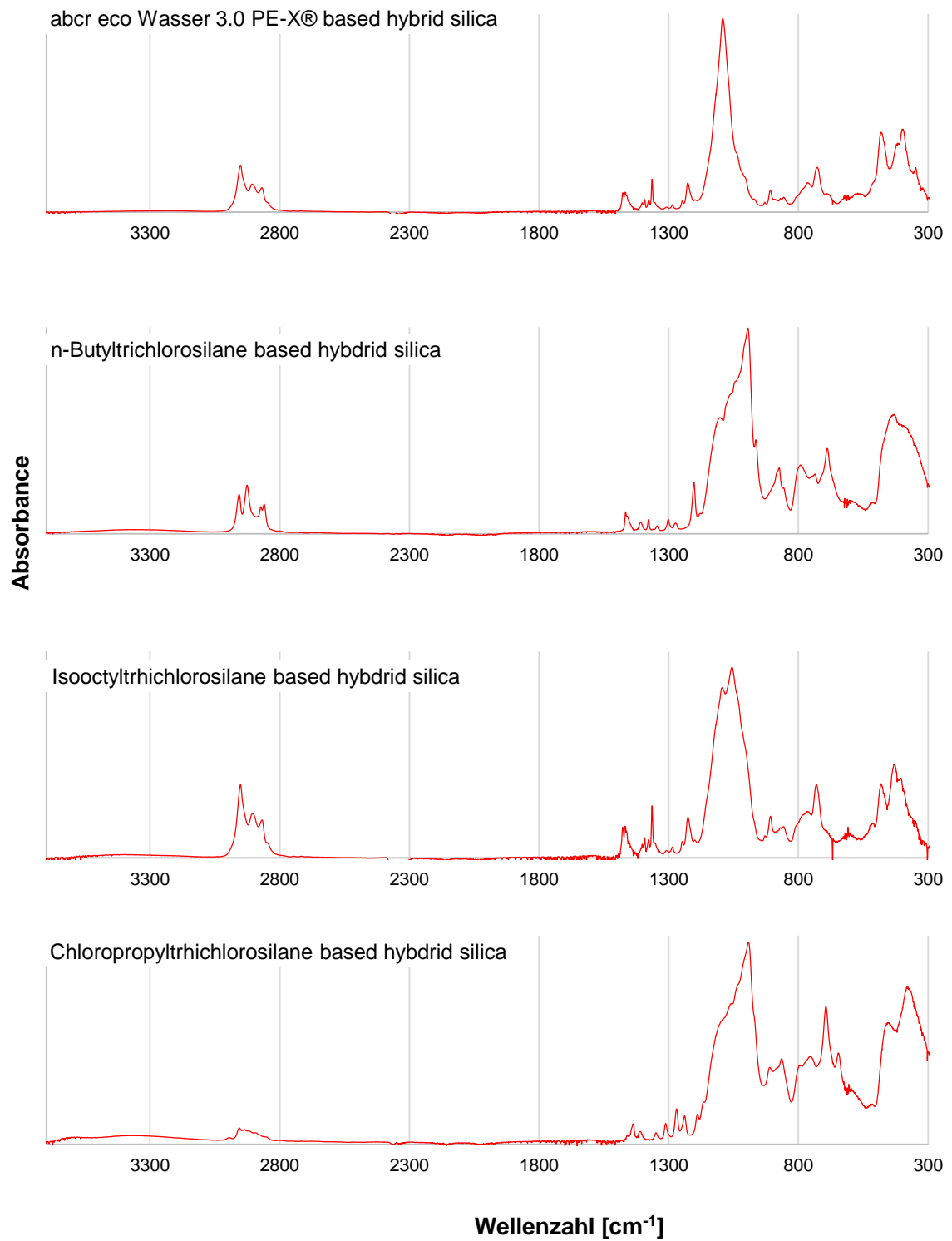


Figure A2-3: FTIR-Spectra of the hybrid silica formed by adding the respective organosilane to water and stir for 20 minutes.

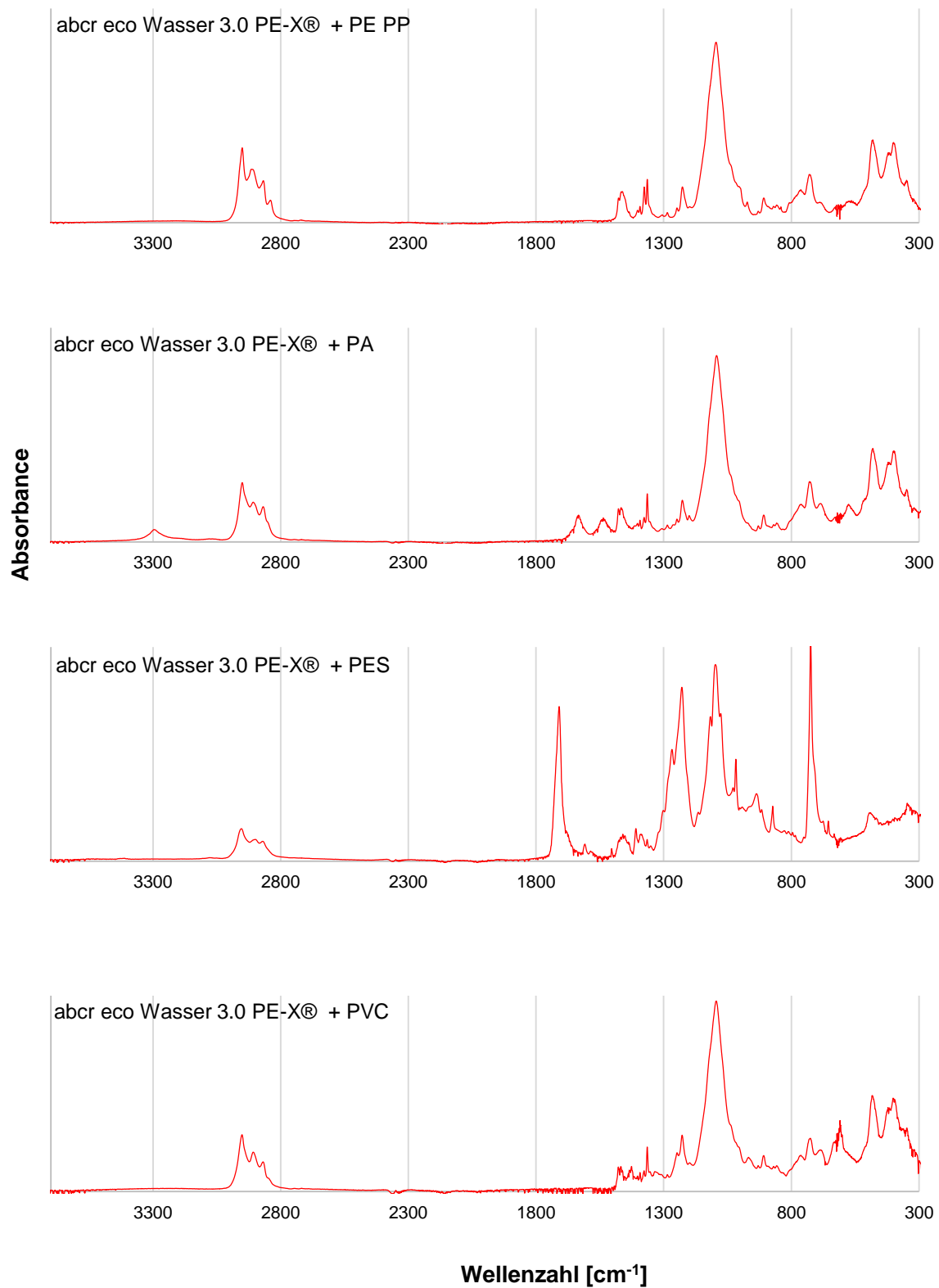


Figure A2-4: FTIR-Spectra of the agglomerates formed during the fixation process using PE-X and different polymers.

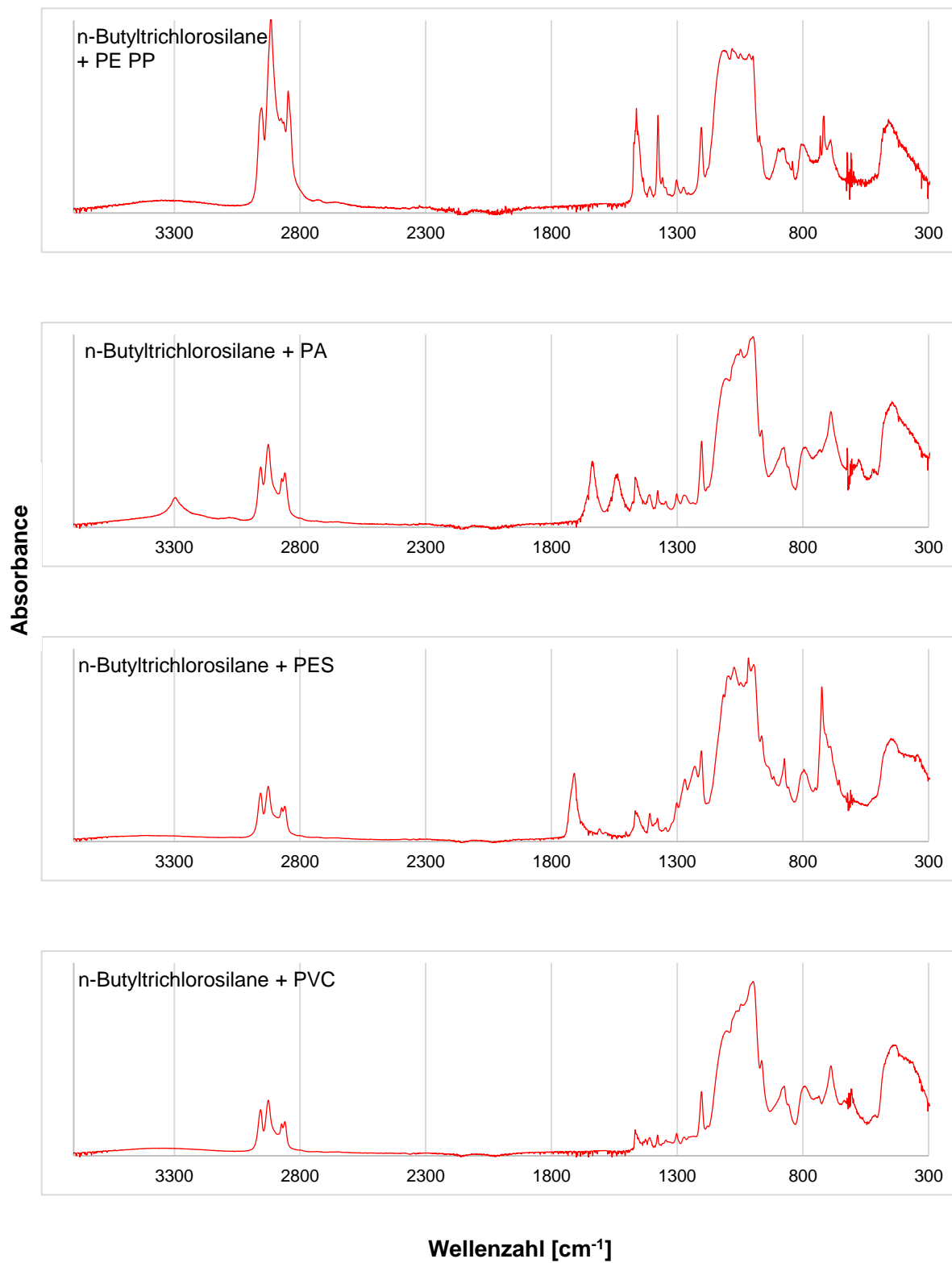


Figure A2-5: FTIR-Spectra of the agglomerates formed during the fixation process using *n*-butyltrichlorosilane and different polymers.

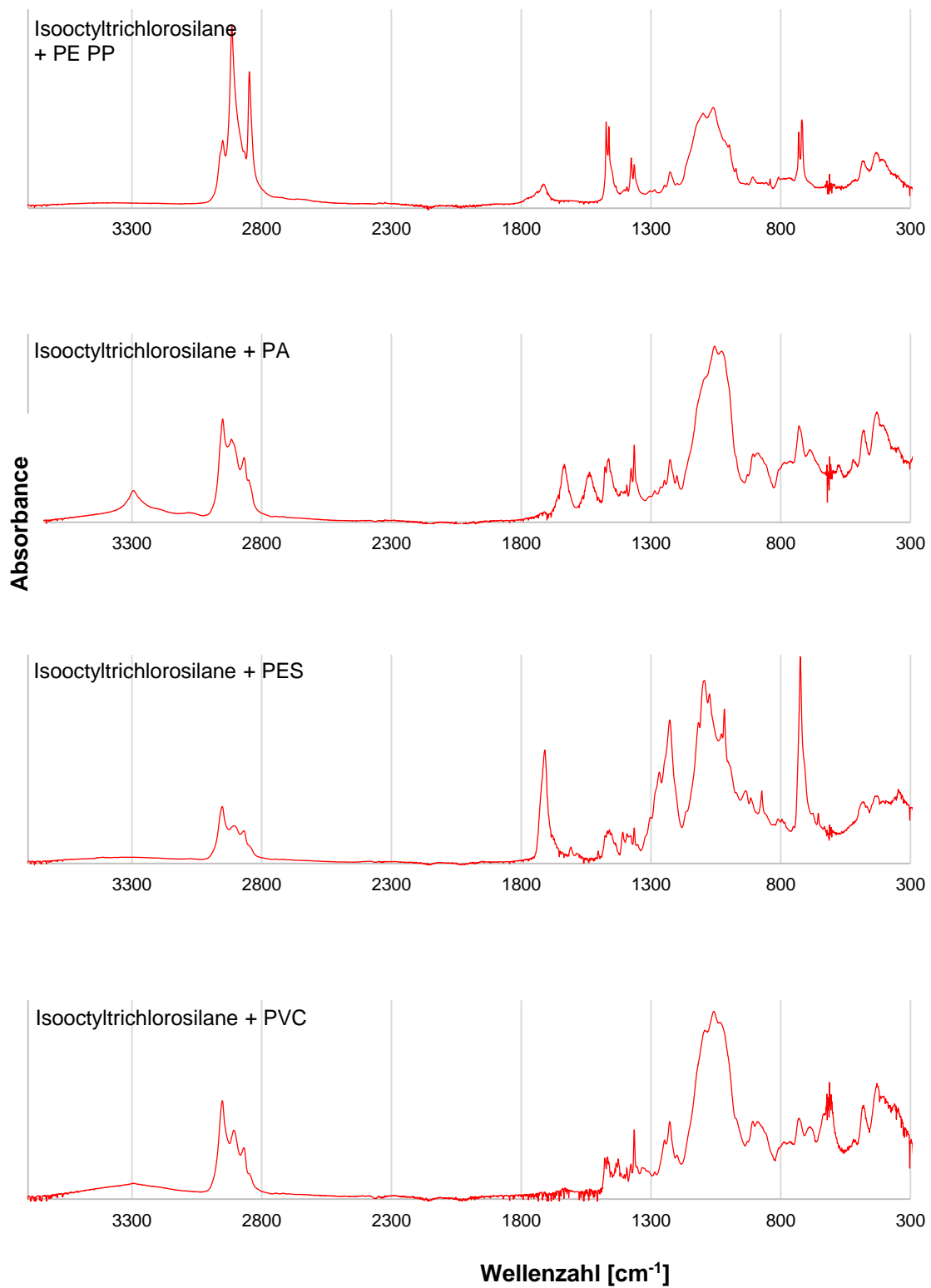


Figure A2-6: FTIR-Spectra of the agglomerates formed during the fixation process using isooctyltrichlorosilane and different polymers.

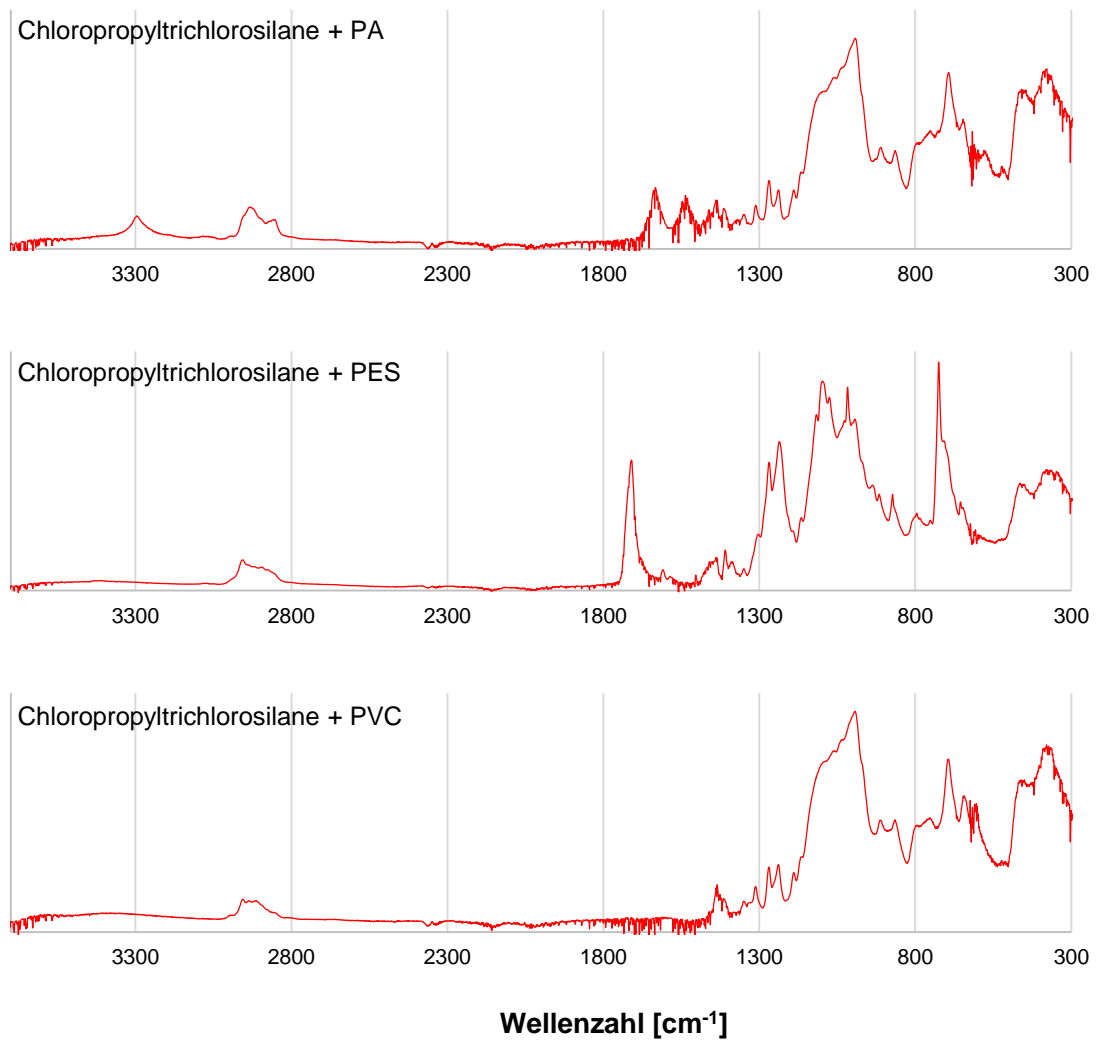


Figure A2-7: FTIR-Spectra of the agglomerates formed during the fixation process using (3-Chloropropyl)trichlorosilane and different polymers. Note: Using (3-Chloropropyl)trichlorosilane and PE / PP no agglomerates were formed during the fixation experiments.

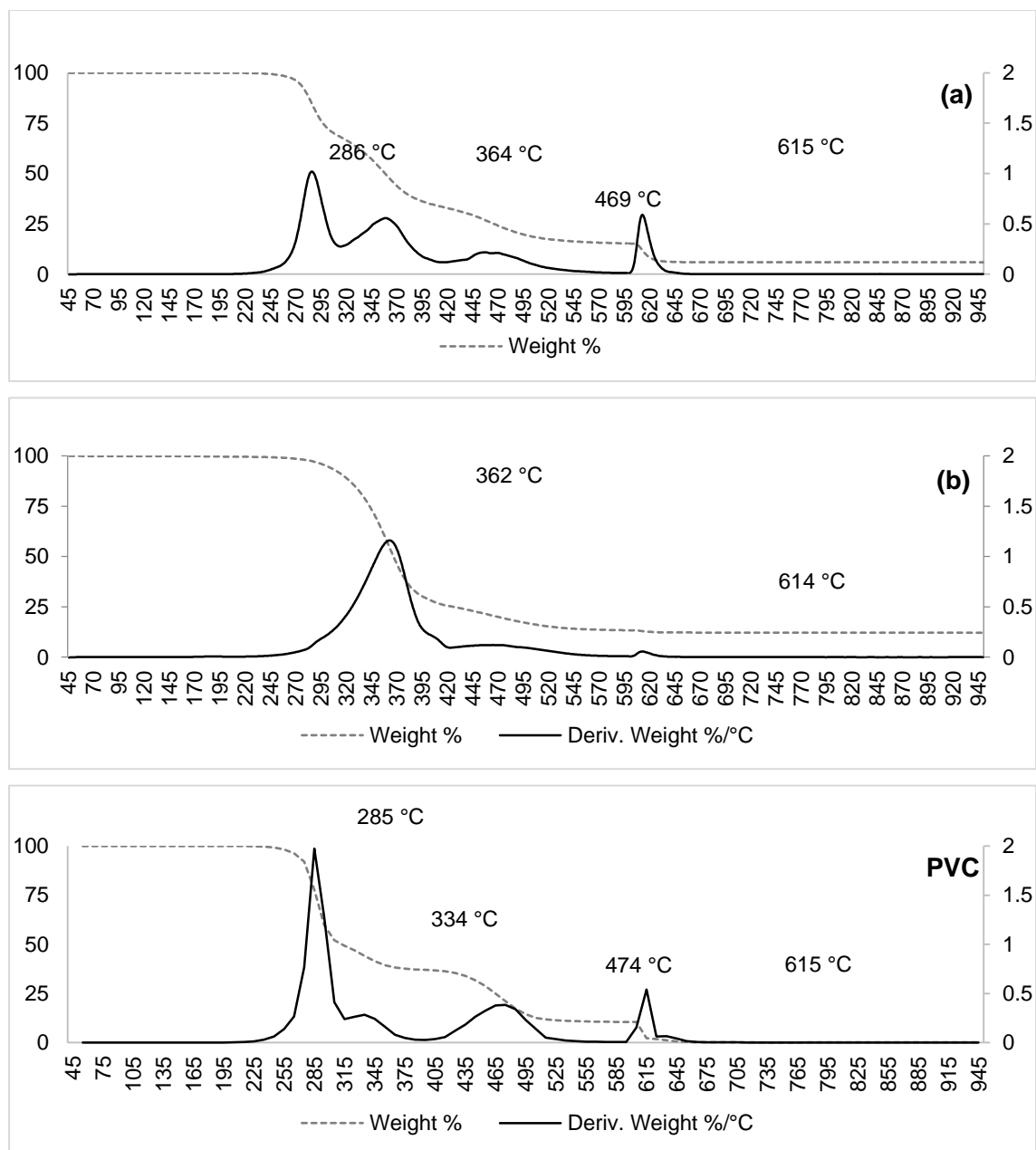


Figure A2-8: TGA curves of (a) agglomerate formed in removal process 100 mg of PVC from 1l demin. water using 100 µl PE-X; (b) hybrid silica formed by adding 100 µl PE-X in 1l demin. water and of the different polymer types used in experiments. Grey dashed line = weight in %; black line = derived weight in %/°C.

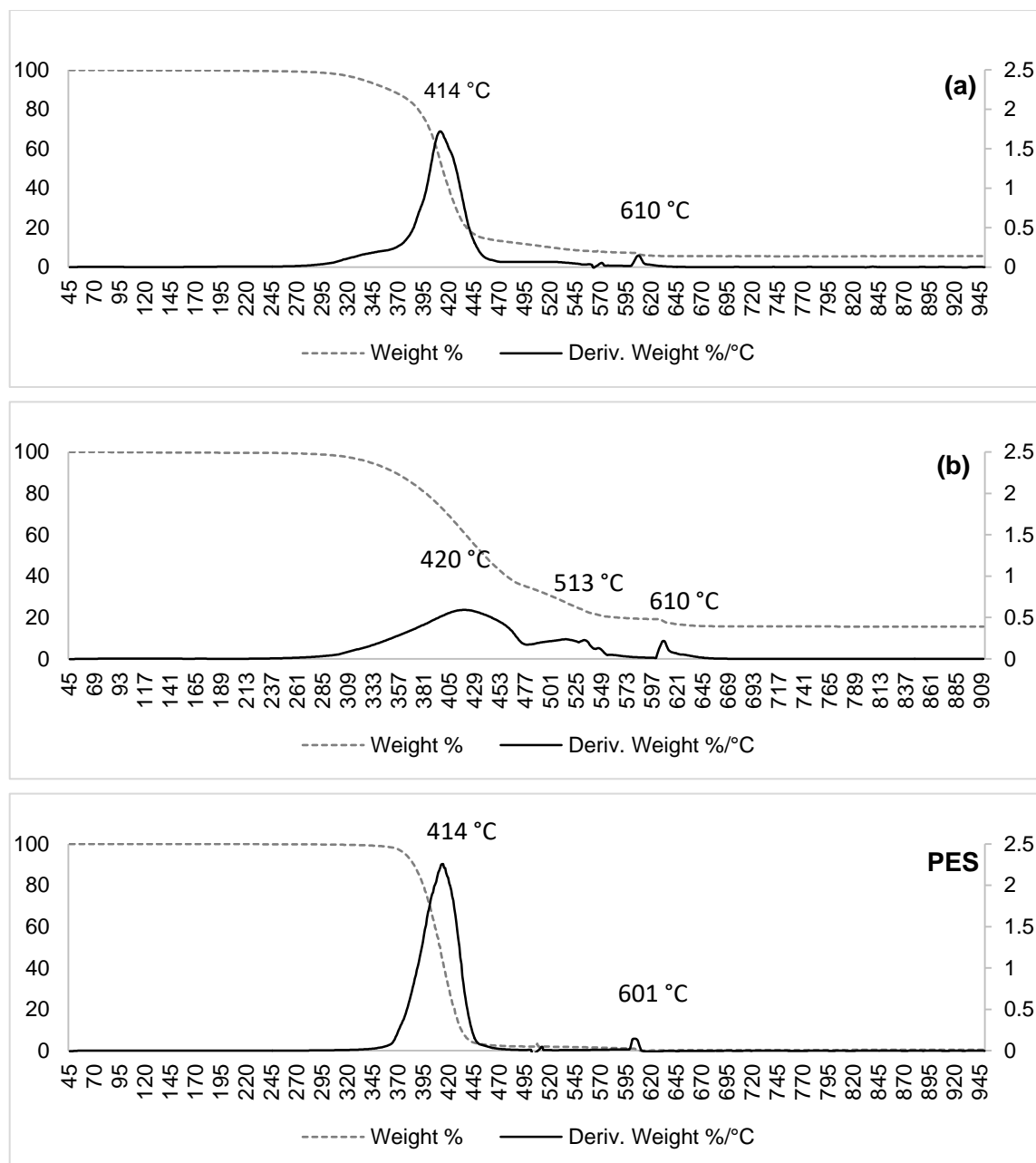


Figure A2-9: TGA curves of (a) agglomerate formed in removal process 100 mg of PES from 1l demin. water using 100 μ l Isooctyltrichlorosilane; (b) hybrid silica formed by adding 100 μ l Isooctyltrichlorosilane in 1l demin. water and of PES.. Grey dashed line = weight in %; black line = derived weight in %/°C.

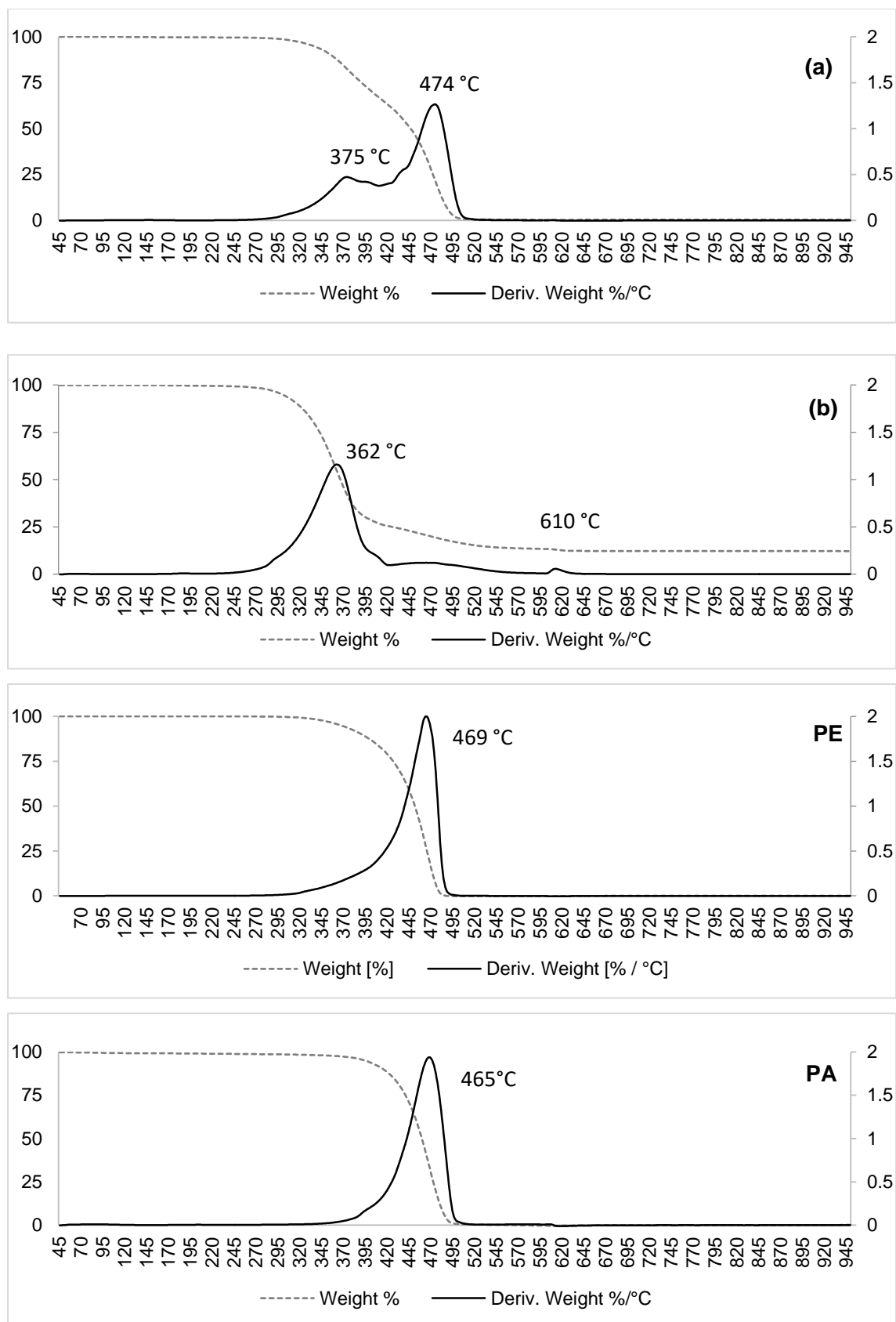


Figure A2-10: TGA curves of (a) agglomerate formed in removal process 100 mg of PE / PA (1:1) from 1l demin. water using 100 μ l PE-X; (b) hybrid silica formed by adding 100 μ l PE-X in 1l demin. water and of the polymer types used in experiments. Grey dashed line = weight in %; black line = derived weight in % / $^{\circ}$ C.

A3 Supplementary material for chapter 4

Supplementary materials: Method for rapid biofilm cultivation on microplastics and investigation of its effect on the agglomeration and removal of microplastics using organosilanes

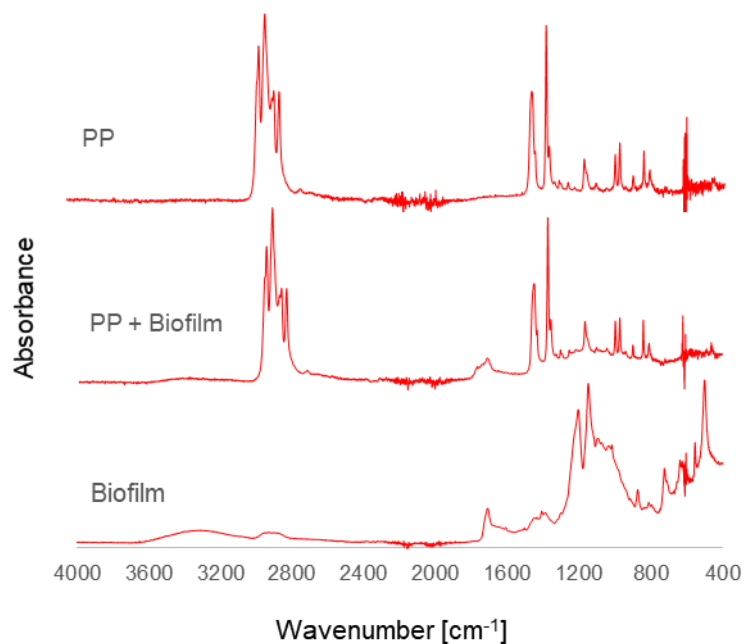


Figure A3-1: FTIR spectra of virgin PP, a pure biofilm sample, and PP covered with biofilm. Both signals can be seen in the sample of PP with Biofilm. Overlapping of bands in the area of 1400-400 cm⁻¹ makes the separation more difficult than for PE (Fig 1).

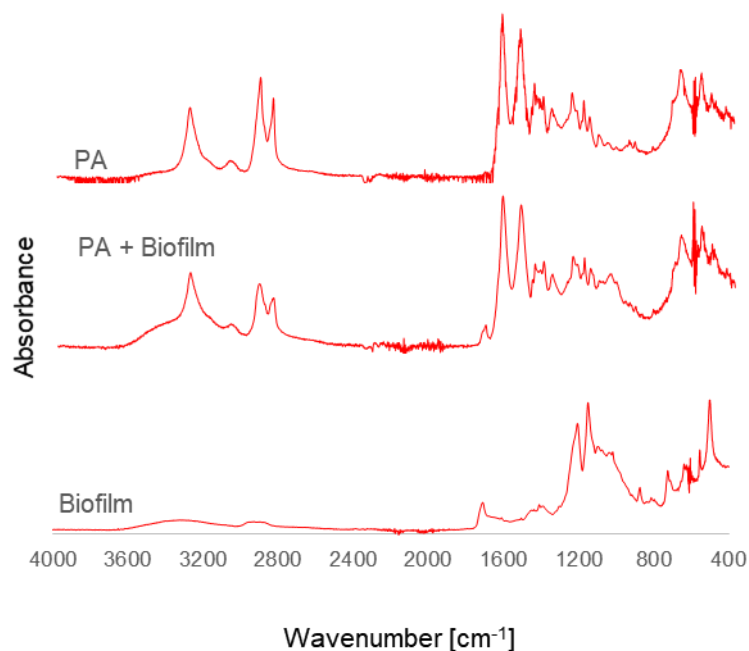


Figure A3-2: FTIR spectra of virgin PA, a pure biofilm sample, and PA covered with biofilm. Both signals can be seen in the sample of PA with Biofilm, but there is strong overlapping of bands in the area of 1700-400 cm⁻¹, which is why the signals are difficult to separate

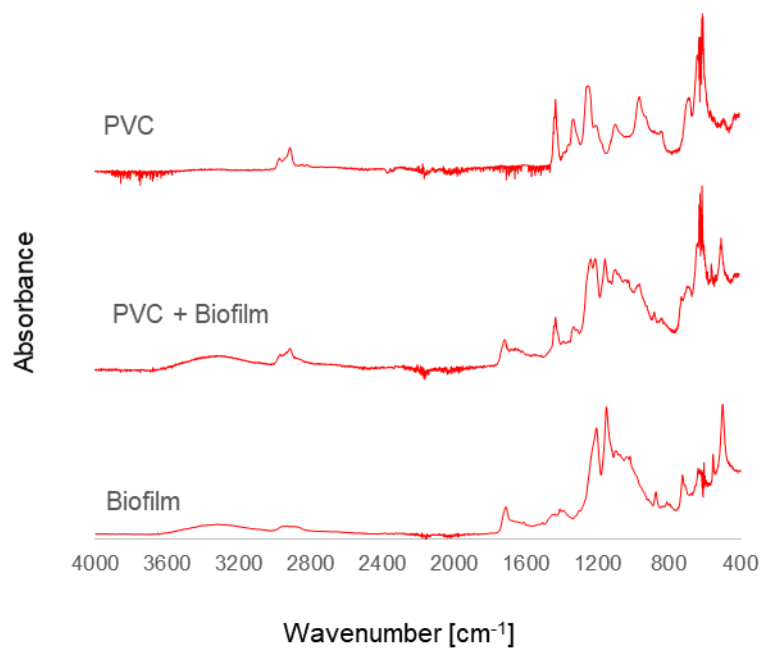


Figure A3-4: FTIR spectra of virgin PVC, a pure biofilm sample, and PVC covered with biofilm. Both signals can be seen in the sample of PVC with Biofilm.

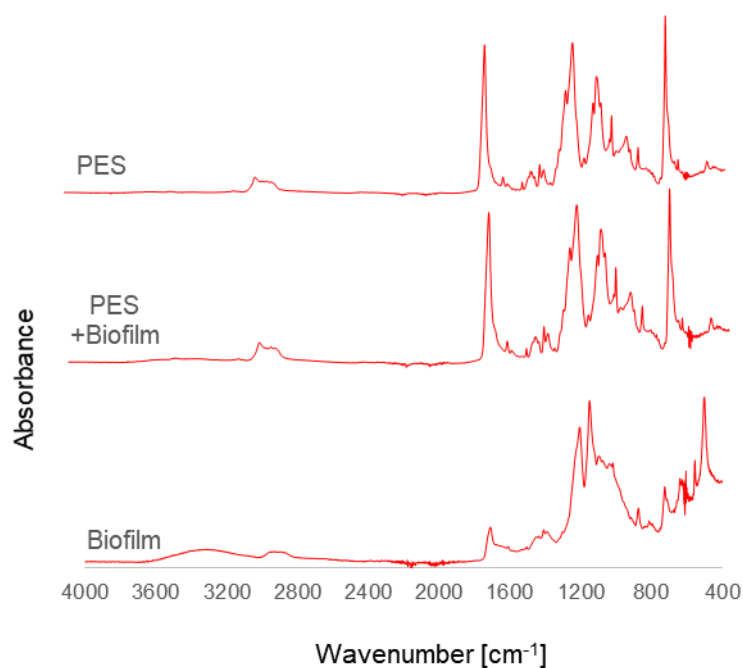


Figure A3-5: FTIR spectra of virgin PES, a pure biofilm sample, and PES covered with biofilm. Both signals cannot be separated in the sample of PES with Biofilm, as there is strong overlapping of bands in the area of 1400-400 cm⁻¹ and the band from 3600-3000 cm⁻¹ is very weak.

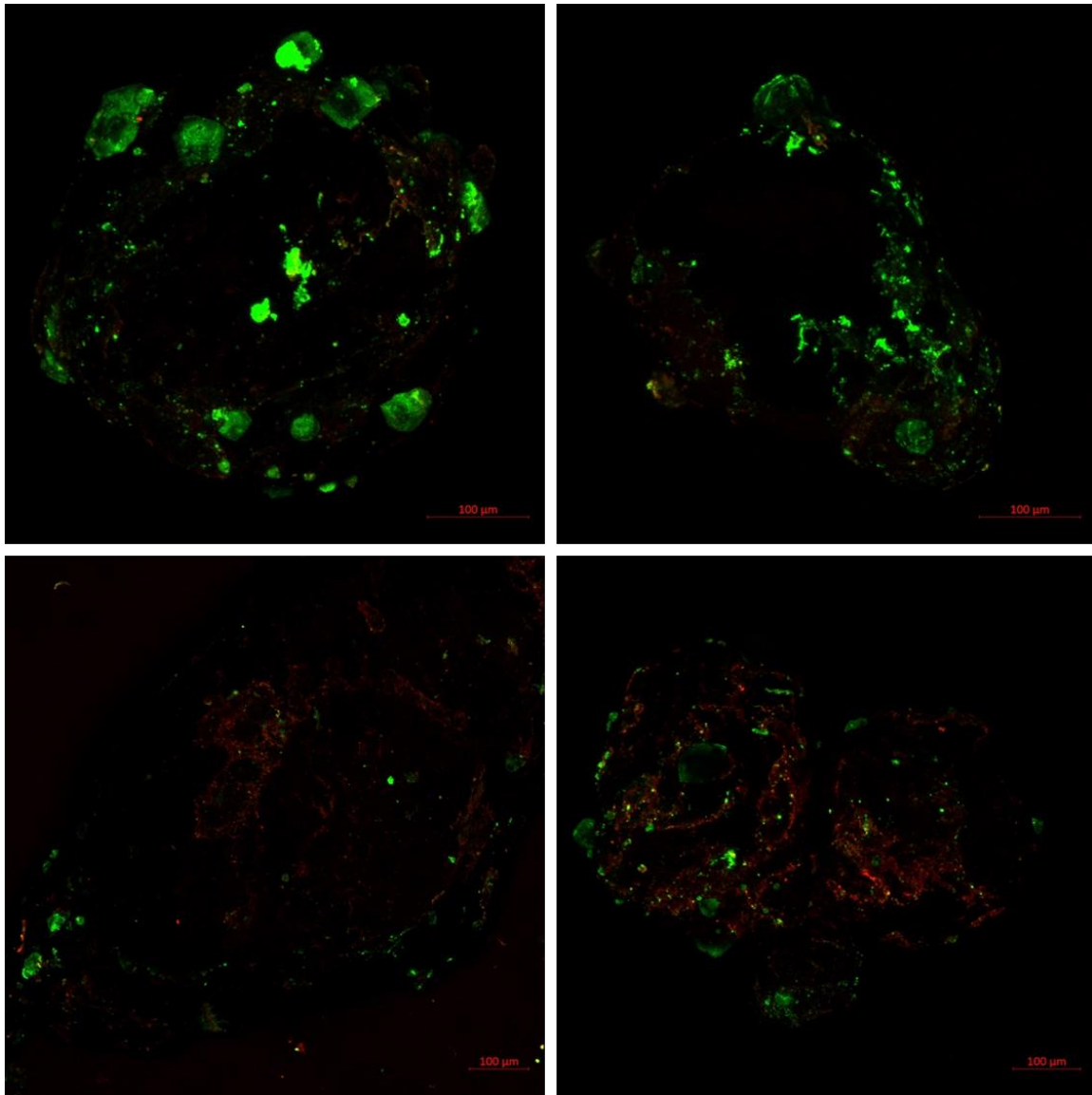


Figure A3-6: CLSM images of Biofilm covered PE after 15 minutes treatment with ultrasound in 35% H₂O₂. Red areas (Syto 60, nucleic acids) are strongly colonized with bacteria, and green areas (AAL-FITC, EPS) show EPS coverage. Compared to untreated PE with Biofilm, the signals are much weaker, as the ultrasound treatment removes the biofilm. Rests of the biofilm are still attached to the surface.

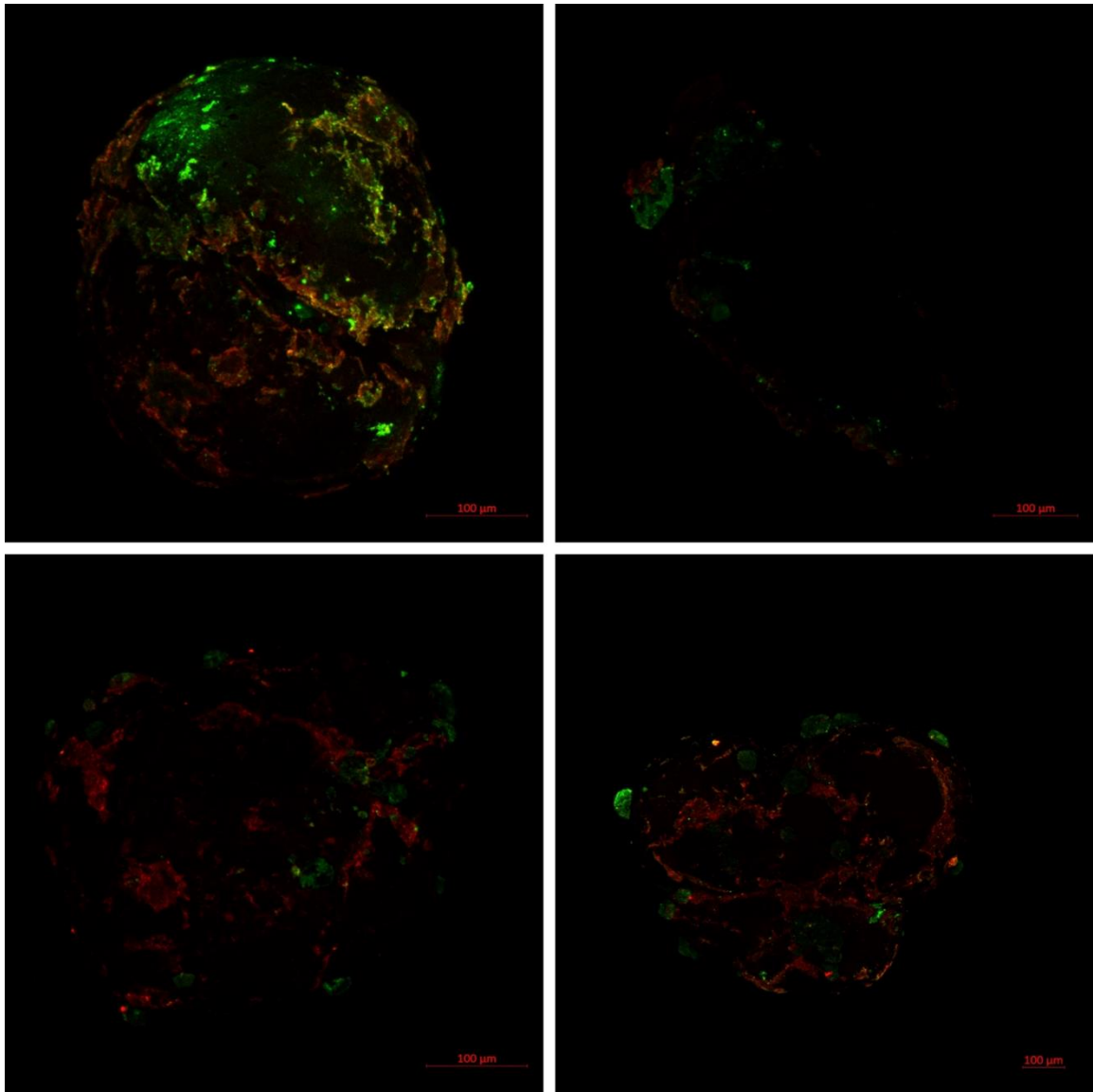


Figure A3-7: CLSM images of Biofilm covered PE after 15 minutes treatment with ultrasound in 35% H_2O_2 . Red areas (Syto 60, nucleic acids) are strongly colonized with bacteria, and green areas (AAL-FITC, EPS) show EPS coverage. Compared to simple ultrasound treatment, the signals, especially of the eps, seem weaker. As it is not possible to quantify the biofilm coverage, this cannot be proven.

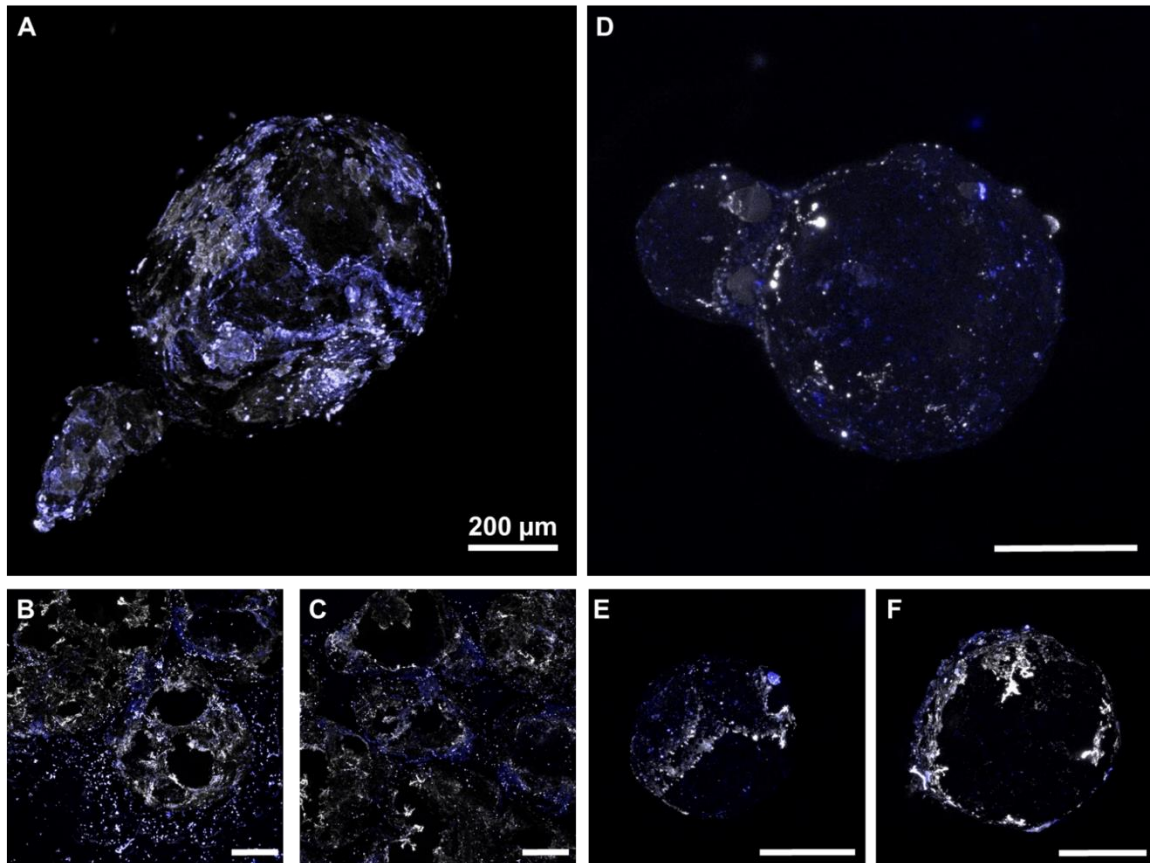


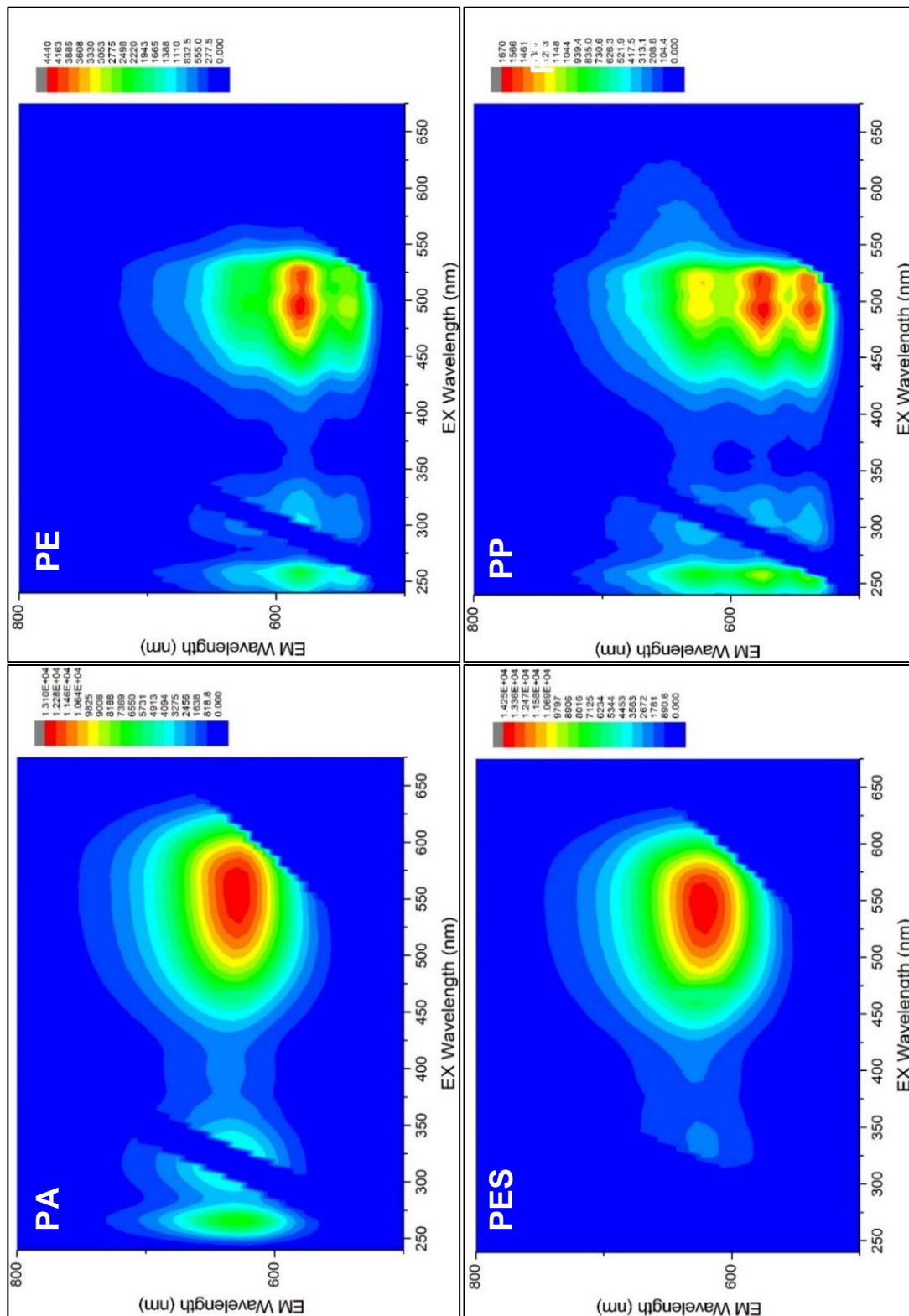
Figure A3-8: CLSM images (maximum intensity projection) of PE and PP based microplastics covered with biofilm. Blue areas (Syto 60, nucleic acids) are strongly colonized with bacteria, and white areas (AAL-FITC, EPS) show EPS coverage. A = PE fresh, B+C= PE stirred in water for 20 min, D = PP fresh, E+F = PP stirred in water for 20 minutes.

A4 Supplementary material for chapter 5

Supplementary material: The potential of fluorescence dyes – Comparative study of Nile red and three derivatives for the detection of microplastics

Table A4-1: Overview of spectroscopy methods and their properties regarding microplastic detection [221].

Properties	Spectroscopy					Thermo-analytical characterization					Chemical Analysis
	μ -Raman	μ FTIR (trans)	FPA FTIR (trans)	μ ATR-FTIR	ATR-FTIR / Raman	NIR	Py-GCMS	LV Py-GCMS	TED-GCMS	DSC	
Dimensions of the sample mass to be examined	ng- μ g	ng- μ g	ng- μ g	mg	mg	mg	μ g	mg	mg	mg	mg
Maximum number of measurable particles per sample	$10^3 - 10^5$	$10^3 - 10^5$	$10^3 - 10^5$	1	1	undefined	undefined	undefined	undefined	undefined	undefined
Measuring time including sample preparation and measurement	h-d	d	h	min	min	min	h	h	h	h	min
Lower detection limit (practice)	1-10 μ m	20 μ m	20 μ m	25-50 μ m	500 μ m	1%	0.5 - 2.5 μ m	0.5 - 2.5 μ m	0.5 - 2.5 μ m	n/a	ppm
Sample preparation for measurement	on filter	on special filter	on special filter	isolated particle	isolated particle	on filter	isolated particles	filtrate or with filter	filtrate or with filter	filtrate	filtrate
Statement on polymer type	Yes	yes	yes	yes	yes	yes	Yes	yes	yes	only PE, PP	no
Detectable additive grade	pigments	no	no	no	no	n/a	Yes	no	no	no	no
Particle surface characterization (chemical)	Yes	no	no	yes	yes	yes	No	no	no	no	no
State of aging	surface oxidation	no	no	surface oxidation	surface oxidation	no	surface oxidation	no	no	molecular mass	no
Particle counting, size, shape, morphology	Yes	yes	yes	yes	yes	no	No	no	no	no	no
Mass balance	No	no	no	no	no	no	No	yes	yes	yes	yes



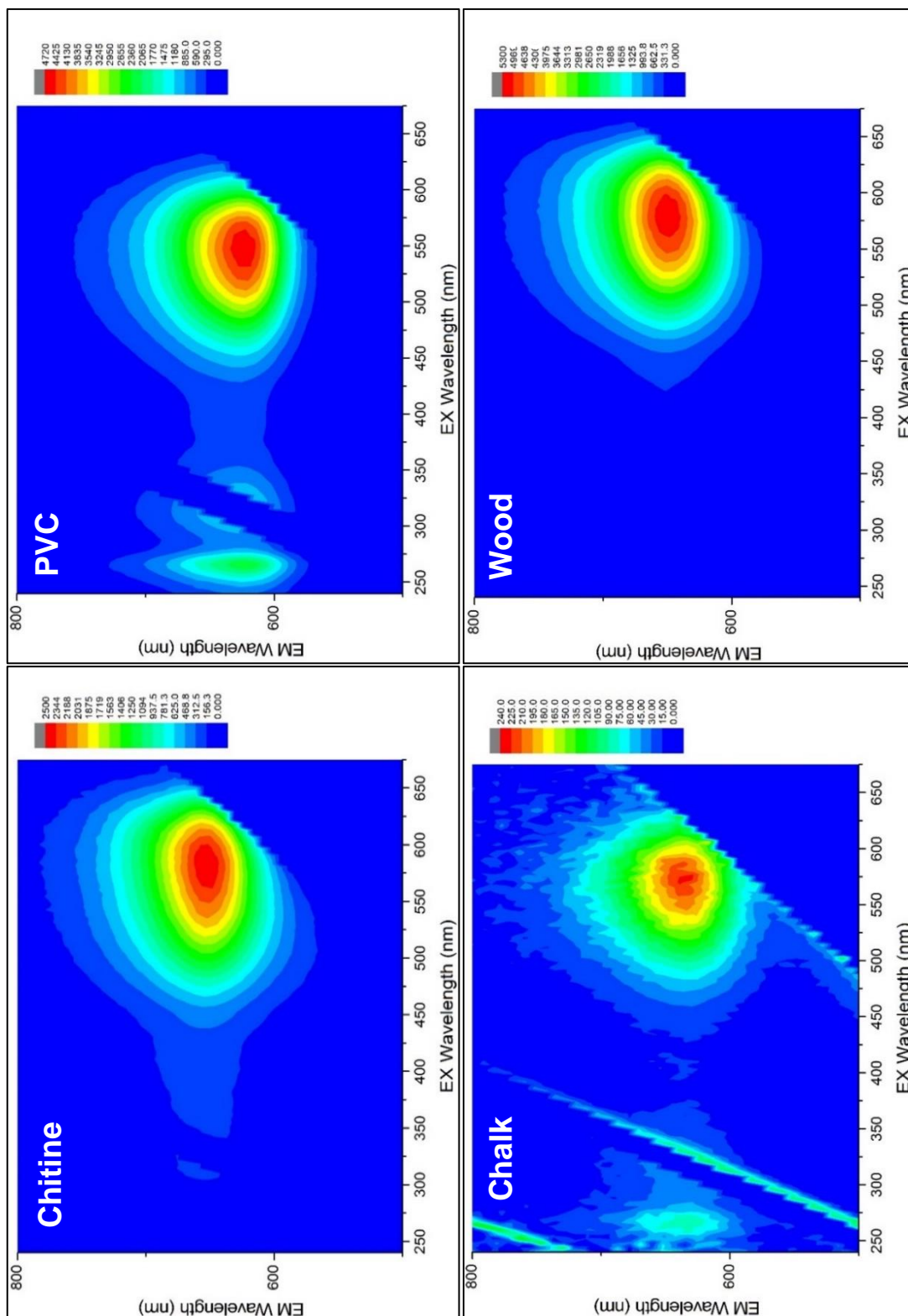


Figure A4-1: 3D Emission fluorescence spectra of different microplastics and natural particles dyed with Nile red in water at acidic pH-value (pH=2.5).
 Note: Color scale for fluorescence signal intensity differs between the spectra.

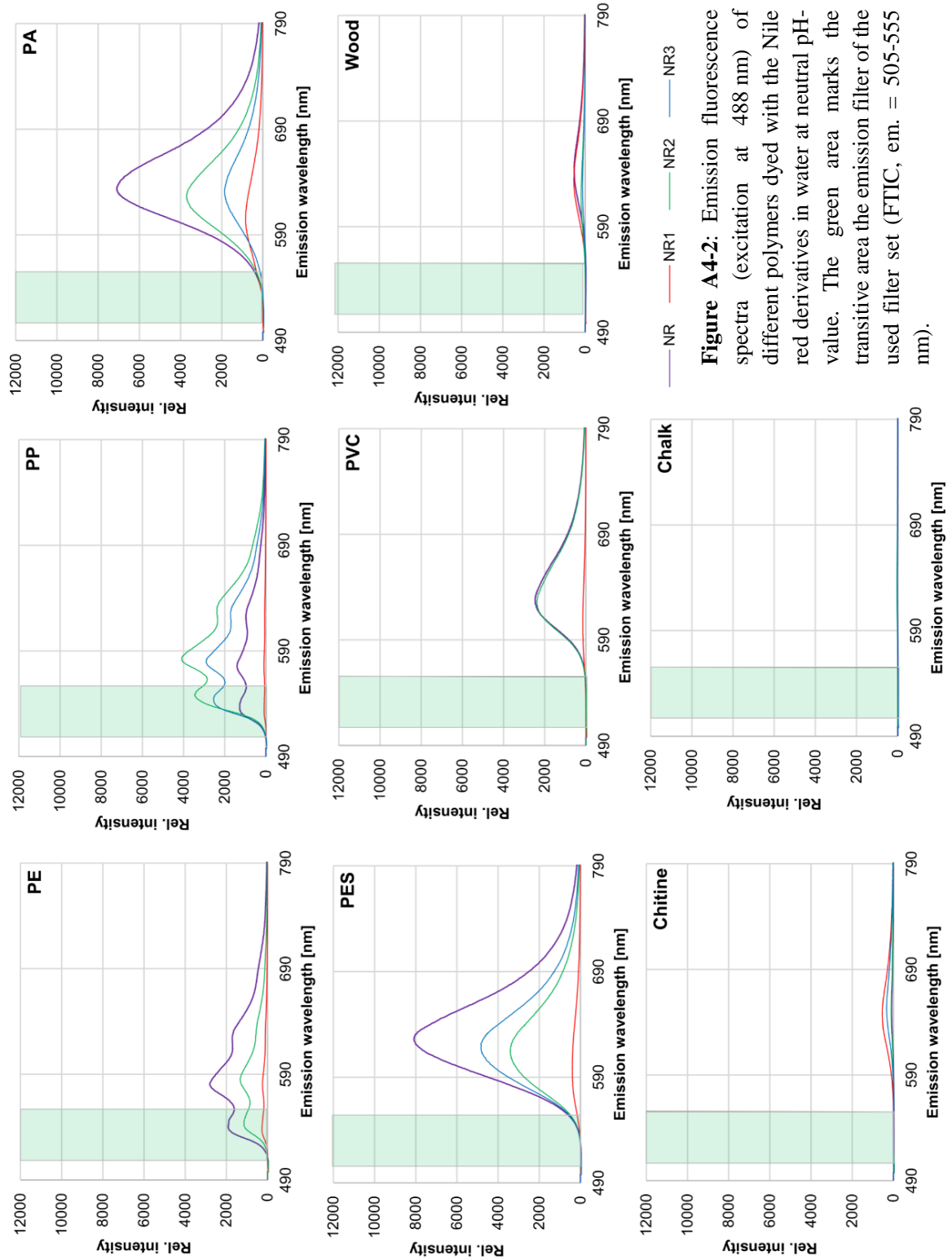


Figure A4-2: Emission fluorescence spectra (excitation at 488 nm) of different polymers dyed with the Nile red derivatives in water at neutral pH-value. The green area marks the transitive area of the emission filter of the used filter set (FTIC, em. = 505-555 nm).

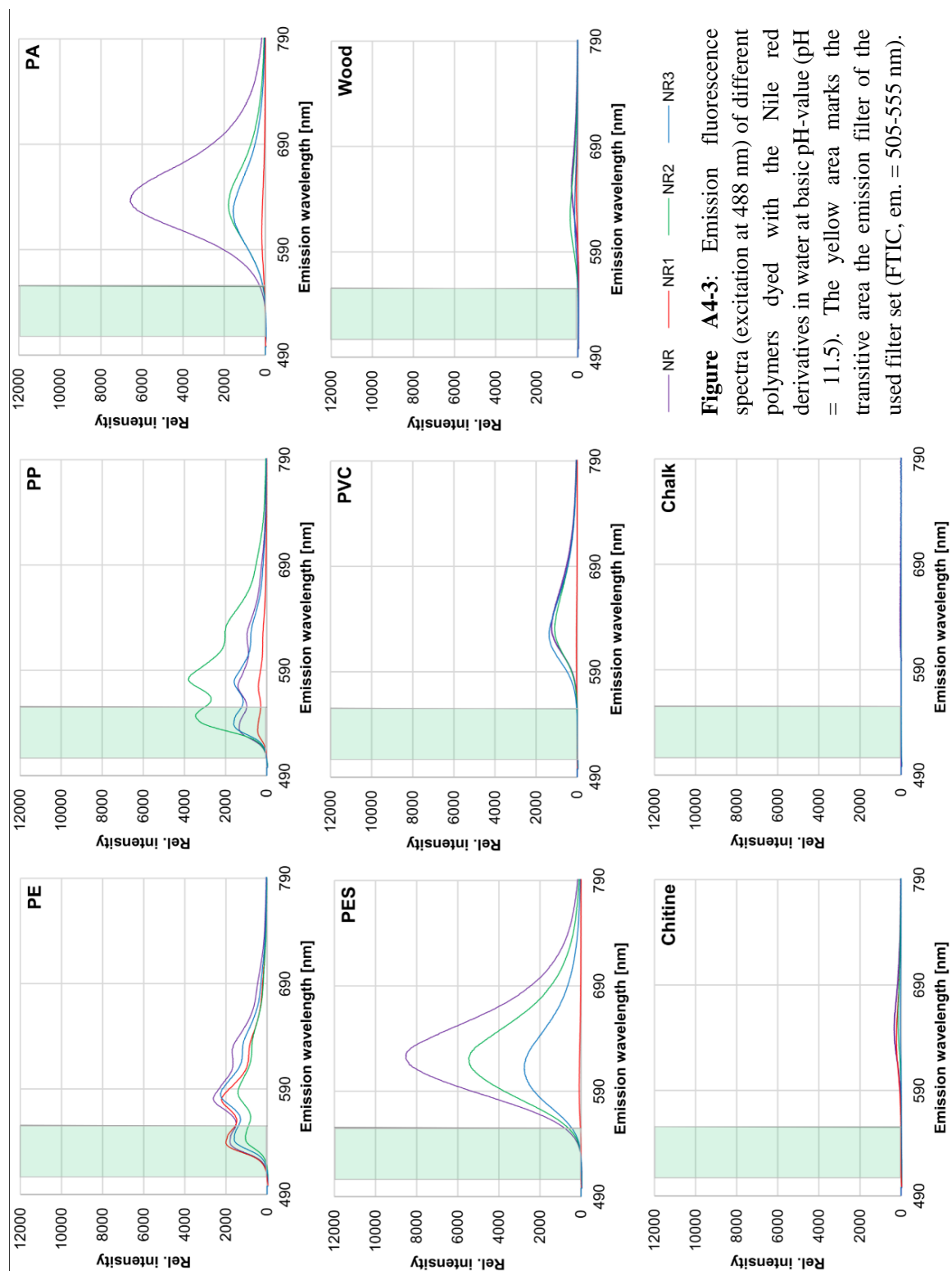


Figure A4-3: Emission fluorescence spectra (excitation at 488 nm) of different polymers dyed with the Nile red derivatives in water at basic pH-value (pH = 11.5). The yellow area marks the transitive area the emission filter of the used filter set (FTIC, em. = 505-555 nm).

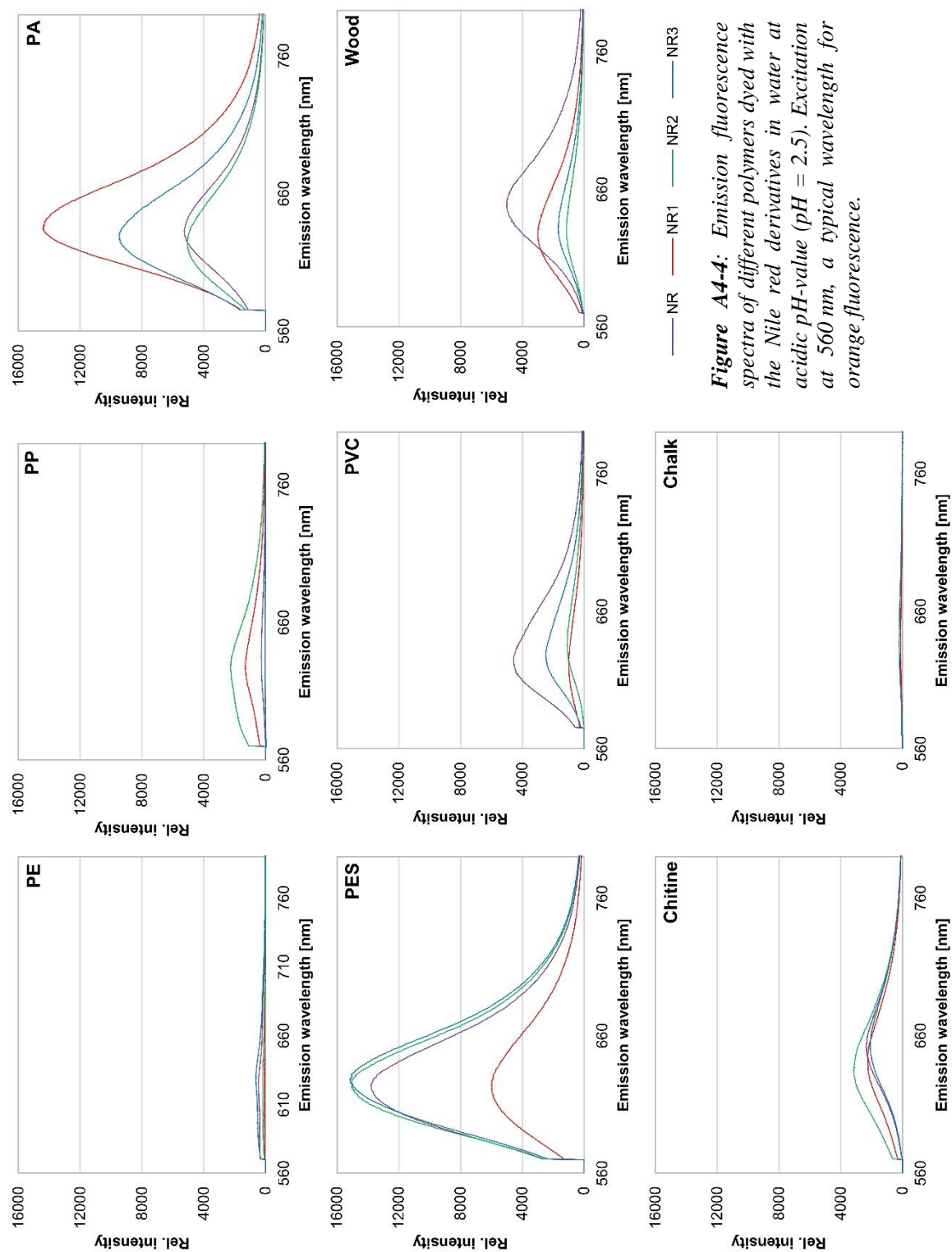


Figure A4-4: Emission fluorescence spectra of different polymers dyed with the Nile red derivatives in water at acidic pH-value (pH = 2.5). Excitation at 560 nm, a typical wavelength for orange fluorescence.

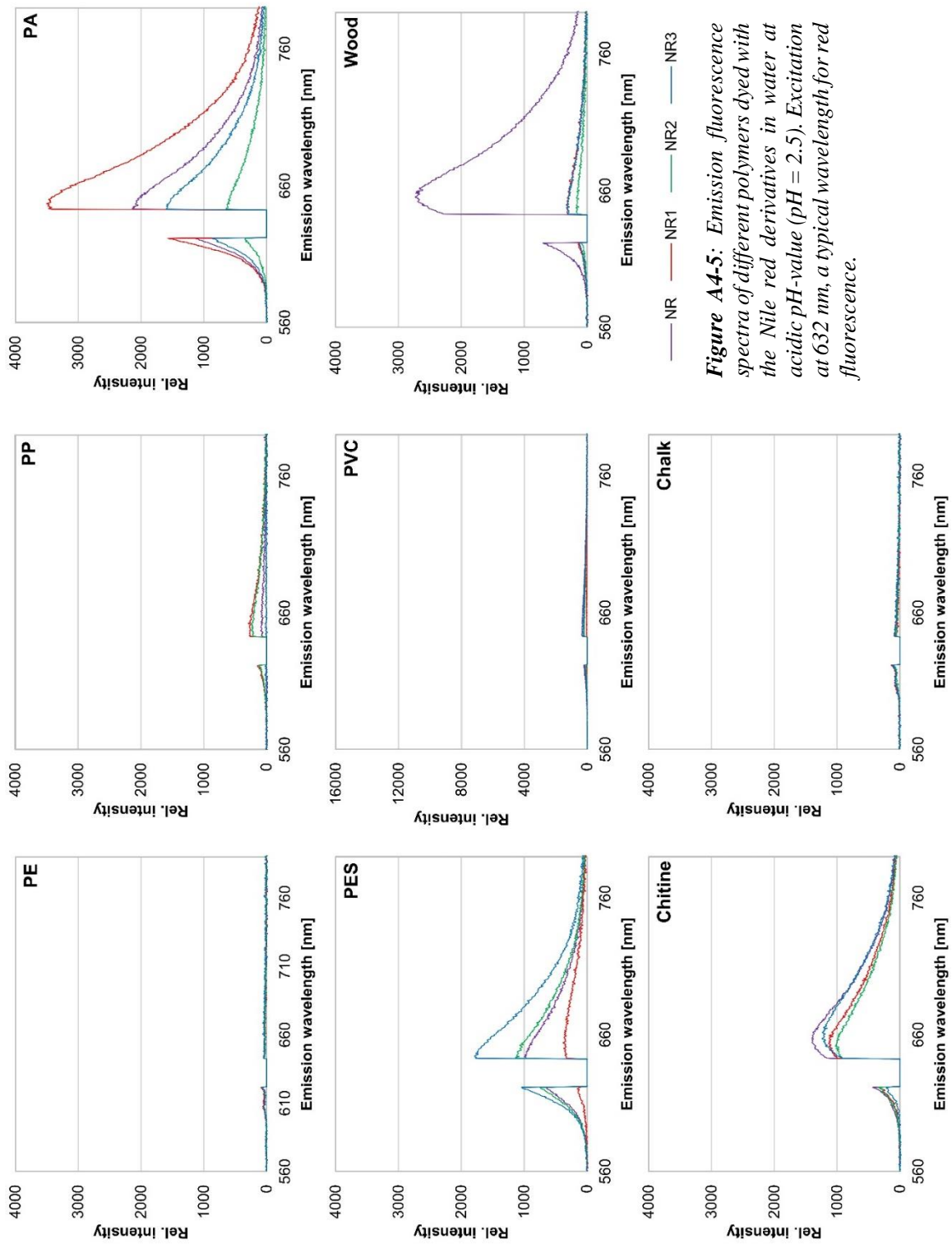
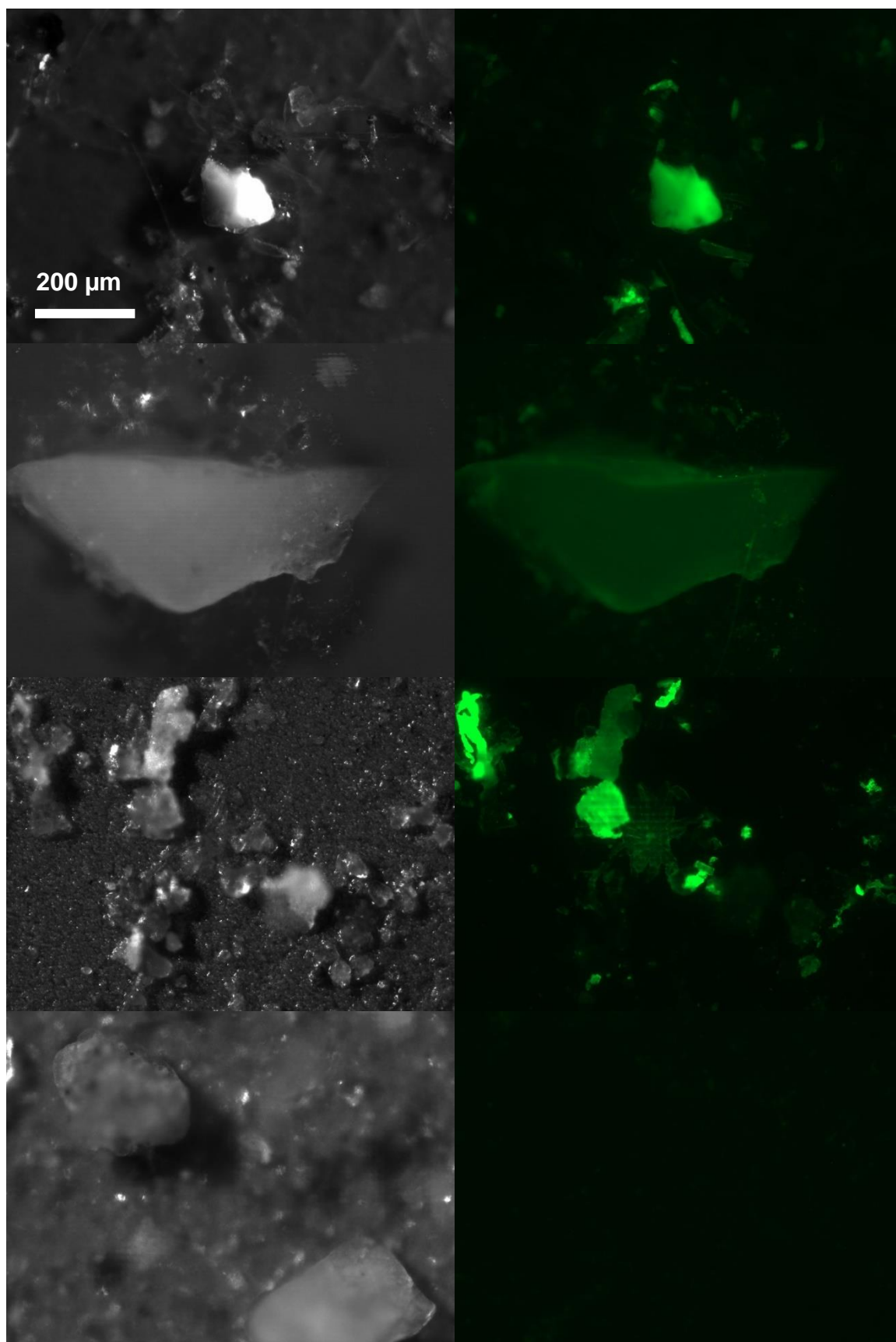
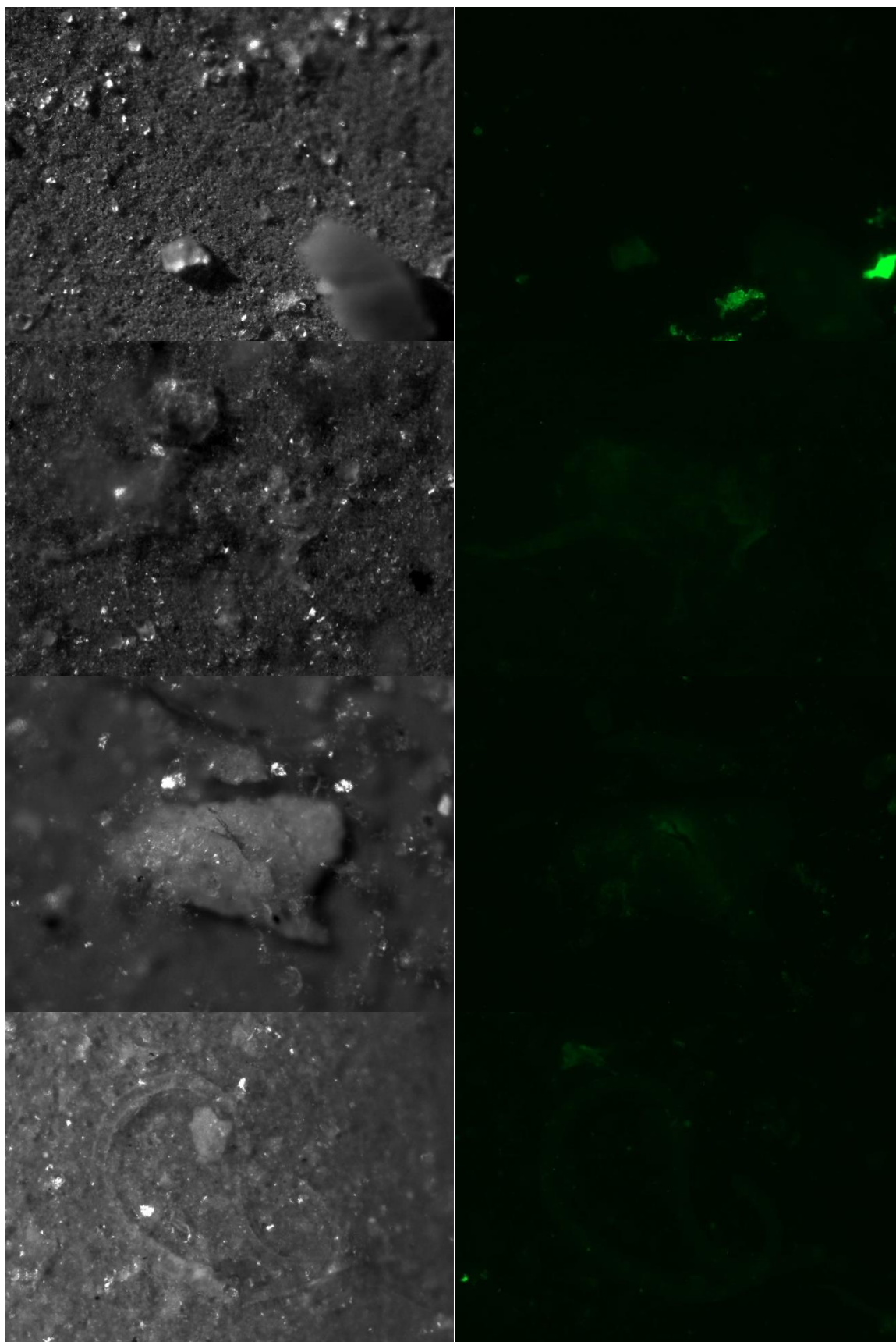


Figure A4-5: Emission fluorescence spectra of different polymers dyed with the Nile red derivatives in water at acidic pH-value (pH = 2.5). Excitation at 632 nm, a typical wavelength for red fluorescence.





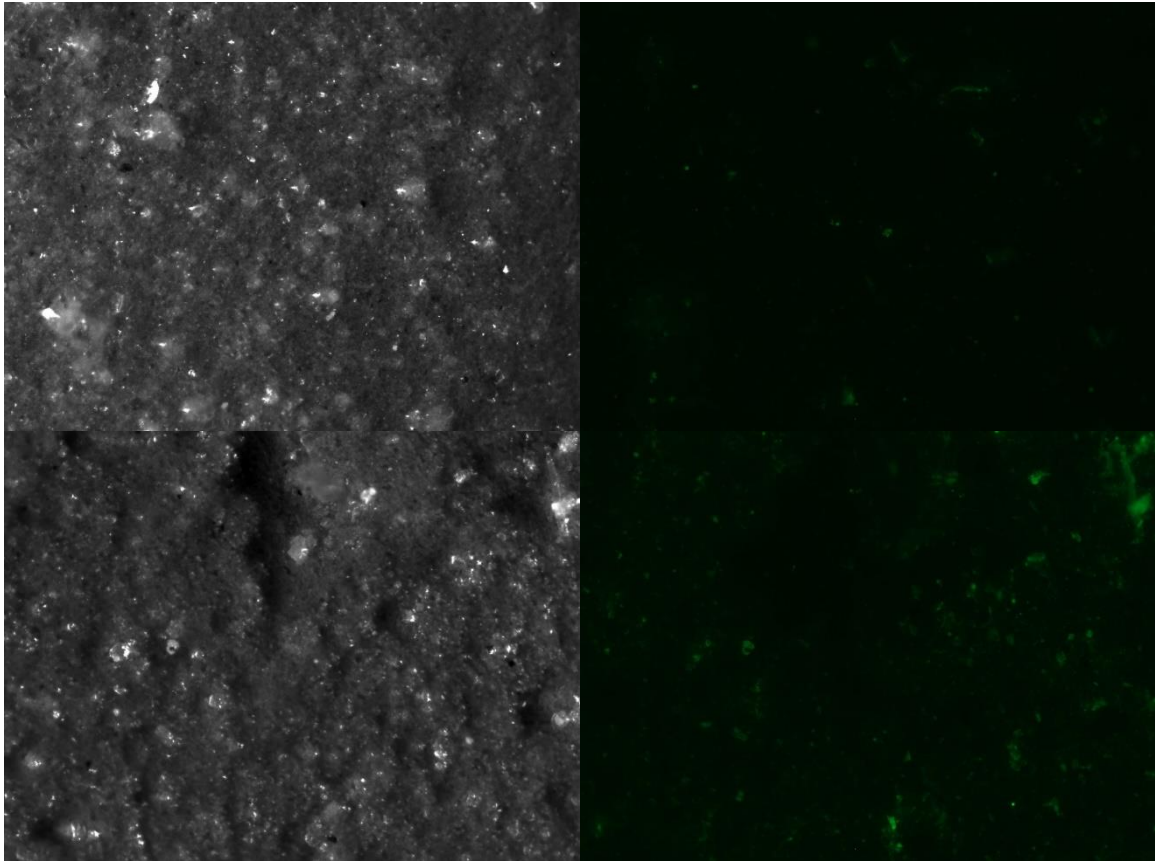


Figure A4-6: *Microscope images taken of the processed and dyed sea salt samples using epiluminescence mode (left) and green fluorescence (right). In most cases the green fluorescence helped to distinguish clearly non-fluorescent particles fluorescent particles, respective microplastics. In some cases the fluorescence signal was of intermediate strength, which made it difficult to say whether it comes from a natural polymer or plastic. Since these cases mainly occurred with small particles in size ranges below 50 μm , we have set the lower size limit for microplastics to this size in order to reduce the uncertainties with this method.*

A5 Verification of the contribution from the co-authors

Chapter 2

Title: Comparative study of the influence of linear and branched alkyltrichlorosilanes on the removal efficiency of polyethylene and polypropylene based microplastic particles from water

Journal: Environmental Science and Pollution Research. 2020;27:10888–98.

Authors: Sturm MT, Herbort AF, Horn H, Schuhen K

Link / DOI: <https://doi.org/10.1007/s11356-020-07712-9>

Position in the dissertation

The content of this paper has been included in Chapter 2

Contribution of Michael Toni Sturm (first author) (75 %)

- Conceived the concept
- Designed and conducted experiments for the investigation of reaction kinetics and analysis of agglomerates. Conducted the experiments for the removal of 13 of the 18 organosilanes tested
- Analyzed and visualized the results
- Wrote the manuscript (80%)

Contribution of Adrian Frank Herbort (second author) (15 %)

- Conceived the concept
- Designed experiments for microplastics removal and conducted the experiments for the removal for 5 of the 18 organosilanes tested
- Analyzed the results
- Wrote the manuscript (20%)

Contribution of Harald Horn (third author) (4 %)

- Discussed the results
- Corrected the manuscript

Contribution of Katrin Schuhen (fourth author) (6 %)

- Designed the experiments
- Discussed the results
- Corrected the manuscript

Signature of the authors:

Author	Signature / electronic signature
Michael Toni Sturm	
Adrian Frank Herbort	
Harald Horn	
Katrin Schuhen	

Permission from Springer

“The author retains the right to use his/her article for his/her further scientific career by including the final published journal article in other publications such as dissertations and postdoctoral qualifications provided acknowledgement is given to the original source of publication.”

Source: Copyright Transfer Statement from Springer

(<https://resource-cms.springernature.com/springer-cms/rest/v1/content/19752/data/v3>),

Accessed on the 15th of October 2021

Chapter 3

Title: Removal of Microplastics from Waters through Agglomeration-Fixation Using Organosilanes—Effects of Polymer Types, Water Composition and Temperature.
Journal: Water, 13, 675 (2021).
Authors: Sturm, M.T., Horn, H., Schuhen, K.
Link / DOI: <https://doi.org/10.3390/w13050675>

Position in the dissertation

The content of this paper has been included in Chapter 3

Contribution of Michael Toni Sturm (first author) (90 %)

- Conceived the concept
- Designed and conducted the experiments
- Analyzed and visualized the results
- Wrote the manuscript

Contribution of Harald Horn (second author) (4 %)

- Discussed the results
- Corrected the manuscript

Contribution of Katrin Schuhen (third author) (6 %)

- Designed the experiments
- Discussed the results
- Corrected the manuscript

Signature of the authors:

Author	Signature / electronic signature
Michael Toni Sturm	
Harald Horn	
Katrin Schuhen	

Permission from MDPI

“This is an open access article distributed under the Creative Commons Attribution License which permits unrestricted use, distribution, and reproduction in any medium, provided the original work is properly cited”

Source: MDPI website of the paper, copyright statement,
(<https://www.mdpi.com/2073-4441/13/5/675>),

Accessed on the 16th of October 2021

Chapter 4

Title: Method for rapid biofilm cultivation on microplastics and investigation of its effect on the agglomeration and removal of microplastics using organosilanes

Journal: Science of The Total Environment, 151388 (2021)

Authors: Sturm, M.T., Schuhen, K., Horn, H.

Link / DOI: <https://doi.org/10.1016/j.scitotenv.2021.151388>

Position in the dissertation

The content of this paper has been included in Chapter 4

Contribution of Michael Toni Sturm (first author) (90 %)

- Conceived the concept
- Designed and conducted the experiments
- Analyzed and visualized the results
- Wrote the manuscript

Contribution of Katrin Schuhen (second author) (4 %)

- Discussed the results
- Corrected the manuscript

Contribution of Harald Horn (third author) (6 %)

- Designed experiments
- Discussed the results
- Corrected the manuscript

Signature of the authors:

Author	Signature / electronic signature
Michael Toni Sturm	
Harald Horn	
Katrin Schuhen	

Permission from Elsevier

„Authors can include their articles in full or in part in a thesis or dissertation for non-commercial purposes.”

Source: Homepage Elsevier

(<https://www.elsevier.com/about/policies/copyright/permissions>),

Accessed on the 14th of November 2019

Chapter 5

Title: The potential of fluorescent dyes—comparative study of Nile red and three derivatives for the detection of microplastics.

Journal: Analytical and Bioanalytical Chemistry 413, 1059–1071 (2021).

Authors: Sturm, M.T., Horn, H., Schuhen, K.

Link / DOI: <https://doi.org/10.1007/s00216-020-03066-w>

Position in the dissertation

The content of this paper has been included in Chapter 3

Contribution of Michael Toni Sturm (first author) (90 %)

- Conceived the concept
- Designed and conducted the experiments
- Analyzed and visualized the results
- Wrote the manuscript

Contribution of Harald Horn (second author) (4 %)

- Discussed the results
- Corrected the manuscript

Contribution of Katrin Schuhen (third author) (6 %)

- Designed the experiments
- Discussed the results
- Corrected the manuscript

Signature of the authors:

Author	Signature / electronic signature
Michael Toni Sturm	
Harald Horn	
Katrin Schuhen	

Permission from Springer

“The author retains the right to use his/her article for his/her further scientific career by including the final published journal article in other publications such as dissertations and postdoctoral qualifications provided acknowledgement is given to the original source of publication.”

Source: Copyright Transfer Statement from Springer

(<https://resource-cms.springernature.com/springer-cms/rest/v1/content/19752/data/v3>),

Accessed on the 15th of October 2021

List of abbreviations

²⁹ Si-MAS-NMR	Silicon-29 magic-angle-spinning magnetic resonance spectroscopy
ABS	Acrylonitrile butadiene styrene
ATR	Attenuated total reflectance
AAL	Aleuria aurantia lectin
BP	Bandpass
CLSM	Confocal laser scanning microscopy (CLSM),
DOC	Dissolved organic carbon
DSC	Differential scanning calorimetry
DW	demineralized water
EPS	Extracellular polymeric substances
FPA	Focal Plane Array
FT	Color splitter (“Farb Teiler”)
FTIR	Fourier-transform infrared spectroscopy
FITC	Fluorescein isothiocyanate
HDPE	High-density polyethylene
ICP-MS	Inductively coupled plasma mass spectrometry
ICP-OES	Inductively coupled plasma atomic emission spectroscopy
k	Reaction constant
LDPE	Low-density polyethylene
PA	Polyamide
PE	Polyethylene
PE-X	abcr eco Wasser 3.0 PE-X®
PES	Polyester
PP	Polypropylene
PS	Polystyrene
PUR	Polyurethane
PVC	Polyvinyl chloride
MP	Microplastics
NR	Nile red
NR 1	Nile red derivative (2-propionicacid modified)
NR 2	Nile red derivative (n-hexyl modified)
NR 3	Nile red derivative (ethylhexyl modified)
NIR	Near-infrared spectroscopy
OCT	Optical coherence tomography
Py-GC/MS	Pyrolysis–gas chromatography–mass spectrometry
SEM	scanning electron microscopy

List of abbreviations

SW	salt water
$t_{1/2}$	Half-life time
TED GC/MS	Thermal extraction and –desorption combined with gas chromatography-mass spectrometry
TGA	Thermogravimetric analysis
TOC	Total organic carbon
WW	biologically treated wastewater

References

1. PlasticsEurope. *Plastics – the Facts 2020, An analysis of European latest plastics production, demand and waste data*, Brussels, Belgium: Association of Plastics Manufacturers. 2020. <https://www.plasticseurope.org/de/resources/publications/196-plastics-facts-2013>. Accessed 30 Mar 2021.
2. Juergen Bertling, Hamann L, Bertling R. *Kunststoffe in der Umwelt*. Oberhausen: Fraunhofer UMSICHT; 2018.
3. Buchanan JB. Pollution by synthetic fibres. *Marine Pollution Bulletin*. 1971;2:23. doi:10.1016/0025-326X(71)90136-6.
4. Kenyon KW, Kridler E. Laysan Albatrosses Swallow Indigestible Matter. *The Auk*. 1969;86:339–43. doi:10.2307/4083505.
5. Colton JB, JR, Burns BR, Knapp FD. Plastic particles in surface waters of the northwestern atlantic. *Science*. 1974;185:491–7. doi:10.1126/science.185.4150.491.
6. Thompson RC, Olsen Y, Mitchell RP, Davis, A., Rowland, S.J., John AWG. Lost at Sea: Where Is All the Plastic? *Science*. 2004;304:838. doi:10.1126/science.1094559.
7. Frias, J. P. G. L., Nash R. Microplastics: Finding a consensus on the definition. *Marine Pollution Bulletin*. 2019;138:145–7. doi:10.1016/j.marpolbul.2018.11.022.
8. Braun U. Statuspapier Mikroplastik-Analytik - Probenahme, Probenaufbereitung und Detektionsverfahren. 2020. https://bmbf-plastik.de/sites/default/files/2020-11/Statuspapier_Mikroplastik%20Analytik_Plastik%20in%20der%20Umwelt_2020.pdf. Accessed 4 Oct 2021.
9. Cole M, Lindeque P, Halsband C, Galloway TS. Microplastics as contaminants in the marine environment: a review. *Marine Pollution Bulletin*. 2011;62:2588–97. doi:10.1016/j.marpolbul.2011.09.025.
10. Ivleva NP, Wiesheu AC, Niessner R. Microplastic in Aquatic Ecosystems. *Angew Chem Int Ed Engl* 2016. doi:10.1002/anie.201606957.
11. Geyer R, Jambeck JR, Law KL. Production, use, and fate of all plastics ever made. *Sci. Adv*. 2017;3:e1700782. doi:10.1126/sciadv.1700782.
12. Jambeck JR, Geyer R, Wilcox C, Siegler TR, Perryman M, Andrady A, et al. Plastic waste inputs from land into the ocean. *Science*. 2015;347:768–71. doi:10.1126/science.1260352.
13. Law KL, Starr N, Siegler TR, Jambeck JR, Mallos NJ, Leonard GH. The United States' contribution of plastic waste to land and ocean. *Sci. Adv*. 2020. doi:10.1126/sciadv.abd0288.
14. Borrelle SB, Ringma J, Law KL, Monnahan CC, Lebreton L, McGivern A, et al. Predicted growth in plastic waste exceeds efforts to mitigate plastic pollution. *Science*. 2020;369:1515–8. doi:10.1126/science.aba3656.
15. Li WC, Tse HF, Fok L. Plastic waste in the marine environment: A review of sources, occurrence and effects. *Sci Total Environ*. 2016;566-567:333–49. doi:10.1016/j.scitotenv.2016.05.084.

16. Horton AA, Dixon SJ. Microplastics: An introduction to environmental transport processes. *WIREs Water*. 2018;5:1. doi:10.1002/wat2.1268.
17. Hale RC, Seeley ME, La Guardia MJ, Mai L, Zeng EY. A Global Perspective on Microplastics. *J. Geophys. Res. Oceans*. 2020;125:1. doi:10.1029/2018JC014719.
18. van Wijnen J, Ragas AMJ, Kroeze C. Modelling global river export of microplastics to the marine environment: Sources and future trends. *Sci Total Environ*. 2019;673:392–401. doi:10.1016/j.scitotenv.2019.04.078.
19. Law KL, Thompson RC. Microplastics in the seas. *Science*. 2014;345:144–5. doi:10.1126/science.1254065.
20. van Sebille E, Wilcox C, Lebreton L, Maximenko N, Hardesty BD, van Franeker JA, et al. A global inventory of small floating plastic debris. *Environ. Res. Lett*. 2015;10:124006. doi:10.1088/1748-9326/10/12/124006.
21. Peeken I, Primpke S, Beyer B, Gütermann J, Katlein C, Krumpen T, et al. Arctic sea ice is an important temporal sink and means of transport for microplastic. *Nat Commun*. 2018;9:1505. doi:10.1038/s41467-018-03825-5.
22. Bergmann M, Wirzberger V, Krumpen T, Lorenz C, Primpke S, Tekman MB, Gerdts G. High Quantities of Microplastic in Arctic Deep-Sea Sediments from the HAUSGARTEN Observatory. *Environ Sci Technol*. 2017;51:11000–10. doi:10.1021/acs.est.7b03331.
23. van Cauwenberghe L, Vanreusel A, Mees J, Janssen CR. Microplastic pollution in deep-sea sediments. *Environ Pollut*. 2013;182:495–9. doi:10.1016/j.envpol.2013.08.013.
24. Germanov ES, Marshall AD, Bejder L, Fossi MC, Loneragan NR. Microplastics: No Small Problem for Filter-Feeding Megafauna. *Trends Ecol Evol (Amst)*. 2018;33:227–32. doi:10.1016/j.tree.2018.01.005.
25. Girard EB, Fuchs A, Kaliwoda M, Lasut M, Ploetz E, Schmahl WW, Wörheide G. Sponges as bioindicators for microparticulate pollutants; 2020.
26. Bergmann M, Gutow L, Klages M, editors. *Marine Anthropogenic Litter*. Cham: Springer International Publishing; 2015.
27. Horton AA, Walton A, Spurgeon DJ, Lahive E, Svendsen C. Microplastics in freshwater and terrestrial environments: Evaluating the current understanding to identify the knowledge gaps and future research priorities. *Sci Total Environ*. 2017;586:127–41. doi:10.1016/j.scitotenv.2017.01.190.
28. Dris R, Gasperi J, Rocher V, Saad M, Renault N, Tassin B. Microplastic contamination in an urban area: a case study in Greater Paris. *Environ. Chem*. 2015;12:592. doi:10.1071/en14167.
29. Rillig MC, Lehmann A. Microplastic in terrestrial ecosystems. *Science*. 2020;368:1430–1. doi:10.1126/science.abb5979.
30. Dris R, Gasperi J, Mirande C, Mandin C, Guerrouache M, Langlois V, Tassin B. A first overview of textile fibers, including microplastics, in indoor and outdoor environments. *Environ Pollut*. 2017;221:453–8. doi:10.1016/j.envpol.2016.12.013.

31. González-Pleiter M, Edo C, Aguilera Á, Viúdez-Moreiras D, Pulido-Reyes G, González-Toril E, et al. Occurrence and transport of microplastics sampled within and above the planetary boundary layer. *Sci Total Environ.* 2021;761:143213. doi:10.1016/j.scitotenv.2020.143213.
32. Evangeliou N, Grythe H, Klimont Z, Heyes C, Eckhardt S, Lopez-Aparicio S, Stohl A. Atmospheric transport is a major pathway of microplastics to remote regions. *Nat Commun.* 2020;11:3381. doi:10.1038/s41467-020-17201-9.
33. Zhang K, Hamidian AH, Tubić A, Zhang Y, Fang JKH, Wu C, Lam PKS. Understanding plastic degradation and microplastic formation in the environment: A review. *Environ Pollut.* 2021;274:116554. doi:10.1016/j.envpol.2021.116554.
34. Chamas A, Moon H, Zheng J, Qiu Y, Tabassum T, Jang JH, et al. Degradation Rates of Plastics in the Environment. *ACS Sustainable Chem. Eng.* 2020;8:3494–511. doi:10.1021/acssuschemeng.9b06635.
35. Gewert B, Plassmann MM, MacLeod M. Pathways for degradation of plastic polymers floating in the marine environment. *Environ Sci Process Impacts.* 2015;17:1513–21. doi:10.1039/C5EM00207A.
36. Adam V, Yang T, Nowack B. Toward an ecotoxicological risk assessment of microplastics: Comparison of available hazard and exposure data in freshwaters. *Environ Toxicol Chem.* 2019;38:436–47. doi:10.1002/etc.4323.
37. Du J, Zhou Q, Li H, Xu S, Wang C, Fu L, Tang J. Environmental distribution, transport and ecotoxicity of microplastics: A review. *J Appl Toxicol.* 2021;41:52–64. doi:10.1002/jat.4034.
38. Galloway TS, Cole M, Lewis C. Interactions of microplastic debris throughout the marine ecosystem. *Nat Ecol Evol.* 2017;1:116. doi:10.1038/s41559-017-0116.
39. Lambert S, Scherer C, Wagner M. Ecotoxicity testing of microplastics: Considering the heterogeneity of physicochemical properties. *Integr Environ Assess Manag.* 2017;13:470–5. doi:10.1002/ieam.1901.
40. Wright SL, Thompson RC, Galloway TS. The physical impacts of microplastics on marine organisms: A review. *Environmental Pollution.* 2013;178:483–92. doi:10.1016/j.envpol.2013.02.031.
41. Jemec A, Horvat P, Kunej U, Bele M, Kržan A. Uptake and effects of microplastic textile fibers on freshwater crustacean *Daphnia magna*. *Environ Pollut.* 2016;219:201–9. doi:10.1016/j.envpol.2016.10.037.
42. Prinz N, Korez Š. Understanding How Microplastics Affect Marine Biota on the Cellular Level Is Important for Assessing Ecosystem Function: A Review. In: Jungblut S, Liebich V, Bode-Dalby M, editors. *YOUMARES 9 - The Oceans: Our Research, Our Future*. Cham: Springer International Publishing; 2020. p. 101–120. doi:10.1007/978-3-030-20389-4_6.
43. Kalčíková G, Skalar T, Marolt G, Jemec Kokalj A. An environmental concentration of aged microplastics with adsorbed silver significantly affects aquatic organisms. *Water Research.* 2020;175:115644. doi:10.1016/j.watres.2020.115644.

44. Beiras R, Verdejo E, Campoy-López P, Vidal-Liñán L. Aquatic toxicity of chemically defined microplastics can be explained by functional additives. *J Hazard Mater.* 2021;406:124338. doi:10.1016/j.jhazmat.2020.124338.
45. Teuten EL, Rowland SJ, Galloway TS, Thompson RC. Potential for plastics to transport hydrophobic contaminants. *Environ. Sci. Technol.* 2007;41:7759–64. doi:10.1021/es071737s.
46. Atugoda T, Vithanage M, Wijesekara H, Bolan N, Sarmah AK, Bank MS, et al. Interactions between microplastics, pharmaceuticals and personal care products: Implications for vector transport. *Environ Int.* 2021;149:106367. doi:10.1016/j.envint.2020.106367.
47. Viršek MK, Lovšin MN, Koren Š, Kržan A, Peterlin M. Microplastics as a vector for the transport of the bacterial fish pathogen species *Aeromonas salmonicida*. *Marine Pollution Bulletin.* 2017;125:301–9. doi:10.1016/j.marpolbul.2017.08.024.
48. Rillig MC, Hoffmann M, Lehmann A, Liang Y, Lück M, Augustin J. Microplastic fibers affect dynamics and intensity of CO₂ and N₂O fluxes from soil differently. *Micropl.&Nanopl.* 2021;1:894. doi:10.1186/s43591-021-00004-0.
49. Rocha-Santos T, Costa M, Mouneyrac C, editors. *Handbook of Microplastics in the Environment.* Cham: Springer International Publishing; 2020.
50. Prata JC. Airborne microplastics: Consequences to human health? *Environ Pollut.* 2018;234:115–26. doi:10.1016/j.envpol.2017.11.043.
51. Yong CQY, Valiyaveetill S, Tang BL. Toxicity of Microplastics and Nanoplastics in Mammalian Systems. *Int J Environ Res Public Health* 2020. doi:10.3390/ijerph17051509.
52. Lusher A, Hollman PCH, Mendoza-Hill J. *Microplastics in fisheries and aquaculture: Status of knowledge on their occurrence and implications for aquatic organisms and food safety.* Rome: Food and Agriculture Organization of the United Nations; 2017.
53. Ju P, Zhang Y, Zheng Y, Gao F, Jiang F, Li J, Sun C. Probing the toxic interactions between polyvinyl chloride microplastics and Human Serum Albumin by multispectroscopic techniques. *Sci Total Environ.* 2020;734:139219. doi:10.1016/j.scitotenv.2020.139219.
54. Rafiee M, Dargahi L, Eslami A, Beirami E, Jahangiri-Rad M, Sabour S, Amereh F. Neurobehavioral assessment of rats exposed to pristine polystyrene nanoplastics upon oral exposure. *Chemosphere.* 2018;193:745–53. doi:10.1016/j.chemosphere.2017.11.076.
55. Ragusa A, Svelato A, Santacroce C, Catalano P, Notarstefano V, Carnevali O, et al. Plasticenta: First evidence of microplastics in human placenta. *Environ Int.* 2021;146:106274. doi:10.1016/j.envint.2020.106274.
56. Sturm M, Hiller C, Schuhen K. Ursprung und Auswirkungen synthetischer Polymere in der Umwelt, Teil 2: Wie kann man das Risikopotential von Mikroplastik für Mensch, Tier und Umwelt einschätzen? *GIT Labor-Fachzeitschrift WileyVCH.* 2019:16–8.
57. Vethaak AD, Legler J. Microplastics and human health. *Science.* 2021;371:672–4. doi:10.1126/science.abe5041.

58. Rist S, Carney Almroth B, Hartmann NB, Karlsson TM. A critical perspective on early communications concerning human health aspects of microplastics. *Sci Total Environ.* 2018;626:720–6. doi:10.1016/j.scitotenv.2018.01.092.
59. Schuhen K, Sturm MT. Microplastic Pollution and Reduction Strategies. In: Rocha-Santos T, Costa M, Mouneyrac C, editors. *Handbook of Microplastics in the Environment*. Cham: Springer International Publishing; 2020. p. 1–33. doi:10.1007/978-3-030-10618-8_53-1.
60. Lange K, Magnusson K, Viklander M, Blecken G-T. Removal of rubber, bitumen and other microplastic particles from stormwater by a gross pollutant trap - bioretention treatment train. *Water Research.* 2021;202:117457. doi:10.1016/j.watres.2021.117457.
61. Amy G, Ghaffour N, Li Z, Francis L, Linares RV, Missimer T, Lattemann S. Membrane-based seawater desalination: Present and future prospects. *Desalination.* 2017;401:16–21. doi:10.1016/j.desal.2016.10.002.
62. Golgoli M, Khiadani M, Shafieian A, Sen TK, Hartanto Y, Johns ML, Zargar M. Microplastics fouling and interaction with polymeric membranes: A review. *Chemosphere.* 2021;283:131185. doi:10.1016/j.chemosphere.2021.131185.
63. Pinnekamp J, Firk J, Keysers C, Mousel, D, Ruppelt JP, Katharina T. Elimination von Mikroschadstoffen, Mikroplastik und multiresistenten Keimen. Bochum, Germany: 34. Bochumer Workshop Siedlungswasserwirtschaft; 2016.
64. Peixoto D, Pinheiro C, Amorim J, Oliva-Teles L, Guilhermino L, Vieira MN. Microplastic pollution in commercial salt for human consumption: A review. *Estuarine, Coastal and Shelf Science.* 2019;219:161–8. doi:10.1016/j.ecss.2019.02.018.
65. Dwiyoitno D, Sturm MT, Januar HI, Schuhen K. Influence of various production methods on the microplastic contamination of sea salt produced in Java, Indonesia. *Environmental Science and Pollution Research* 2021. doi:10.1007/s11356-021-14411-6+#.
66. Padervand M, Lichtfouse E, Robert D, Wang C. Removal of microplastics from the environment. A review. *Environ Chem Lett.* 2020;25:7287. doi:10.1007/s10311-020-00983-1.
67. Wang Y, Li Y'n, Tian L, Ju L, Liu Y. The removal efficiency and mechanism of microplastic enhancement by positive modification dissolved air flotation. *Water Environ Res* 2020. doi:10.1002/wer.1352.
68. Talvitie J, Mikola A, Koistinen A, Setälä O. Solutions to microplastic pollution - Removal of microplastics from wastewater effluent with advanced wastewater treatment technologies. *Water Research.* 2017;123:401–7. doi:10.1016/j.watres.2017.07.005.
69. Simon M, Vianello A, Vollertsen J. Removal of >10 µm Microplastic Particles from Treated Wastewater by a Disc Filter. *Water.* 2019;11:1935. doi:10.3390/w11091935.
70. Sembiring E, Fajar M, Handajani M. Performance of rapid sand filter – single media to remove microplastics. *Water Supply.* 2021;21:2273–84. doi:10.2166/ws.2021.060.

71. Sembiring E, Mahapati WOSW, Hidayat S. Microplastics particle size affects cloth filter performance. *Journal of Water Process Engineering*. 2021;42:102166. doi:10.1016/j.jwpe.2021.102166.
72. Poerio T, Piacentini E, Mazzei R. Membrane Processes for Microplastic Removal. *Molecules* 2019. doi:10.3390/molecules24224148.
73. Lapointe M, Farner JM, Hernandez LM, Tufenkji N. Understanding and Improving Microplastic Removal during Water Treatment: Impact of Coagulation and Flocculation. *Environ Sci Technol*. 2020;54:8719–27. doi:10.1021/acs.est.0c00712.
74. Ma B, Xue W, Hu C, Liu H, Qu J, Li L. Characteristics of microplastic removal via coagulation and ultrafiltration during drinking water treatment. *Chemical Engineering Journal*. 2019;359:159–67. doi:10.1016/j.cej.2018.11.155.
75. Harford AJ, Hogan AC, Jones DR, van Dam RA. Ecotoxicological assessment of a polyelectrolyte flocculant. *Water Research*. 2011;45:6393–402. doi:10.1016/j.watres.2011.09.032.
76. Shen M, Zhang Y, Almatrafi E, Hu T, Zhou C, Song B, et al. Efficient removal of microplastics from wastewater by an electrocoagulation process. *Chemical Engineering Journal*. 2022;428:131161. doi:10.1016/j.cej.2021.131161.
77. Perren W, Wojtasik A, Cai Q. Removal of Microbeads from Wastewater Using Electrocoagulation. *ACS Omega*. 2018;3:3357–64. doi:10.1021/acsomega.7b02037.
78. Kiendrebeogo M, Karimi Estahbanati MR, Khosravanipour Mostafazadeh A, Drogui P, Tyagi RD. Treatment of microplastics in water by anodic oxidation: A case study for polystyrene. *Environ Pollut*. 2021;269:116168. doi:10.1016/j.envpol.2020.116168.
79. Magalhães S, Alves L, Medronho B, Romano A, Rasteiro MdG. Microplastics in Ecosystems: From Current Trends to Bio-Based Removal Strategies. *Molecules* 2020. doi:10.3390/molecules25173954.
80. Herbort AF, Sturm MT, Schuhen K. A new approach for the agglomeration and subsequent removal of polyethylene, polypropylene, and mixtures of both from freshwater systems - a case study. *Environ Sci Pollut Res Int*. 2018:15226–34. doi:10.1007/s11356-018-1981-7.
81. Herbort AF, Schuhen K. A concept for the removal of microplastics from the marine environment with innovative host-guest relationships. *Environmental Science and Pollution Research*. 2016:1–5. doi:10.1007/s11356-016-7216-x.
82. Rudloff M, Herbort A, Bimmler P, Hiller C, Poppelreiter N, Schuhen K. Quo vadis Spurenstoffelimination mittels Aktivkohlen Laborpraxis Teil 1-3. 2018. <https://www.laborpraxis.vogel.de/kohle-am-limit-quo-vadis-spurenstoffelimination-mittels-aktivkohlen-a-720974/>. Accessed 3 Jun 2019.
83. Löder MGJ, Gerdts G. Methodology Used for the Detection and Identification of Microplastics—A Critical Appraisal. In: Bergmann M, Gutow L, Klages M, editors. *Marine Anthropogenic Litter*. Cham: Springer International Publishing; 2015. p. 201–227. doi:10.1007/978-3-319-16510-3_8.

84. Prata JC, da Costa JP, Duarte AC, Rocha-Santos T. Methods for sampling and detection of microplastics in water and sediment: A critical review. *TrAC Trends in Analytical Chemistry*. 2019;110:150–9. doi:10.1016/j.trac.2018.10.029.
85. Möller JN, Löder MGJ, Laforsch C. Finding Microplastics in Soils: A Review of Analytical Methods. *Environ Sci Technol*. 2020;54:2078–90. doi:10.1021/acs.est.9b04618.
86. Chen G, Fu Z, Yang H, Wang J. An overview of analytical methods for detecting microplastics in the atmosphere. *TrAC Trends in Analytical Chemistry*. 2020;130:115981. doi:10.1016/j.trac.2020.115981.
87. Sturm MT, Horn H, Schuhen K. The potential of fluorescent dyes-comparative study of Nile red and three derivatives for the detection of microplastics. *Anal Bioanal Chem*. 2021;413:1059–71. doi:10.1007/s00216-020-03066-w.
88. Imhof HK, Schmid J, Niessner R, Ivleva NP, Laforsch C. A novel, highly efficient method for the separation and quantification of plastic particles in sediments of aquatic environments. *Limnol. Oceanogr. Methods*. 2012;10:524–37. doi:10.4319/lom.2012.10.524.
89. Prata JC, da Costa JP, Girão AV, Lopes I, Duarte AC, Rocha-Santos T. Identifying a quick and efficient method of removing organic matter without damaging microplastic samples. *Sci Total Environ*. 2019;686:131–9. doi:10.1016/j.scitotenv.2019.05.456.
90. Löder MGJ, Imhof HK, Ladehoff M, Löschel LA, Lorenz C, Mintenig S, et al. Enzymatic Purification of Microplastics in Environmental Samples. *Environ Sci Technol*. 2017;51:14283–92. doi:10.1021/acs.est.7b03055.
91. Löder MGJ, Kuczera M, Mintenig S, Lorenz C, Gerdts G. Focal plane array detector-based micro-Fourier-transform infrared imaging for the analysis of microplastics in environmental samples. *Environ. Chem*. 2015;12:563. doi:10.1071/EN14205.
92. Giese A, Kerpen J, Weber F, Prediger J. A Preliminary Study of Microplastic Abrasion from the Screw Cap System of Reusable Plastic Bottles by Raman Microspectroscopy. *ACS EST Water*. 2021;1:1363–8. doi:10.1021/acsestwater.0c00238.
93. Zhang Q, Zhao Y, Du F, Cai H, Wang G, Shi H. Microplastic Fallout in Different Indoor Environments. *Environ Sci Technol*. 2020;54:6530–9. doi:10.1021/acs.est.0c00087.
94. Chen W, Zhang C, Song L, Sommerfeld M, Hu Q. A high throughput Nile red method for quantitative measurement of neutral lipids in microalgae. *J Microbiol Methods*. 2009;77:41–7. doi:10.1016/j.mimet.2009.01.001.
95. Erni-Cassola G, Gibson MI, Thompson RC, Christie-Oleza JA. Lost, but Found with Nile Red: A Novel Method for Detecting and Quantifying Small Microplastics (1 mm to 20 μ m) in Environmental Samples. *Environ Sci Technol*. 2017;51:13641–8. doi:10.1021/acs.est.7b04512.
96. Shim WJ, Song YK, Hong SH, Jang M. Identification and quantification of microplastics using Nile Red staining. *Marine Pollution Bulletin*. 2016;113:469–76. doi:10.1016/j.marpolbul.2016.10.049.

97. Maes T, Jessop R, Wellner N, Haupt K, Mayes AG. A rapid-screening approach to detect and quantify microplastics based on fluorescent tagging with Nile Red. *Sci. Rep.* 2017;7:44501. doi:10.1038/srep44501.
98. Shruti VC, Pérez-Guevara F, Roy PD, Kuttralam-Muniasamy G. Analyzing microplastics with Nile Red: Emerging trends, challenges, and prospects. *J Hazard Mater.* 2021;423:127171. doi:10.1016/j.jhazmat.2021.127171.
99. Prata JC, Reis V, Matos JTV, da Costa JP, Duarte AC, Rocha-Santos T. A new approach for routine quantification of microplastics using Nile Red and automated software (MP-VAT). *Sci Total Environ.* 2019;690:1277–83. doi:10.1016/j.scitotenv.2019.07.060.
100. Lv L, Qu J, Yu Z, Chen D, Zhou C, Hong P, et al. A simple method for detecting and quantifying microplastics utilizing fluorescent dyes - Safranin T, fluorescein isophosphate, Nile red based on thermal expansion and contraction property. *Environ Pollut.* 2019;255:113283. doi:10.1016/j.envpol.2019.113283.
101. Prata JC, da Costa JP, Fernandes AJS, da Costa FM, Duarte AC, Rocha-Santos T. Selection of microplastics by Nile Red staining increases environmental sample throughput by micro-Raman spectroscopy. *Sci Total Environ.* 2021;783:146979. doi:10.1016/j.scitotenv.2021.146979.
102. Sancataldo G, Avellone G, Vetri V. Nile Red lifetime reveals microplastic identity. *Environ Sci Process Impacts.* 2020;22:2266–75. doi:10.1039/d0em00348d.
103. Bergmann M, Gutow L, Klages M. Marine Anthropogenic Litter 2015. doi:10.1007/978-3-319-16510-3.
104. Barnes DKA, Galgani F, Thompson RC, Barlaz M. Accumulation and fragmentation of plastic debris in global environments. *Philosophical Transactions of the Royal Society B: Biological Sciences.* 2009;364:1985–98. doi:10.1098/rstb.2008.0205.
105. Herbort AF, Sturm MT, Hiller C, Schuhen K. Ökologische Chemie von Mikroplastik – Ab wann werden Alltagshelfer zum Umweltproblem? Nachhaltiger Gewässerschutz durch die Implementierung einer Partikelelimination in der Kläranlage. *GWF Abwasser/Wasser.* 2017:1–9.
106. Sundt P, Schulze P-E, Syversen F. Sources of microplastics-pollution to the marine environment. 2014. <http://www.miljodirektoratet.no/Documents/publikasjoner/M321/M321.pdf>. Accessed 6 Dec 2016.
107. Suaria G, Avio CG, Mineo A, Lattin GL, Magaldi MG, Belmonte G, et al. The Mediterranean Plastic Soup: synthetic polymers in Mediterranean surface waters. *Sci Rep.* 2016;6:37551. doi:10.1038/srep37551.
108. Lechner A, Ramler D. The discharge of certain amounts of industrial microplastic from a production plant into the River Danube is permitted by the Austrian legislation. *Environ Pollut.* 2015;200:159–60. doi:10.1016/j.envpol.2015.02.019.
109. Browne MA, Crump P, Niven SJ, Teuten E, Tonkin A, Galloway T, Thompson R. Accumulation of Microplastic on Shorelines Worldwide: Sources and Sinks. *Environ. Sci. Technol.* 2011;45:9175–9. doi:10.1021/es201811s.

110. Mintenig SM, Int-Veen I, Loder MGJ, Primpke S, Gerdt G. Identification of microplastic in effluents of waste water treatment plants using focal plane array-based micro-Fourier-transform infrared imaging. *Water Research* 2016. doi:10.1016/j.watres.2016.11.015.
111. Simon M, van Alst N, Vollertsen J. Quantification of microplastic mass and removal rates at wastewater treatment plants applying Focal Plane Array (FPA)-based Fourier Transform Infrared (FT-IR) imaging. *Water Research*. 2018;142:1–9. doi:10.1016/j.watres.2018.05.019.
112. Brinker CJ, Scherer GW. *Sol-gel science: The physics and chemistry of sol-gel processing*. Boston: Academic Press; 1990.
113. Iler RK. *The chemistry of silica: Solubility, polymerization, colloid and surface properties, and biochemistry*. New York, NY: Wiley; 2004.
114. Sakka S. Sol-gel technology as representative processing for nanomaterials: case studies on the starting solution. *J Sol-Gel Sci Technol*. 2008;46:241–9. doi:10.1007/s10971-007-1651-6.
115. Perchacz M, Beneš H, Kobera L, Walterová Z. Influence of sol-gel conditions on the final structure of silica-based precursors. *J Sol-Gel Sci Technol*. 2015;75:649–63. doi:10.1007/s10971-015-3735-z.
116. Corriu R, Nguyễn TA. *Molecular chemistry of sol-gel derived nanomaterials*. Chichester, U.K: Wiley; 2009.
117. Brinker CJ. Hydrolysis and condensation of silicates: Effects on structure. *Journal of Non-Crystalline Solids*. 1988;100:31–50. doi:10.1016/0022-3093(88)90005-1.
118. Hench LL, West JK. The sol-gel process. *Chem. Rev.* 1990;90:33–72. doi:10.1021/cr00099a003.
119. Hook RJ. A ²⁹Si NMR study of the sol-gel polymerisation rates of substituted ethoxysilanes. *Journal of Non-Crystalline Solids*. 1996;195:1–15. doi:10.1016/0022-3093(95)00508-0.
120. Loy DA, Baugher BM, Baugher CR, Schneider DA, Rahimian K. Substituent Effects on the Sol-Gel Chemistry of Organotrialkoxysilanes. *Chem. Mater.* 2000;12:3624–32. doi:10.1021/cm000451i.
121. Moreau, J. J. E., Pichon BP, Man, M. W. C., Bied C, Pritzkow H, Bantignies J-L, et al. A Better Understanding of the Self-Structuration of Bridged Silsesquioxanes. *Angew. Chem. Int. Ed.* 2004;43:203–6. doi:10.1002/anie.200352485.
122. Hoffmann F, Cornelius M, Morell J, Fröba M. Silica-Based Mesoporous Organic-Inorganic Hybrid Materials. *Angew. Chem. Int. Ed.* 2006;45:3216–51. doi:10.1002/anie.200503075.
123. Bögershausen A. *Sol-Gel-Synthese und Poreneigenschaften von anorganisch organischen Hybridgelen für die kontrollierte Wirkstofffreisetzung*. Münster: Westfälische Wilhelms-Universität Münster; 2004.
124. Herbort AF, Sturm MT, Fiedler S, Abkai G, Schuhen K. Alkoxy-silyl Induced Agglomeration: A New Approach for the Sustainable Removal of Microplastic from Aquatic Systems. *J Polym Environ.* 2018;62:1–13. doi:10.1007/s10924-018-1287-3.
125. Pietschnig R, Spirk S. The chemistry of organo silanetriols. *Coordination Chemistry Reviews*. 2016;323:87–106. doi:10.1016/j.ccr.2016.03.010.

126. Hurkes N, Ehmann HMA, List M, Spirk S, Bussiek M, Belaj F, Pietschnig R. Silanol-based surfactants: synthetic access and properties of an innovative class of environmentally benign detergents. *Chemistry*. 2014;20:9330–5. doi:10.1002/chem.201402857.
127. Kim K, Jang KY, Upadhye RS. Hollow Silica Spheres of Controlled Size and Porosity by Sol-Gel Processing. *J American Ceramic Society*. 1991;74:1987–92. doi:10.1111/j.1151-2916.1991.tb07819.x.
128. Levy D, Zayat M. *The Sol-Gel Handbook*. Weinheim, Germany: Wiley-VCH Verlag GmbH & Co. KGaA; 2015.
129. Brochier Salon M-C, Belgacem MN. Hydrolysis-Condensation Kinetics of Different Silane Coupling Agents. *Phosphorus, Sulfur, and Silicon and the Related Elements*. 2011;186:240–54. doi:10.1080/10426507.2010.494644.
130. Al-Oweini R, El-Rassy H. Synthesis and characterization by FTIR spectroscopy of silica aerogels prepared using several Si(OR)₄ and R''Si(OR)₃ precursors. *Journal of Molecular Structure*. 2009;919:140–5. doi:10.1016/j.molstruc.2008.08.025.
131. Majewsky M, Bitter H, Eiche E, Horn H. Determination of microplastic polyethylene (PE) and polypropylene (PP) in environmental samples using thermal analysis (TGA-DSC). *Sci Total Environ*. 2016;568:507–11. doi:10.1016/j.scitotenv.2016.06.017.
132. Siegfried M, Koelmans AA, Besseling E, Kroeze C. Export of microplastics from land to sea. A modelling approach. *Water Research*. 2017;127:249–57. doi:10.1016/j.watres.2017.10.011.
133. da Costa JP, Santos PSM, Duarte AC, Rocha-Santos T. (Nano)plastics in the environment - Sources, fates and effects. *Sci Total Environ*. 2016;566-567:15–26. doi:10.1016/j.scitotenv.2016.05.041.
134. Gasperi J, Wright SL, Dris R, Collard F, Mandin C, Guerrouache M, et al. Microplastics in air: Are we breathing it in? *Current Opinion in Environmental Science & Health*. 2018;1:1–5. doi:10.1016/j.coesh.2017.10.002.
135. Wright SL, Kelly FJ. Plastic and Human Health: A Micro Issue? *Environ Sci Technol*. 2017;51:6634–47. doi:10.1021/acs.est.7b00423.
136. Sun J, Dai X, Wang Q, van Loosdrecht MCM, Ni B-J. Microplastics in wastewater treatment plants: Detection, occurrence and removal. *Water Research*. 2019;152:21–37. doi:10.1016/j.watres.2018.12.050.
137. EFSA CONTAM Panel. Presence of microplastics and nanoplastics in food, with particular focus on seafood. *EFS2*. 2016;14:30 pp. doi:10.2903/j.efsa.2016.4501.
138. Bui X-T, Vo T-D-H, Nguyen P-T, Nguyen V-T, Dao T-S, Nguyen P-D. Microplastics pollution in wastewater: Characteristics, occurrence and removal technologies. *Environmental Technology & Innovation*. 2020;19:101013. doi:10.1016/j.eti.2020.101013.
139. Pico Y, Alfathan A, Barcelo D. Nano- and microplastic analysis: Focus on their occurrence in freshwater ecosystems and remediation technologies. *TrAC Trends in Analytical Chemistry*. 2019;113:409–25. doi:10.1016/j.trac.2018.08.022.

140. Sturm MT, Herbort AF, Horn H, Schuhen K. Comparative study of the influence of linear and branched alkyltrichlorosilanes on the removal efficiency of polyethylene and polypropylene-based microplastic particles from water. *Environmental Science and Pollution Research*. 2020;27:10888–98. doi:10.1007/s11356-020-07712-9.
141. Schuhen K, Sturm MT, Herbort AF. Technological Approaches for the Reduction of Microplastic Pollution in Seawater Desalination Plants and for Sea Salt Extraction. In: Gomiero A, editor. *Plastics in the Environment*: IntechOpen; 2019. doi:10.5772/intechopen.81180.
142. Gurung K, Ncibi MC, Sillanpää M. Assessing membrane fouling and the performance of pilot-scale membrane bioreactor (MBR) to treat real municipal wastewater during winter season in Nordic regions. *Sci Total Environ*. 2017;579:1289–97. doi:10.1016/j.scitotenv.2016.11.122.
143. Shore JL, M'Coy WS, Gunsch CK, Deshusses MA. Application of a moving bed biofilm reactor for tertiary ammonia treatment in high temperature industrial wastewater. *Bioresource Technology*. 2012;112:51–60. doi:10.1016/j.biortech.2012.02.045.
144. Henze M. *Wastewater treatment: Biological and chemical processes*. 3rd ed. New Delhi (India): Springer; 2010.
145. Akarsu C, Kumbur H, Gökdağ K, Kıdeys AE, Sanchez-Vidal A. Microplastics composition and load from three wastewater treatment plants discharging into Mersin Bay, north eastern Mediterranean Sea. *Marine Pollution Bulletin*. 2020;150:110776. doi:10.1016/j.marpolbul.2019.110776.
146. Ben-David EA, Habibi M, Haddad E, Hasanin M, Angel DL, Booth AM, Sabbah I. Microplastic distributions in a domestic wastewater treatment plant: Removal efficiency, seasonal variation and influence of sampling technique. *Sci Total Environ*. 2021;752:141880. doi:10.1016/j.scitotenv.2020.141880.
147. Ranade VV, Bhandari VM, Ahirrao S. *Industrial wastewater treatment, recycling, and reuse*. Kidlington, Oxford, UK, Waltham, MA: Butterworth-Heinemann; 2014.
148. Elderfield H, Holland HD, editors. *The oceans and marine geochemistry*. 1st ed. Amsterdam: Elsevier; 2006.
149. Hammer UT. *Saline lake ecosystems of the world*. Dordrecht: Junk; 1986.
150. Rosner D, Markowitz G. Persistent pollutants: a brief history of the discovery of the widespread toxicity of chlorinated hydrocarbons. *Environmental Research*. 2013;120:126–33. doi:10.1016/j.envres.2012.08.011.
151. Baby DK. Rheology of hydrogels. In: *Rheology of Polymer Blends and Nanocomposites*: Elsevier; 2020. p. 193–204. doi:10.1016/B978-0-12-816957-5.00009-4.
152. Noda I, Dowrey AE, Haynes JL, Marcott C. Group Frequency Assignments for Major Infrared Bands Observed in Common Synthetic Polymers. In: Mark JE, editor. *Physical Properties of Polymers Handbook*. New York, NY: Springer New York; 2007. p. 395–406. doi:10.1007/978-0-387-69002-5_22.

153. Jung MR, Horgen FD, Orski SV, Rodriguez C V, Beers KL, Balazs GH, et al. Validation of ATR FT-IR to identify polymers of plastic marine debris, including those ingested by marine organisms. *Marine Pollution Bulletin*. 2018;127:704–16. doi:10.1016/j.marpolbul.2017.12.061.
154. Ajith N, Arumugam S, Parthasarathy S, Manupoori S, Janakiraman S. Global distribution of microplastics and its impact on marine environment-a review. *Environmental Science and Pollution Research*. 2020;27:25970–86. doi:10.1007/s11356-020-09015-5.
155. Karimi Estahbanati MR, Kiendrebeogo M, Khosravanipour Mostafazadeh A, Drogui P, Tyagi RD. Treatment processes for microplastics and nanoplastics in waters: State-of-the-art review. *Marine Pollution Bulletin*. 2021;168:112374. doi:10.1016/j.marpolbul.2021.112374.
156. Mohana AA, Farhad SM, Haque N, Pramanik BK. Understanding the fate of nano-plastics in wastewater treatment plants and their removal using membrane processes. *Chemosphere*. 2021;284:131430. doi:10.1016/j.chemosphere.2021.131430.
157. Bratby J. *Coagulation and Flocculation in Water and Wastewater Treatment - Third Edition*. 3rd ed. London: IWA Publishing; 2016.
158. Lee PS, Jung SM. Quantitative analysis of microplastics coagulation-removal process for clean sea salt production. *Int. J. Environ. Sci. Technol*. 2021;133:336. doi:10.1007/s13762-021-03469-x.
159. Pereira JL, Vidal T, Gonçalves FJM, Gabriel RG, Costa R, Rasteiro MG. Is the aquatic toxicity of cationic polyelectrolytes predictable from selected physical properties? *Chemosphere*. 2018;202:145–53. doi:10.1016/j.chemosphere.2018.03.101.
160. Costa R, Pereira JL, Gomes J, Gonçalves F, Hunkeler D, Rasteiro MG. The effects of acrylamide polyelectrolytes on aquatic organisms: relating toxicity to chain architecture. *Chemosphere*. 2014;112:177–84. doi:10.1016/j.chemosphere.2014.03.096.
161. Lengar Ž, Klun K, Dogsa I, Rotter A, Stopar D. Sequestration of Polystyrene Microplastics by Jellyfish Mucus. *Front. Mar. Sci*. 2021;8:35. doi:10.3389/fmars.2021.690749.
162. Sarcletti M, Park H, Wirth J, Englisch S, Eigen A, Drobek D, et al. The remediation of nano-/microplastics from water. *Materials Today*. 2021;225:28. doi:10.1016/j.mattod.2021.02.020.
163. Peydayesh M, Suta T, Uselli M, Handschin S, Canelli G, Bagnani M, Mezzenga R. Sustainable Removal of Microplastics and Natural Organic Matter from Water by Coagulation-Flocculation with Protein Amyloid Fibrils. *Environ Sci Technol*. 2021;55:8848–58. doi:10.1021/acs.est.1c01918.
164. Sturm MT, Horn H, Schuhen K. Removal of Microplastics from Waters through Agglomeration-Fixation Using Organosilanes—Effects of Polymer Types, Water Composition and Temperature. *Water*. 2021;13:675. doi:10.3390/w13050675.
165. Tu C, Chen T, Zhou Q, Liu Y, Wei J, Waniek JJ, Luo Y. Biofilm formation and its influences on the properties of microplastics as affected by exposure time and depth in the seawater. *Sci Total Environ*. 2020;734:139237. doi:10.1016/j.scitotenv.2020.139237.

166. Kovács ÁT, Dragoš A. Evolved Biofilm: Review on the Experimental Evolution Studies of *Bacillus subtilis* Pellicles. *J Mol Biol.* 2019;431:4749–59. doi:10.1016/j.jmb.2019.02.005.
167. Michels J, Stippkugel A, Lenz M, Wirtz K, Engel A. Rapid aggregation of biofilm-covered microplastics with marine biogenic particles. *Proc Biol Sci* 2018. doi:10.1098/rspb.2018.1203.
168. Miao L, Yu Y, Adyel TM, Wang C, Liu Z, Liu S, et al. Distinct microbial metabolic activities of biofilms colonizing microplastics in three freshwater ecosystems. *J Hazard Mater.* 2021;403:123577. doi:10.1016/j.jhazmat.2020.123577.
169. Tu C, Zhou Q, Zhang C, Liu Y, Luo Y. Biofilms of Microplastics. In: He D, Luo Y, editors. *Microplastics in Terrestrial Environments*. Cham: Springer International Publishing; 2020. p. 299–317. doi:10.1007/978-90-00-461-461.
170. Shabbir S, Faheem M, Ali N, Kerr PG, Wang L-F, Kuppusamy S, Li Y. Periphytic biofilm: An innovative approach for biodegradation of microplastics. *Sci Total Environ.* 2020;717:137064. doi:10.1016/j.scitotenv.2020.137064.
171. Guan J, Qi K, Wang J, Wang W, Wang Z, Lu N, Qu J. Microplastics as an emerging anthropogenic vector of trace metals in freshwater: Significance of biofilms and comparison with natural substrates. *Water Research.* 2020;184:116205. doi:10.1016/j.watres.2020.116205.
172. Feng L, He L, Jiang S, Chen J, Zhou C, Qian Z-J, et al. Investigating the composition and distribution of microplastics surface biofilms in coral areas. *Chemosphere.* 2020;252:126565. doi:10.1016/j.chemosphere.2020.126565.
173. McGivney E, Cederholm L, Barth A, Hakkarainen M, Hamacher-Barth E, Ogonowski M, Gorokhova E. Rapid Physicochemical Changes in Microplastic Induced by Biofilm Formation. *Front Bioeng Biotechnol.* 2020;8:205. doi:10.3389/fbioe.2020.00205.
174. Ramsperger AFRM, Narayana VKB, Gross W, Mohanraj J, Thelakkat M, Greiner A, et al. Environmental exposure enhances the internalization of microplastic particles into cells. *Sci. Adv.* 2020. doi:10.1126/sciadv.abd1211.
175. Ivleva NP, Wagner M, Horn H, Niessner R, Haisch C. Towards a nondestructive chemical characterization of biofilm matrix by Raman microscopy. *Anal Bioanal Chem.* 2009;393:197–206. doi:10.1007/s00216-008-2470-5.
176. Atashgahi S, Liebensteiner MG, Janssen DB, Smidt H, Stams AJM, Sipkema D. Microbial Synthesis and Transformation of Inorganic and Organic Chlorine Compounds. *Front Microbiol.* 2018;9:3079. doi:10.3389/fmicb.2018.03079.
177. Giacomucci L, Raddadi N, Soccio M, Lotti N, Fava F. Polyvinyl chloride biodegradation by *Pseudomonas citronellolis* and *Bacillus flexus*. *N Biotechnol.* 2019;52:35–41. doi:10.1016/j.nbt.2019.04.005.
178. Singh R, Pant D. Bio-inspired dechlorination of poly vinyl chloride. *Chemical Engineering Research and Design.* 2018;132:505–17. doi:10.1016/j.cherd.2018.01.043.
179. Wang J, Wu Y, Cao Y, Li G, Liao Y. Influence of surface roughness on contact angle hysteresis and spreading work. *Colloid Polym Sci.* 2020;298:1107–12. doi:10.1007/s00396-020-04680-x.

180. Kubiak KJ, Wilson MCT, Mathia TG, Carval P. Wettability versus roughness of engineering surfaces. *Wear*. 2011;271:523–8. doi:10.1016/j.wear.2010.03.029.
181. Jansen B, Kohnen W. Prevention of biofilm formation by polymer modification. *J Ind Microbiol*. 1995;15:391–6. doi:10.1007/BF01569996.
182. Miao L, Wang P, Hou J, Yao Y, Liu Z, Liu S, Li T. Distinct community structure and microbial functions of biofilms colonizing microplastics. *Sci Total Environ*. 2019;650:2395–402. doi:10.1016/j.scitotenv.2018.09.378.
183. Chen X, Chen X, Zhao Y, Zhou H, Xiong X, Wu C. Effects of microplastic biofilms on nutrient cycling in simulated freshwater systems. *Sci Total Environ*. 2020;719:137276. doi:10.1016/j.scitotenv.2020.137276.
184. Liu N, Skauge T, Landa-Marbán D, Hovland B, Thorbjørnsen B, Radu FA, et al. Microfluidic study of effects of flow velocity and nutrient concentration on biofilm accumulation and adhesive strength in microchannels; 2018.
185. Wang C, Miao L, Hou J, Wang P, Qian J, Dai S. The effect of flow velocity on the distribution and composition of extracellular polymeric substances in biofilms and the detachment mechanism of biofilms. *Water Science & Technology*. 2014;69:825–32. doi:10.2166/wst.2013.785.
186. Stoodley P, Dodds I, Boyle JD, Lappin-Scott HM. Influence of hydrodynamics and nutrients on biofilm structure. *J Appl Microbiol*. 1998;85 Suppl 1:19S-28S. doi:10.1111/j.1365-2672.1998.tb05279.x.
187. Othman AR, Hasan HA, Muhamad MH, Ismail N'I, Abdullah SRS. Microbial degradation of microplastics by enzymatic processes: a review. *Environ Chem Lett*. 2021;744:140984. doi:10.1007/s10311-021-01197-9.
188. Andrady AL. The plastic in microplastics: A review. *Marine Pollution Bulletin*. 2017;119:12–22. doi:10.1016/j.marpolbul.2017.01.082.
189. Rivas D, Ginebreda A, Pérez S, Quero C, Barceló D. MALDI-TOF MS Imaging evidences spatial differences in the degradation of solid polycaprolactone diol in water under aerobic and denitrifying conditions. *Sci Total Environ*. 2016;566-567:27–33. doi:10.1016/j.scitotenv.2016.05.090.
190. Ha J, Yeo M-K. The environmental effects of microplastics on aquatic ecosystems. *Mol. Cell. Toxicol*. 2018;14:353–9. doi:10.1007/s13273-018-0039-8.
191. Boucher J, Friot D. Primary microplastics in the oceans: A global evaluation of sources. Gland, Switzerland: IUCN; 2017.
192. Shim WJ, Thomposon RC. Microplastics in the Ocean. *Arch Environ Contam Toxicol*. 2015;69:265–8. doi:10.1007/s00244-015-0216-x.
193. Prata JC, da Costa JP, Lopes I, Duarte AC, Rocha-Santos T. Environmental exposure to microplastics: An overview on possible human health effects. *Sci Total Environ*. 2020;702:134455. doi:10.1016/j.scitotenv.2019.134455.

194. Prata JC, Silva ALP, da Costa JP, Mouneyrac C, Walker TR, Duarte AC, Rocha-Santos T. Solutions and Integrated Strategies for the Control and Mitigation of Plastic and Microplastic Pollution. *Int J Environ Res Public Health*. 2019;16:2411–30. doi:10.3390/ijerph16132411.
195. Lindeque PK, Cole M, Coppock RL, Lewis CN, Miller RZ, Watts AJR, et al. Are we underestimating microplastic abundance in the marine environment? A comparison of microplastic capture with nets of different mesh-size. *Environmental Pollution*. 2020;265:114721. doi:10.1016/j.envpol.2020.114721.
196. Hidalgo-Ruz V, Gutow L, Thompson RC, Thiel M. Microplastics in the marine environment: a review of the methods used for identification and quantification. *Environ Sci Technol*. 2012;46:3060–75. doi:10.1021/es2031505.
197. Paul-Pont I, Tallec K, Gonzalez-Fernandez C, Lambert C, Vincent D, Mazurais D, et al. Constraints and Priorities for Conducting Experimental Exposures of Marine Organisms to Microplastics. *Front. Mar. Sci*. 2018;5:1518. doi:10.3389/fmars.2018.00252.
198. Watteau F, Dignac M-F, Bouchard A, Revallier A, Houot S. Microplastic Detection in Soil Amended With Municipal Solid Waste Composts as Revealed by Transmission Electronic Microscopy and Pyrolysis/GC/MS. *Front. Sustain. Food Syst*. 2018;2:253. doi:10.3389/fsufs.2018.00081.
199. Renner G, Schmidt TC, Schram J. Analytical methodologies for monitoring micro(nano)plastics: Which are fit for purpose? *Current Opinion in Environmental Science & Health*. 2018;1:55–61. doi:10.1016/j.coesh.2017.11.001.
200. Bhargava R, Wang S-Q, Koenig JL. FTIR Microspectroscopy of Polymeric Systems. In: Abe A, Albertsson A-C, Cantow H-J, Dusek K, Edwards S, Höcker H, et al., editors. *Liquid Chromatography / FTIR Microspectroscopy / Microwave Assisted Synthesis*. Berlin, Heidelberg: Springer Berlin Heidelberg; 2003. p. 137–191. doi:10.1007/b11052.
201. Kappler A, Windrich F, Loder MGJ, Malanin M, Fischer D, Labrenz M, et al. Identification of microplastics by FTIR and Raman microscopy: a novel silicon filter substrate opens the important spectral range below 1300 cm⁻¹ for FTIR transmission measurements. *Anal Bioanal Chem*. 2015;407:6791–801. doi:10.1007/s00216-015-8850-8.
202. Andrady AL. Using flow cytometry to detect micro- and nano-scale polymer particles on Proceedings of the Second Research Workshop on Microplastic Marine Debris.: Tacoma, November 5-6, 2010. NOAA Technical Memorandum NOS-OR&R-39; 2011.
203. Ra H, Piyawattanametha W, Mandella MJ, Hsiung P-L, Hardy J, Wang TD, et al. Three-dimensional in vivo imaging by a handheld dual-axes confocal microscope. *Optics express*. 2008;16:7224–32. doi:10.1364/OE.16.007224.
204. Tamminga M, Hengstmann E, Fischer H. Nile Red Staining as a Subsidiary Method for Microplastic Quantification: A Comparison of Three Solvents and Factors Influencing Application Reliability. *JESES*. 2017;2:1–8. doi:10.15436/JESES.2.2.1.

205. Erni-Cassola G, Gibson MI, Thompson RC, Christie-Oleza JA. Lost, but Found with Nile Red: A Novel Method for Detecting and Quantifying Small Microplastics (1 mm to 20 μm) in Environmental Samples. *Environ Sci Technol*. 2017;51:13641–8. doi:10.1021/acs.est.7b04512.
206. Guido CA, Mennucci B, Jacquemin D, Adamo C. Planar vs. twisted intramolecular charge transfer mechanism in Nile Red: new hints from theory. *Phys Chem Chem Phys*. 2010;12:8016–23. doi:10.1039/B927489H.
207. Cser A, Nagy K, Biczók L. Fluorescence lifetime of Nile Red as a probe for the hydrogen bonding strength with its microenvironment. *Chemical Physics Letters*. 2002;360:473–8. doi:10.1016/S0009-2614(02)00784-4.
208. Boldrini B, Cavalli E, Painelli A, Terenziani F. Polar Dyes in Solution: A Joint Experimental and Theoretical Study of Absorption and Emission Band Shapes. *J. Phys. Chem. A*. 2002;106:6286–94. doi:10.1021/jp020031b.
209. Nagy K, Göktürk S, Biczók L. Effect of Microenvironment on the Fluorescence of 2-Hydroxy-Substituted Nile Red Dye: A New Fluorescent Probe for the Study of Micelles. *J. Phys. Chem. A*. 2003;107:8784–90. doi:10.1021/jp035357e.
210. Jee A-Y, Park S, Kwon H, Lee M. Excited state dynamics of Nile Red in polymers. *Chemical Physics Letters*. 2009;477:112–5. doi:10.1016/j.cplett.2009.06.088.
211. Jose J, Burgess K. Benzophenoxazine-based fluorescent dyes for labeling biomolecules. *Tetrahedron*. 2006;62:11021–37. doi:10.1016/j.tet.2006.08.056.
212. Baur E, Ruhrberg K, Woishnis W, editors. *Chemical resistance of engineering thermoplastics*. Norwich: William Andrew; 2016.
213. Metzger AP, Matlack JD. Comparative swelling behavior of various thermoplastic polymers. *Polym. Eng. Sci*. 1968;8:110–5. doi:10.1002/pen.760080206.
214. Sackett DL, Knutson JR, Wolff J. Hydrophobic surfaces of tubulin probed by time-resolved and steady-state fluorescence of Nile Red. *J Biol Chem*. 1990;265:14899–906.
215. Hungerford G, Ferreira JA. The effect of the nature of retained solvent on the fluorescence of Nile Red incorporated in sol–gel-derived matrices. *Journal of Luminescence*. 2001;93:155–65. doi:10.1016/S0022-2313(01)00181-8.
216. Meinershagen JL, Bein T. Optical Sensing in Nanopores. Encapsulation of the Solvatochromic Dye Nile Red in Zeolites. *J. Am. Chem. Soc*. 1999;121:448–9. doi:10.1021/ja982647d.
217. Sackett DL, Wolff J. Nile red as a polarity-sensitive fluorescent probe of hydrophobic protein surfaces. *Analytical Biochemistry*. 1987;167:228–34. doi:10.1016/0003-2697(87)90157-6.
218. Tang R, Ji W, Wang C. pH-Responsive Micelles Based on Amphiphilic Block Copolymers Bearing Ortho Ester Pendants as Potential Drug Carriers. *Macromol. Chem. Phys*. 2011;212:1185–92. doi:10.1002/macp.201100007.
219. Hendriks J, Gensch T, Hviid L, van der Horst MA, Hellingwerf KJ, van Thor JJ. Transient Exposure of Hydrophobic Surface in the Photoactive Yellow Protein Monitored with Nile Red. *Biophysical Journal*. 2002;82:1632–43. doi:10.1016/S0006-3495(02)75514-8.

220. Moreno EM, Levy D. Role of the Comonomer GLYMO in ORMOSILs As Reflected by Nile Red Spectroscopy. *Chem. Mater.* 2000;12:2334–40. doi:10.1021/cm001048e.
221. Braun U, Jekel M, Gerds G, Ivleva NP, Reiber J. *Diskussionspapier Mikroplastik-Analytik*. Berlin, Germany: BMBF Forschungsschwerpunkt „Plastik in der Umwelt“; 2018.